Trinity College Dublin
Coláiste na Tríonóide, Baile Átha Cliath
The University of Dublin

School of Computer Science and Statistics

# Deriving and implementing a model to predict the most energy efficient route for a solar powered vehicle

Julie Gallagher

April 19, 2022

A dissertation submitted in partial fulfilment
of the requirements for the degree of
MAI (Computer Engineering)

# Declaration

I hereby declare that this dissertation is entirely my own work and that it has not been submitted as an exercise for a degree at this or any other university.

I have read and I understand the plagiarism provisions in the General Regulations of the University Calendar for the current year, found at `http://www.tcd.ie/calendar`.

I have also completed the Online Tutorial on avoiding plagiarism 'Ready Steady Write', located at `http://tcd-ie.libguides.com/plagiarism/ready-steady-write`.

I agree that this thesis will not be publicly available but will be available to TCD staff and students in the University's open access institutional repository on the Trinity domain only.

# Abstract

Solar powered vehicles are currently being developed as entirely self-sustaining vehicles that harness their energy directly from the sun. This paper tackles the problem that a crucial aspect of energy consumption for solar vehicles is driving them in as much solar exposed areas as possible. With increased energy absorption these vehicles can become more widespread and aid in reducing energy consumption through fossil fuels in the transport industry.

This project derives and implements a model that can predict the most energy efficient route for a solar powered vehicle in a variety of different conditions. Unlike previous work, this project focuses on building a model using aspects of other research in areas of weather, mapping and energy management. The goal is to build a model that can be applied to any city using a digital surface model.

This project uses the ArcGIS tool and the open weather API to develop a model that predicts the solar potential of a vehicle by taking into account shade based on surrounding topography, vehicle type, weather, distance and time of day.

This model was then implemented into a user mobile application; ‘Drive Solar’ that can calculate the optimal route for the user based on their preferences. A data management application was also built to support the transfer of data from ArcGIS and help this application be scalable for larger road networks.

The prediction model was then tested using a solar irradiance sensor on the bonnet of a car in Dublin city. This test aids in understanding the effectiveness of the model in a variety of conditions.

The results found that the model designed in this experiment predicts the route with the most energy absorbed with a 51.65% accuracy and chooses the route with the most energy consumed with a 86.65% accuracy. It was found that some vehicle types such as Aptera and Lightyear One could be self-sustaining with the help of some solar parking. Other vehicles such as solar vans or buses could currently only support energy consumption in a hybrid vehicle. By increasing the energy absorbed by a solar vehicle, Drive Solar can aid in the transition to the widespread use of self-sustaining solar vehicles.

# Acknowledgements

Firstly, I would like to thank my supervisor Dr. Siobhan Clarke for all her guidance throughout this project. She provided assistance when needed and helped shape and mould this project into what it is.

I would also like to thank Dr. Sarah McCormack for providing me with technical support in her area of expertise relating to solar energy.

Thank you to senior technical officer, Mary O'Shea who helped me source the equipment required for this project.

Thank you also to Dr. John Connolly who provided me with resources required for the digital surface model which created the foundations of this dissertation.

And finally I would like to thank my family and friends for all of their help throughout the last 5 years in Trinity.

# Contents


**1 Introduction** **1**
1.1 Introduction . . . . . 1
1.2 Motivation . . . . . 1
1.3 Approach . . . . . 2
1.4 Research questions . . . . . 3
1.5 Contributions of research . . . . . 3
1.6 Roadmap of project . . . . . 4

**2 Background and state of the art** **5**
2.1 Background . . . . . 5
2.1.1 ArcGIS Tool . . . . . 5
2.2 State of the Art . . . . . 7
2.2.1 Solar vehicle developments . . . . . 7
2.2.2 Solar mapping . . . . . 9
2.2.3 Impact of weather on solar irradiance . . . . . 11
2.2.4 Energy efficient shortest route problem . . . . . 13
2.2.5 Solar Car Optimised Route Estimation . . . . . 14
2.3 Summary . . . . . 16

**3 Derivation of the prediction model** **18**
3.1 Road network and length . . . . . 18
3.2 Shade and time of day calculations . . . . . 19
3.2.1 Urban analysis . . . . . 20
3.2.2 Data conversion . . . . . 20
3.2.3 Solar mapping . . . . . 22
3.2.4 Solar radiation analysis . . . . . 22
3.2.5 Clear sky solar irradiance . . . . . 23
3.3 Weather impact . . . . . 24
3.4 Vehicle type . . . . . 25
3.4.1 Lightyear one . . . . . 25

3.4.2 Aptera motors . . . . . . . . . . . . . . . . . . . . . . . . 26
3.4.3 Solar bus . . . . . . . . . . . . . . . . . . . . . . . . . . . 26
3.4.4 Solar van . . . . . . . . . . . . . . . . . . . . . . . . . . . 27
3.4.5 Contribution to prediction model . . . . . . . . . . . . . . . . . . 27
3.5 Summary . . . . . . . . . . . . . . . . . . . . . . . . . . . . . 28

**4 Implementation 29**
4.1 Data . . . . . . . . . . . . . . . . . . . . . . . . . . . . . . . 29
4.1.1 Graph databases . . . . . . . . . . . . . . . . . . . . . . . 29
4.1.2 Document databases . . . . . . . . . . . . . . . . . . . . . 30
4.1.3 Firebase . . . . . . . . . . . . . . . . . . . . . . . . . . . 30
4.1.4 Architecture . . . . . . . . . . . . . . . . . . . . . . . . . 31
4.2 Implementation algorithms . . . . . . . . . . . . . . . . . . . . . . 31
4.2.1 Graph design . . . . . . . . . . . . . . . . . . . . . . . . . 32
4.2.2 Bellman Ford algorithm . . . . . . . . . . . . . . . . . . . . 32
4.2.3 Johnsons algorithm . . . . . . . . . . . . . . . . . . . . . . 33
4.2.4 Dijkstra algorithm . . . . . . . . . . . . . . . . . . . . . . 33
4.2.5 A* algorithm . . . . . . . . . . . . . . . . . . . . . . . . . 34
4.3 Drive Solar: User mobile application . . . . . . . . . . . . . . . . . 35
4.3.1 Objectives . . . . . . . . . . . . . . . . . . . . . . . . . . 36
4.3.2 Code structure . . . . . . . . . . . . . . . . . . . . . . . . 36
4.3.3 Inputs . . . . . . . . . . . . . . . . . . . . . . . . . . . . 37
4.3.4 Outputs . . . . . . . . . . . . . . . . . . . . . . . . . . . 38
4.3.5 Calculation . . . . . . . . . . . . . . . . . . . . . . . . . . 38
4.4 Data Management application . . . . . . . . . . . . . . . . . . . . 39
4.4.1 Objectives . . . . . . . . . . . . . . . . . . . . . . . . . . 39
4.4.2 Code structure . . . . . . . . . . . . . . . . . . . . . . . . 40
4.4.3 Functions . . . . . . . . . . . . . . . . . . . . . . . . . . . 40
4.5 Summary . . . . . . . . . . . . . . . . . . . . . . . . . . . . . 41

**5 Testing methodology 43**
5.1 Planning . . . . . . . . . . . . . . . . . . . . . . . . . . . . . 43
5.1.1 The Route . . . . . . . . . . . . . . . . . . . . . . . . . . 43
5.1.2 Test timing . . . . . . . . . . . . . . . . . . . . . . . . . . 44
5.2 Iterations . . . . . . . . . . . . . . . . . . . . . . . . . . . . . 45
5.2.1 Iteration 1 . . . . . . . . . . . . . . . . . . . . . . . . . . 45
5.2.2 Iteration 2 . . . . . . . . . . . . . . . . . . . . . . . . . . 45
5.3 Final testing method . . . . . . . . . . . . . . . . . . . . . . . . 46
5.4 Analysing routes . . . . . . . . . . . . . . . . . . . . . . . . . . 47

5.5 Summary . . . . . . . . . . 48

**6 Results and Discussion** **49**
6.1 Road segment analysis in clear sky conditions . . . . . . . . . . 49
6.1.1 Road segment analysis at 7:00 UTC . . . . . . . . . . 49
6.1.2 Discussion of limitations . . . . . . . . . . 50
6.2 Route analysis in clear sky conditions . . . . . . . . . . 54
6.3 Analysis in cloudy weather conditions . . . . . . . . . . 57
6.3.1 Predicting and classifying weather . . . . . . . . . . 57
6.3.2 Analysis of individual road segments under heavy and light cloud . . 58
6.3.3 Route analysis in cloudy conditions . . . . . . . . . . 59
6.4 Comparison of vehicles . . . . . . . . . . 61
6.5 Comparison of time vs energy . . . . . . . . . . 62
6.6 Summary . . . . . . . . . . 63

**7 Conclusion** **64**
7.1 Result Conclusions . . . . . . . . . . 64
7.1.1 Other key findings . . . . . . . . . . 66
7.1.2 To what extent can a model predict the optimal solar energy efficient route for a solar vehicle? . . . . . . . . . . 66
7.2 Project analysis . . . . . . . . . . 67
7.2.1 Challenges . . . . . . . . . . 67
7.2.2 Strengths and Limitations . . . . . . . . . . 67
7.3 Future work . . . . . . . . . . 68
7.4 Summary . . . . . . . . . . 69

**A1 Solar Maps** **75**

**A2 Individual road segment analysis at 11am and 3pm** **77**

**A3 Route analysis in clear sky conditions** **79**

**A4 Individual road segment analysis in cloudy conditions** **83**

**A5 Route analysis in cloudy conditions** **85**

**A6 Vehicle Analysis** **91**

# List of Figures


2.1 Lobaccaro's 6 step solar mapping approach . . . . . . . . . . . . . . . . . . 10
2.2 Wergertseder's solar mapping approach . . . . . . . . . . . . . . . . . . . . . 11
2.3 Bonkaney's solar irradiance profiles corresponding to cloudy days . . . . . . 12

3.1 Map of nodes and edges used as sample road network . . . . . . . . . . . . 18
3.2 Flight paths of aerial laser photogrammetry . . . . . . . . . . . . . . . . . . . 20
3.3 LAS files where each square shows the outer bounds of the data for that file 21
3.4 Digital surface model at intersection of D'Oiler street and O'Connell Bridge 21
3.5 Raster dataset of the digital surface model . . . . . . . . . . . . . . . . . . . 22
3.6 Solar map around Trinity College at 11am on March $26^{th}$ . . . . . . . . . . 22
3.7 Zonal data recorded over raster dataset . . . . . . . . . . . . . . . . . . . . . 23
3.8 Lighyear one solar vehicle . . . . . . . . . . . . . . . . . . . . . . . . . . . . 26
3.9 Aptera solar vehicle . . . . . . . . . . . . . . . . . . . . . . . . . . . . . . . 26

4.1 Sample data in nodes collection . . . . . . . . . . . . . . . . . . . . . . . . 30
4.2 Sample data in edges collection . . . . . . . . . . . . . . . . . . . . . . . . . 31
4.3 Architecture diagram . . . . . . . . . . . . . . . . . . . . . . . . . . . . . . . 31
4.4 User Interface of Drive Solar before and after search . . . . . . . . . . . . . 35
4.5 User mobile application class diagram . . . . . . . . . . . . . . . . . . . . . 36
4.6 Sequence diagram when a user wants to calculate the most energy efficient route . . . . . . . . . . . . . . . . . . . . . . . . . . . . . . . . . . . . . . . 39
4.7 Data Management Class Diagram . . . . . . . . . . . . . . . . . . . . . . . . 40
4.8 Sequence diagram for reading the predicted data from a CSV file . . . . . . 41

5.1 Final set of edges . . . . . . . . . . . . . . . . . . . . . . . . . . . . . . . . 44
5.2 Test set up for the final methodology . . . . . . . . . . . . . . . . . . . . . . 46

6.1 Comparison of predicted and tested data on March $26^{th}$ and $27^{th}$ at 7:00 UTC 50
6.2 An image showing how the sensor was shaded by the car . . . . . . . . . . . 51
6.3 A representation of how traffic can impact the prediction model . . . . . . . 51
6.4 Road segment from node 5 to 6 at 3pm on April 3rd . . . . . . . . . . . . . 52

6.5 Representation of changes in solar irradiance due to construction . . . . . . 53
6.6 A representation of how an overhead bridge can impact the prediction model 53
6.7 An image of the test car being shaded by another vehicle. . . . . . . . . . . 54
6.8 Comparison of predicted and tested data for solar absorption along a Journey 55
6.9 Comparison of predicted and tested data for solar energy consumed along Journey 1 . . . . . . . . . . . . . . . . . . . . . . . . . . . . . . . . . 56
6.10 Comparison of predicted and tested data at each edge under heavy and light cloud conditions . . . . . . . . . . . . . . . . . . . . . . . . . . . . . 58
6.11 Comparison of predicted and tested data for Journey 1 under heavy and light cloud conditions . . . . . . . . . . . . . . . . . . . . . . . . . . . . . 59
6.12 Comparison of Vehicle type across journeys on March 26 at 11am . . . . . 61
6.13 2 routes highlighted for Journey 3 . . . . . . . . . . . . . . . . . . . . . 62

A1.1 Sample of a generated solar map on April 3 at 7am . . . . . . . . . . . . . 75
A1.2 Sample of a generated solar map on April 3 at 11am . . . . . . . . . . . . . 76
A1.3 Sample of a generated solar map on April 3 at 3pm . . . . . . . . . . . . . 76

A2.1 Comparison of predicted and tested data on March 26 and 27 at 11:00 UTC 77
A2.2 Comparison of predicted and tested data on March 26 and 27 at 15:00 UTC 78

A3.1 Route analysis conducted on March 26th for the energy absorbed by a solar vehicle . . . . . . . . . . . . . . . . . . . . . . . . . . . . . . . . . . . 80
A3.2 Route analysis conducted on March 26th for energy consumed by a solar vehicle 81
A3.3 Route analysis conducted on March 27th for energy consumed by a solar vehicle 82

A4.1 Individual road segment analysis for light cloud . . . . . . . . . . . . . . . . 83
A4.2 Individual road segment analysis for medium cloud . . . . . . . . . . . . . . 84
A4.3 Individual road segment analysis for heavy cloud . . . . . . . . . . . . . . . 84

A5.1 Route analysis conducted in light cloud conditions for the energy absorbed by a solar vehicle . . . . . . . . . . . . . . . . . . . . . . . . . . . . . . . 86
A5.2 Route analysis conducted in light cloud conditions for the energy consumed by a solar vehicle . . . . . . . . . . . . . . . . . . . . . . . . . . . . . . . 87
A5.3 Route analysis conducted in medium cloud conditions for the energy absorbed by a solar vehicle . . . . . . . . . . . . . . . . . . . . . . . . . . . . . . 88
A5.4 Route analysis conducted in medium cloud conditions for the energy consumed by a solar vehicle . . . . . . . . . . . . . . . . . . . . . . . . . . . . . . 88
A5.5 Route analysis conducted in heavy cloud conditions for the energy absorbed by a solar vehicle . . . . . . . . . . . . . . . . . . . . . . . . . . . . . . 89
A5.6 Route analysis conducted in heavy cloud conditions for the energy consumed by a solar vehicle . . . . . . . . . . . . . . . . . . . . . . . . . . . . . . 90

A6.1 Comparison of vehicles travelling optimal route for each journey March 26 . . 91

# List of Tables


2.1 Summary of State of the art . . . . . . . . . . . . . . . . . . . . . . . . . 17

3.1 Sample data for 10 edges produced by the 'Zonal Statistics as Table' tool . . 23
3.2 Standard values for solar vehicles . . . . . . . . . . . . . . . . . . . . . . 27

5.1 Sample data for 5 test data edges on April 2 at 7 and 11 am . . . . . . . . 47
5.2 Journeys and routes selected for analysis . . . . . . . . . . . . . . . . . . . 48

6.1 Limitations that caused large discrepancy in data March 26 and 27 at 7 am 50
6.2 Cloud classifications . . . . . . . . . . . . . . . . . . . . . . . . . . . . . 57
6.3 Sample of how different variables effect what route is selected by Drive Solar 63
6.4 Accuracy Table . . . . . . . . . . . . . . . . . . . . . . . . . . . . . . . . 63

A2.1 Reasons for large discrepancy in data March 26 and 27 at 11 am . . . . . . 78
A2.2 Reasons for large discrepancy in data March 26 and 27 at 3 pm . . . . . . . 78

# List of Algorithms


1 Bellman Ford Algorithm . . . . . . . . . . . . . . . . . . . . . . . . . . . . 32
2 Johnson's Algorithm . . . . . . . . . . . . . . . . . . . . . . . . . . . . . 33
3 Dijkstra's Algorithm . . . . . . . . . . . . . . . . . . . . . . . . . . . . . 34
4 A* Algorithm . . . . . . . . . . . . . . . . . . . . . . . . . . . . . . . . . 34

# Nomenclature

| | |
|---|---|
| G | Graph |
| v | A vertex in a graph |
| V | Set of all vertices in the graph |
| $\omega(u, v)$ | Weight of a graph edge from u to v |
| d[ ] | Array of distances from source node |
| E | Set of all edges in a graph |
| s | Source vertex |
| $\pi[\,]$ | Array to track the path recorded |

# 1 Introduction

## 1.1 Introduction

Whilst automobile transportation is the single most common means of transportation today, researchers still grapple with the pollution issues caused by cars and seek alternatives to power transportation with reduced emission levels. The development of solar vehicles has provided new possibilities, meaning the solar panels on the roof and other parts of the vehicle can generate energy from renewable resources. Research now focuses on increasing the energy absorbed by solar powered vehicles to make them competitive with conventional fossil fuel vehicles.

In the car industry, considerable progression has been made with solar powered cars beginning to enter the market as entirely self-sustaining vehicles. This is confirmed by the announcement of the release of Lightyear One, the first long-range solar car, in late 2022 (1) and Aptera (Aptera Motors) in late 2023 (2). Solar panels are also being considered for buses (3)(4) and are soon to be expanded into all modes of transport. These vehicles are shown to successfully reduce fuel consumption by generating more energy through renewable sources.

With increased use of solar vehicles, understanding and modelling their energy consumption will become more of a focus area of research similar to the energy efficiency research for current electric vehicles. This research project will derive and implement an algorithm to predict the optimal route for a solar vehicle to travel while maximising its solar energy absorption.

## 1.2 Motivation

Solar powered vehicles reduce the consumption of fossil fuels in the transport industry. In Ireland, private-cars account for 14.2% of energy demand (5). Current electric vehicles have already helped convert this energy usage from fossil fuels to more renewable energy sources, although still from the grid. Solar powered vehicles are entirely self-sustaining and do not rely on any other energy source other than the sun. This redirects the energy usage from fossil fuels and charging stations which rely on other forms of energy, directly to the sun.

With current technologies, the energy absorbed from the panels of a solar vehicle is not as high as can be provided from a traditional fossil fuel vehicle. The focus of research has been to reduce energy usage of the vehicle by reconstructing the frames and modifying it to be more aerodynamic. As well as this the solar panels have been increased to cover as much area as possible often including the bonnet, roof and sides. However a crucial part of energy absorption for a solar vehicle is parking and driving it in as much solar exposed areas as possible.

Some research focuses on the parking model of a solar vehicle which is similar to the analysis of a static set of solar panels. This research project focuses on optimising the energy consumption of solar vehicles when driving from point A to B. This tackles the issue of providing the vehicle with as much solar exposure as possible while driving. This was chosen due to the current lack of research in the area. With current technologies, many would consider the solar energy absorbed while driving to have minimal impact on the overall energy consumption. However, as technologies progress and built up environments become more developed the route chosen will have a dramatic impact on the solar energy absorbed. The small amount of research done in the area lacks a solution that can be applied to multiple locations and has little understanding of the effectiveness of the model.

This research fills a gap in the knowledge surrounding increasing the solar exposure of a solar vehicle while driving. It focuses on developing a prediction model to optimise the route that can be applied to a larger road network and tests the effectiveness of this model. With the implementation of a user friendly app to add realism to the research, users can have direct access to this prediction model. Using this prediction model as a more widespread resource will optimise energy consumption in solar vehicles and help increase the momentum towards a greener energy future.

## 1.3 Approach

This project aims to create a prediction model to select the optimal route from point A to B to optimise solar energy consumption in a solar vehicle. The model takes into account shading due to surrounding topography, time of day, time of year, weather conditions, vehicle type and distance to determine the most solar energy efficient route.

This prediction model is implemented into a mobile application, Drive Solar, so that users can effectively find the optimal route by entering all of the required parameters. A second application is developed to manage the data required for this project and make this project scalable for larger road networks.

Testing will be conducted to determine the accuracy of the prediction model and how it compares to real-time recordings. Iterations are performed to improve both test and predictive data and generate a more accurate model.

The tested data is then compared with the predicted data to determine the accuracy of the model. This also aids in understanding what factors are accurately represented by the model and what elements require future work.

## 1.4 Research questions

This research focuses on deriving a model to predict the optimal solar energy efficient route for a solar vehicle. This is then tested to understand the accuracy of the model. The research question is:

**To what extent can a model predict the optimal solar energy efficient route for a solar vehicle?**

This question will be analysed as a whole as well as considering the answers to some research sub-questions:

1. To what extent can a model predict the average solar irradiance of a road segment at a defined time on a clear day or in cloudy weather conditions?
2. To what extent can a model predict the optimal solar energy efficient route for a solar vehicle on a clear day or in cloudy weather conditions?
3. How does the solar vehicle selected determine the feasibility of a self sustaining solar powered vehicle?
4. How can the model include a users desire for the most time efficient as well as the most energy efficient route?

## 1.5 Contributions of research

This research provides a method of solar mapping a road network that combines work done from previous research particularly in the areas of weather and vehicle type. This method can be applied to road networks in other cities. It could also be used to understand the potential of placing solar panels in other locations in the city such as on the road surface.

It also contributes a prediction model for solar vehicle energy consumed and used. This can be used in the field of hybrid vehicle analysis to better understand battery durations and charge for hybrid vehicles.

With increased research to improve the efficiency of solar panels and improve the structure of solar powered vehicles, this project will become more relevant. The benefits gained from using a more energy efficient vehicle will be multiplied by also choosing the most energy efficient route.

Outside of the area of research, this project has implications for car manufacturers and the community as a whole. Car manufacturers can understand better the impact of installing solar panels on the vehicle and encourage the transition to more renewable energy sources, thus impacting the decarbonisation of the transport sector. The community as a whole will benefit from the faster integration of solar vehicles in society. They can use the implemented application to choose the most solar energy efficient route for their vehicles and contribute towards a greener energy future.

## 1.6 Roadmap of project

This section defines the layout of this dissertation and includes what each chapter discusses and contains.

- **Chapter 2 - Background:** This chapter describes background information about tools and formulas used in this project. It details the current state of the art for this paper including sections on solar vehicle developments, solar mapping, weather impact, electric vehicle energy efficiency and SCORE(Solar Car Optimised Route Estimation).
- **Chapter 3 - Derivation of the prediction model:** This chapter explains the methodology behind creating the prediction model to calculate the average solar energy absorption along a strip of road. It highlights the importance of topography, time of day, time of year, vehicle type, weather and distance in this model.
- **Chapter 4 - Implementation:** This chapter discusses the user mobile application, Drive Solar, built to chose the solar energy optimised route. It discusses the way in which the data was handled and stored and the algorithms used for calculation. It also discusses the data management application built to make this project scalable for larger road networks.
- **Chapter 5 - Testing:** This chapter outlines the methodology used to test the accuracy of the prediction model. It discusses iterations and modifications to the testing structure.
- **Chapter 6 - Results and Discussion:** This chapter displays the results of the experiment and discusses the accuracy of the prediction model. It includes error analysis and recommendations for model and testing improvements.
- **Chapter 7 - Conclusions:** This chapter highlights the key findings of the experiment and analyses the effectiveness of the approach. It recommends and discusses how it could be improved in future works.

# 2 Background and state of the art

This chapter discusses the current state of knowledge surrounding solar energy in vehicles. It describes tools and algorithms used throughout this project. As well as this, the state of the art provides a review of related work and how they are relevant to this project.

## 2.1 Background

### 2.1.1 ArcGIS Tool

Geographical Information Systems (GIS) are a set of major tools used for combining spatial data sets and performing calculations. ArcGIS is a widely used software that has a variety of mapping capabilities to create and process large spatial databases. A variety of tools available in the ArcGIS package are used to process the spatial data required for this project. These tools are outlined in this section.

#### LAS Dataset to Raster tool

An LAS Dataset stores references to multiple LAS files. LAS files are the industry standard for storing airborne lidar data in binary format. A raster dataset is a set of compressed rows that are stored as pixels. Each pixel represents a characteristic of the mapped region. Raster datasets are more commonly used in ArcGIS and are a common format for input into other tools. This tool converts data from an LAS dataset into a raster dataset. This tool can specify what value field is used for the conversion and what form of interpolation is desired. The sampling value can be set to determine the definition of the raster dataset (6).

#### Area Solar Radiation tool

This tool uses a digital surface model in the form of a raster dataset to calculate the average solar insolation at each point in an area over a specific time interval. The global solar radiation is calculated by summing the total direct and total diffuse solar radiation. The total direct solar radiation is uninterrupted in a direct line from the sun whereas diffuse radiation is deflected off clouds, dust or other particles. Firstly, a view shed is calculated to understand where the point is shaded from. Next, a sun map is calculated to understand where the sun will be at the defined time. Diffuse radiation comes from all sky directions and thus a sky map is calculated and divided into sectors for better analysis. The viewshed, sunmap and skymap are then overlaid to calculate the direct and diffuse solar irradiation using the following formulas (7).

$$Global_{tot} = Dir_{tot} + Dif_{tot}$$

where $Global_{tot}$ is total global radiation,$Dir_{tot}$ is total direct solar radiation and $Dif_{tot}$ is total diffuse solar radiation.

$$Dir_{tot} = \sum Dir_{\theta,\alpha}$$

where $Dir_{\theta,\alpha}$ is the direct insolation at a solar map sector.

$$Dir\theta, \alpha = S_{Const} * \beta^{m(\theta)} * SunDur_{\theta,\alpha} * SunGap_{\theta,\alpha} * cos(AngIn_{\theta,\alpha})$$

where $S_{Const}$ is the solar constant outside the atmosphere ($1367W/m^2$), $\beta$ is the transmissivity of the atmosphere, $m(\theta)$ is the relative optical path, $SunDur_{\theta,\alpha}$ is the time duration represented by the sky sector, $SunGap_{\theta,\alpha}$ is the gap fraction of the sun map sector, $AngIn_{\theta,\alpha}$ is the angle of incidence between the centroid of the sky sector and the axis normal to the surface.

$$m(\theta) = EXP(-0.000118 * Elev - 1.638 * 10^{-9} * Elev^2)/cos(\theta)$$

where $\theta$ is the solar zenith angle and Elev is the elevation above sea level.

$$AngIn_{\theta,\alpha} = acos(Cos(\theta) * Cos(G_z) + Sin(\theta) * Sin(G_z) * Cos(\alpha - G_a))$$

where $G_z$ is the surface zenith angle and $G_a$ is the surface azimuth angle.

$$Dif_{\theta,\alpha} = R_{glb} * P_{dif} * Dur * SkyGap_{\theta,\alpha} * Weight_{\theta,\alpha} * cos(AngIn_{\theta,\alpha})$$

where $R_{glb}$ is the global normal radiation, $P_{dif}$ is the proportion of global flux radiation that is diffused, Dur is the time interval for analysis, $SkyGap_{\theta,\alpha}$ is the gap fraction of the sky sector and $Weight_{\theta,\alpha}$ is the proportion of diffuse radiation from a single sky sector relative to all other sectors.

$$R_{glb} = (S_{Const} \sum(\beta m(\theta)))/(1 - P_{dif})$$

$$Weight_{\theta,\alpha} = (cos\theta_2 - cos\theta_1)/Div_{azi}$$

where $\theta_1$ and $\theta_2$ are the zenith angles of the sky sector and $Div_{azi}$ is the number of azimuth divisions.

$$Dif_{tot} = \sum Dif_{\theta,\alpha}$$

The majority of these constants are set or calculated by the tool using the inputted raster dataset. The values that are set in this project are $P_{dif}$, $\beta$ and Dur. $P_{dif}$ and $\beta$ are set dependent on current weather conditions, in a very clear sky environment $P_{dif}$ is set to 0.2 and $\beta$ is set to 0.7. The time interval selected (Dur) is set in 15 minute intervals for each run (7).

#### Zonal Statistics as Table tool

Zones can be polygons, lines or points specified on a map layer to differentiate spaces. The 'Zonal statistics as Table' tool can calculate a variety of statistical values in relation to each zone such as mean, maximum, minimum and standard deviation. This tool can be used to convert a set of zones into a table where one column is the zone id and the other column is a mean value for this zone (8).

#### Table to Excel tool

The table to excel tool exports tables created in the ArcGIS application into excel files. This tool can be used to export the data and provide more suitability for graphing and processing (9).

## 2.2 State of the Art

This state of the art begins by highlighting current developments in the field of solar vehicles that would benefit from this project. It then continues to follow the development process of this project by discussing solar mapping, weather impact and energy efficient routes in electric vehicles. It concludes with the most relevant piece of work on solar car optimised route estimation that amalgamates work in the areas of solar vehicles, weather, mapping and energy efficiency. This state of the art is a sample of the work that has been done in the field and an analysis of its relevance to this project. The work highlighted provides a foundation for the choice of methods used in the implementation of this project.

### 2.2.1 Solar vehicle developments

The following section highlights recent developments and use cases in the solar vehicle industry that would benefit from optimised solar routing in urban and rural environments. Based on current viability of a solar vehicle, they are prominently being developed as hybrid vehicles. However, this can present challenges with energy management and charging frequency and often does not obtain the optimal amount of solar energy.

The five energy conversion components in a hybrid solar vehicle are internal combustion engine, electric motor, electric generator, battery and photovoltaic. Rachmanto created an energy balance equation to create decision making algorithms dependent on the vehicles current driving conditions and state of charge (10). The goal was to optimise the energy obtained through the photovoltaic and manage the other energy accordingly. The results showed that the energy management algorithm can reduce fuel consumption by 30% in comparison to that of a conventional vehicle. The photovoltaic delivers 0.6% of power supplied due to the current low efficiency of photovoltaic cells. There is still significant improvement that is needed to make solar vehicles widely used in urban environments.

One of the biggest problems with hybrid vehicles is that users are typically concerned about their driving range and plan to plug-in their vehicle whenever possible. With a solar vehicle however the solar energy is wasted when a vehicle is plugged in or at full capacity and more energy is taken from the grid. Habits around charging can be categorised into at-home only, at-work only or at-home and at-work each effecting the solar potential differently. In the scenario where the user charges the vehicle both at home and at work, nearly 80% of the available solar energy is wasted (11). With greater prediction models for solar energy while driving this solution could advise users when solar energy is plentiful or when they should consider charging their vehicle. This project supports this goal to reduce energy consumed by hybrid vehicles from the grid and optimise the solar energy potential using better prediction models.

There has been experimental research in the area that tested the effectiveness of a prediction model with a real-time experiment. There are many aspects here that can be tested such as energy consumption, solar forecasting or vehicular design.

Bai et al. (12) created a digital twin model of a hybrid solar vehicle to characterise the energy in the vehicle in order to optimise energy management. The hybrid vehicle consists of power battery system, electric drive system, steering system, braking system and driving system. Each system was modelled in the digital twin in a similar way to pure electric vehicles but also including the photovoltaic cell arrays, the solar inverter and the power battery pack. The experiment was run over a period of 30 minutes across an athletic track and resulted in a 5.17% difference from the digital twin to the experiment. This can show the effectiveness of digital prediction and the accuracy it can have to real world scenarios.

Oosthuizen developed the Gridded Model Output Statistics (GMOS) Global Horizontal Irradiance (GHI) model which uses historical data to reduce the average root mean squared of solar energy forecasting by 11.28%, making the model more accurate than previous solutions (13). The model uses four cities in South Africa to predict the model. As a testing ground Oosthuizen used the Sasol Solar challenge 2018 and confirmed that the GMOS model could have improved the accuracy of the state of charge of the vehicle and analysed the possible range benefits. This project will use similar models for weather forecasting predictions and analyse its effectiveness.

A solar powered E-rickshaw has been designed and used in rural India to conduct last mile transportation (14). Through analysis and testing of aerodynamic design and different positioning of the solar panel on the vehicle, Nadimuthu confirmed that with the new aerodynamic design there was a 60% increase in speed and that the solar panel gave maximum average peak power of 90W. Nadimuthu confirmed that this solution was feasible as a more sustainable option for last mile delivery. This broadens the scope to another type of vehicle that could benefit from solar optimisation routing as well as demonstrating feasibility and effectiveness. It also shows the importance of designing an efficient solar vehicle which is discussed as a major topic in this project.

Solar vehicles emphasise a wide range of complex problems from hybrid energy management to weather forecasting to aerodynamic design as highlighted in this relevant work. However it is also evident that the range of applications for these vehicles is vast and minor improvements in solar predictions as demonstrated in this project can greatly affect the efficiency of many other solar vehicle projects. This forms the basis for building the solar energy prediction model.

### 2.2.2 Solar mapping

Solar Mapping is the first stage required to develop the prediction model in this project. With increased use of photovoltaic cells on roofing or in open spaces the importance of mapping and predicting solar energy has increased. Researchers have taken a variety of different models to improve these predictions and minimize error. This section will discuss some of these methods, the different inputs used and the results found.

Lobaccaro et al (15) performed solar potential analysis of buildings in Sluppen, Norway. The 6 step approach outlined in Fig. 2.1 shows how they used an urban map analysis to select optimal buildings for photovoltaic cells. A similar approach will be taken to map the solar potential of roads in Dublin. Following this method the road maps can be extracted and analysed for different vehicles travelling the route.

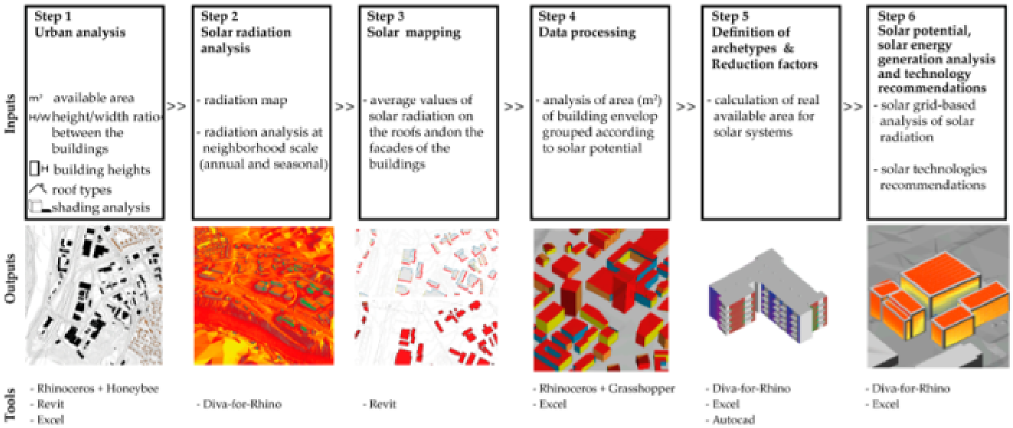


Figure 2.1: Lobaccaro's 6 step solar mapping approach

Another case study was performed across southern India to create maps and explore the solar energy potential across the region (16). The model used satellite given solar data and temperature data over the course of a year. This data was used to produce a series of maps to support business decisions. This shows that it is possible to take other inputs such as temperature and understand its influence over the prediction maps. This work encouraged the consideration of weather impact on solar mapping and how this may effect the outcome of this project.

Hai et al (17) take another approach and use an extreme learning machine (ELM) based prediction model. Unlike others, this is characterised as a method that can reach more remote locations and predict both short term and long term solar irradiance data. Using daily meteorological data as the input, they developed seven ELM models with unique neuronal architectures. The results found that the optimal ELM model produced a root mean squared error of 3.28 $Wm^2$ in comparison to 4.24 $Wm^2$ for a multiple linear regression model. Using machine learning as a model requires a significant amount of historical data to train the model. This project will not incorporate historical data and thus this is not an appropriate model. This is however an interesting consideration to develop future work on.

Wergertseder created a series of models for solar resource mapping (18). Wergertseder's model, unlike previous models, was built on an integrated solar resource and energy consumption approach. They followed a series of steps outlined in Fig. 2.2 to create solar maps of buildings with hourly-time and seasonal-time resolution. This high level of resolution is an advantage of this research as it analyses the impact in detail and not as an average value for the year. The tools used also included ArcGIS, to look at building topology and solar radiation, which is what will be used in this piece of work.

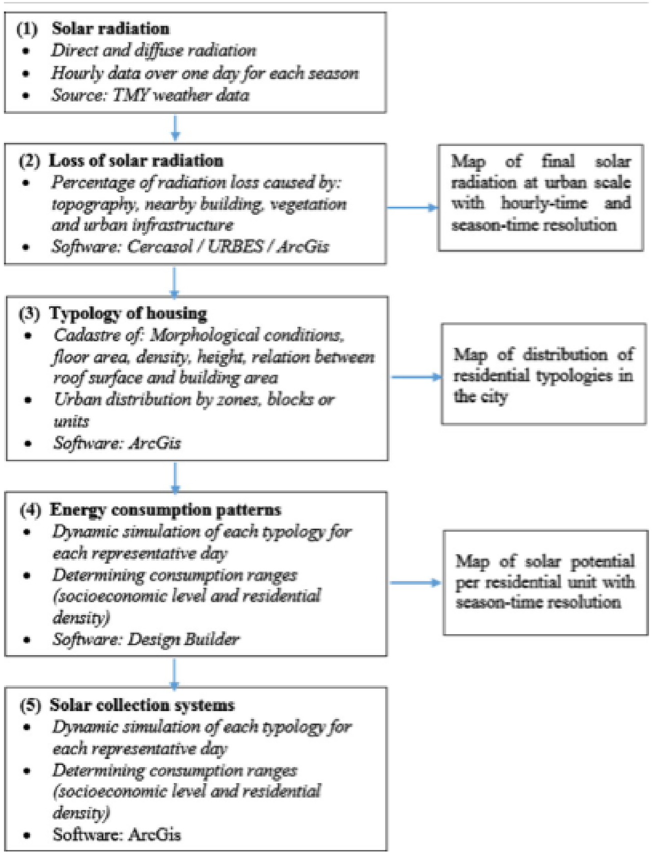


Figure 2.2: Wergertseder's solar mapping approach

Solar mapping technologies and methods have been well researched with solutions including, machine learning, multiple input sources and point of view calculations. This project will incorporate Lobaccaro's 6 step approach in combination with Kumar's weather inclusion to produce weather sensitive solar maps of the road network in Dublin. The way to include this weather information can be further developed through other related works.

### 2.2.3 Impact of weather on solar irradiance

Once the solar irradiance values are calculated from the solar map generated, the weather impact can be analysed and included in the model. Weather conditions can greatly impact the solar energy consumption of photo-voltaic cells as suggested by Kumar in section 2.2.2. This will affect the prediction model for understanding the most optimal route. Research has been conducted in the area to understand and measure this impact which can be used to create more accurate prediction models.

Cloud cover is considered the measurement with largest effect on solar energy consumption. Park presented a paper (19) which used machine learning models to estimate cloud cover from a series of images and thus predict the solar irradiance. The machine learning models were found to be effective at identifying cloud cover and the following formula was used to calculate solar irradiance, where the maximum solar irradiance is the irradiance recorded in clear sky conditions:

$$\textit{solar irradiance} = (1 - \textit{cloud cover ratio}) \times \textit{maximum solar irradiance}$$

This is a successful model and the machine learning algorithms used are very effective at identifying cloud cover. This project focused less on the impact of clouds on solar irradiance and more on identifying clouds. This may not be the optimal solution for understanding the impact of cloud cover on solar irradiance.

On the other hand, Nevins tested this theory over a 3 year period to understand the impact of cloud cover on solar irradiance and deduced that it was a non-linear relationship (20). Using the data collected over 3 years and taking into account the time of day and time of year Nevins used machine learning models to develop a prediction formula which is quadratic.

$$y = 1 - 0.00243x - (4.24 \times 10^{-5})x^2$$

where y is the fraction of clear sky solar irradiance and x is the percentage cloud cover. This formula is tested using a very large dataset and thus is considered to be accurate with a test mean squared error of less than 30%. For this reason this is the formula that will be used to include cloud cover in the prediction calculations.

Bonkaney discusses the impact of dust and cloud cover on solar irradiance through the months of May, June, July and August (21). This research produces graphs illustrated in Fig 2.3 that show the inequalities in solar irradiance on cloudy days directly showing the impact of scattered cloud cover.

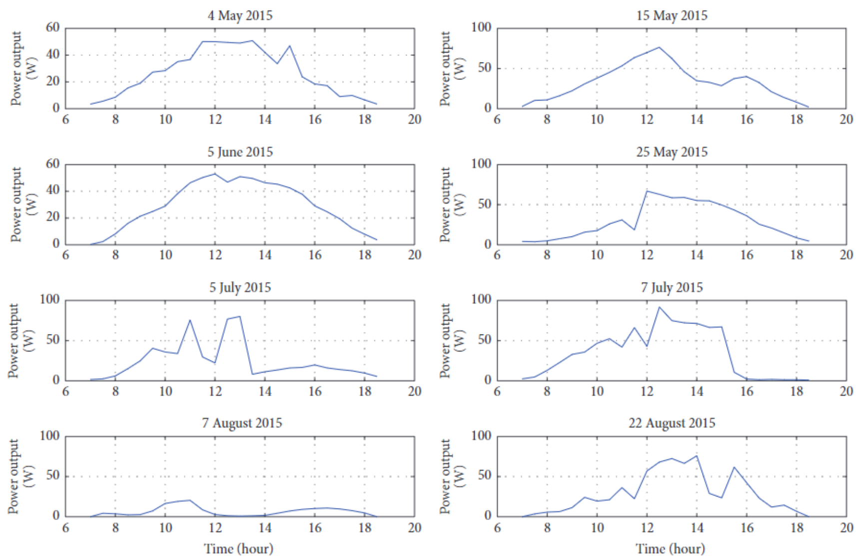


Figure 2.3: Bonkaney's solar irradiance profiles corresponding to cloudy days

As well as this Bonkaney brings to the fore the impact dust can have on solar irradiance which has the potential to reduce the daily energy yield by 15%. This is a point that should be specified to users to ensure these optimal routes are being used to their greatest potential by encouraging users to frequently wash the solar vehicle. The uneven distribution of graphs in Fig. 2.3 also suggests that predicting the solar energy on a route in cloudy conditions may not be feasible due to the ever-changing environment.

Research has been conducted to understand the effect of wind on solar consumption. Waterwoth conducted a study on Westmill solar park in Oxfordshore that showed that southerly winds were increasing the energy output by 20.4-42.9% in comparison to northerly winds (22). This is an interesting finding for static solar parks however due to the movement of solar vehicles and the wind turbulence within a city environment, direction and wind speed are difficult to predict. Consequently, wind will not be considered as a determining factor in this project.

This project will use Nevins formula $y = 1 - 0.00243x - (4.24 \times 10^{-5})x^2$ to calculate the impact of cloud cover on the solar irradiance predicted from the maps. This in combination with solar mapping sets the base solar irradiance values that can be used to calculate the energy efficient shortest route.

### 2.2.4 Energy efficient shortest route problem

Solar vehicles face similar problems to electric vehicles in terms of calculating the most energy efficient route. Electric Vehicles are faced with the problem that the battery life is shorter than desired and thus the most energy efficient route is desired to reduce energy loss from the battery. Research has been conducted in many different areas to improve this problem and thus encourage the use of electric or hybrid vehicles. A prevalent area of research is to calculate the most energy efficient route taking into account elevation gain, stop-start and congestion. This is similar to the weighting of energy consumption in a solar vehicle. This research contains detail on the issues faced when calculating energy optimal routes as well as finding solutions for the most feasible route taking into account distance, parking, battery power and stop-start.

A weighted graph can be used to show energy consumption for each edge in a road network. De Cauwer et al. (23) and Strehler, Merting, and Schwan (24) used this solution and compared the energy efficient, distant efficient and time efficient routes based on the proposed algorithm. The findings concluded that in many cases the optimal energy route was a significant increase in time, up to 170%. This time energy priority will be implemented in the application of this research to directly meet the needs of users.

Storandt (25) had similar findings but focused not only on calculating the most energy efficient route but taking into account the extra time or distance required to travel the route. The research used bounded distances, feasible paths and limited reloading. Similar to the optimisation of solar energy routing it is vital to take into account that even the most eco-friendly of drivers may not drive three times the distance to save energy. Thus the concept of bounding and limiting the feasible distances, can also be applied to solar routing in this project. This further emphasises the need for a time vs energy priority feature in the application so users can decide how much extra time they are willing to spend to save energy.

Sachenbacher et al. (26) discusses the main problems with applying a generic shortest route solution to this problem. Firstly, as it is possible for EVs to recover kinetic energy on deceleration, there is the possibility that the route edge would have a negative value. Secondly, the computations can be challenging and dependent on live constraints that cannot be preprocessed. Thirdly, considering battery power there can be complications dealing with the constraints of a full or empty battery. All of the above problems are prevalent in the route optimization of solar vehicles and thus could follow a similar solution. With some energy optimisations these problems could be solved using Johnson's algorithm as well as the A* search algorithm with a complexity of $O(n^2)$.

Repeated stop-start of a vehicle wastes a significant amount of energy, thus optimal energy routes can be those that minimise deceleration and acceleration. Liu et al.(27) looks at energy optimised routing from a different point of view with connected and automated vehicles (CAVs). The result was that with the automated network the energy efficient route was 15% more efficient than the normal route however without automation there was no significant difference. When applied to a solar vehicle this stop-start prediction would be ineffective without a traffic configuration aspect and thus will not be considered in this project but is highlighted as an area for future work.

Alizadeh et al. (28) , Arslan et al. (29) , Merting et al. (30) , Lee et al. (31) focus on the shortest route for EVs based on recharging locations. A similar logic can be applied to optimal parking for a solar vehicle.

This project will use work done in this area particularly when looking at a time vs energy priority. A* algorithm and Johnsons algorithm have been chosen as a potential solution for the most energy efficient route algorithm.

### 2.2.5 Solar Car Optimised Route Estimation

Building on the work described in solar vehicle development, solar mapping, weather impact and energy efficiency, this most relevant piece of work amalgamates the ideas to create Solar Car Optimised Route Estimation (SCORE). SCORE is a practice developed by Hasicic et al. to optimise a route for solar powered cars. This has the goal of increasing the amount of energy consumed based on historical recordings from a test fleet of vehicles (32). Hasicic et al. have developed preliminary algorithms to solve this problem and analysed the effect of their solution in a series of papers that will be discussed in this section. This is the most relevant related work and will provide a base-line for the work conducted in this project.

In their initial paper they discuss the main objectives of the proposed project (32). The solar data is collected using mobile transmitter sensors on vehicles in the city and the data is sent and fused onto a local server. However these mobile transmitter sensors are light detection sensors, not solar irradiation sensors. The results can be skewed by streetlights, headlights and any other form of non-solar light. This inaccuracy will be improved upon in this project by using solar irradiation sensors to test the accuracy of the solution.

Hasicic also proposed using CAD and GIS software to predict solar radiation at certain locations as well as incorporating the local sunshine forecasts. However the amalgamation and calculations surrounding this data were considered out of scope for this paper.

The proposed solution was expanded upon in 2016 (33) to focus more on the amalgamation of the online and offline data, as well as how Dijkstra's algorithm was used. This uses a standard defined solar car in combination with the SCORE algorithm to calculate how much energy would be absorbed on a piece of road and uses this to create the edges for Dijkstra's graph. However, this does not consider that the length of a road and the traffic can contribute to the amount of energy used by the vehicle. With an evaluation of energy usage over distances these graph edge calculations can be made more accurate. This project will incorporate energy used and transform the potentially negative edges using Johnson's algorithm.

They implemented a SCORE system in a vehicle using TI's ARM Cortex-M4F based TM4C123G LaunchPad so the user could enter a destination and the device could collect information from the server and provide the user with the optimal solar route. A similar solution is implemented in this project but on a mobile application so the research is more easily accessed by users.

The results found that the difference in consumption on a solar optimized route is less than 5% based on their currently defined standard solar car. However, with improving technologies the efficiency of solar panels has been increasing and will have a bigger impact when SCORE is applied. The other aspect of this paper, analysed which parking spots were optimal for solar power consumption and results showed that this makes a significant difference to the energy absorbed. A higher priority should be placed on having a sunnier parking spot rather than a parking spot chosen for proximity.

Their next paper (34) focuses more on the details and algorithms for incorporating historical data. This focuses on prioritising more recent values in a closer time frame. The significance of each data point is rated based on recency, time of day and season. This paper will expand on this by having data for solar irradiance at every location, at any time of year and then incorporate the sunshine forecast on top of this value. Using data from a different day or time can have a dramatically different result especially in more diverse climates. Focusing on the prediction from baseline points rather than previous recordings will produce more accurate results. They also incorporated improvements to their parking algorithm by considering the fact that users are less likely to walk a longer distance to their destination from the parking spot. This is included in this project using a time vs energy priority in the application.

In their most recent paper (35), not only do they discuss the experiment but also the effect that a widely accessible SCORE system would have on a smart city. The biggest concern is that with widespread information about the most optimal solar routes, there will be increased congestion and parking density in these areas. These solar optimal zones will still only be able to accommodate a set number of solar vehicles even with increasing demand. They propose a solution to this problem in a city with some SCORE users and some non-SCORE users. This solution provides incentives such as good parking spots or free charging stations for non-SCORE users to take less attractive routes, leaving the well insolated routes for SCORE users.

There are some additional limitations to the SCORE model which will be addressed by this project. Firstly all calculations are based on a standard size vehicle and there is no consideration for alternative modes of transport such as a solar bus or a solar van. With larger surface area for solar panels there is a potential for a dramatic increase in solar consumption with an optimized route. Secondly, although local forecasting and GIS software are mentioned, there is no specifications into how it is incorporated in the calculations. This report will expand on this and provide clear solutions so it can be used in future work. Thirdly, the algorithm does not take into account energy used along an edge. This will be improved in this project and Johnsons algorithm will be used to counteract potentially negative weights. Finally, Hasicic focuses on using historical data based on a test fleet of drivers. This only is practical in an area where this historical data is available. In this project a generic prediction model that can be applied to any location will be created. This will then be tested to understand the accuracy of the prediction model.

## 2.3 Summary

This project will create a body of work that is unique as it will focus on including energy used along edges, accurate weather prediction, vehicle type and generic digital surface data that can be applied to any location. The ArcGIS tool has powerful mapping capabilities that will be used throughout this project to aid in creating the prediction model.

This project will use work conducted by others to create a well researched prediction model. It will follow Lobaccaro's 6 step approach (15) and incorporate Nevins (20) formula to predict solar irradiance base on cloud cover. It will use similar techniques for analysing energy efficient routes as currently explored for electric vehicles such as time vs energy priority and the use of Johnsons algorithm in combination with A*. All of these algorithms will create a solid baseline for an accurate prediction model for the most solar energy efficient route. A summary of this state of the art with relevance to this project can be seen in Table 2.1

| **Section** | **Relevance** |
|---|---|
| Solar Vehicles | Similar strategy for prediction and testing models, sets current state of technology |
| Solar Mapping | Adapts Lobaccaro's 6 step approach (15) to use for a road network |
| Weather Impact | Uses Nevin's formula for effect of cloud cover on solar irradiance (20) |
| Energy Efficiency in electric vehicles | Uses Johnsons algorithm and time vs energy balance |
| SCORE | Builds on SCORE by incorporating vehicle type, weather predictions and generic solution that can be applied to any location |

Table 2.1: Summary of State of the art

# 3 Derivation of the prediction model

This chapter discusses the methodology used to derive the equation to predict the average solar energy consumed by a solar vehicle along a road segment. Elements such as shade from surrounding topography, weather, vehicle type, distance and time of day are all taken into account.

## 3.1 Road network and length

A sample road network was selected in Dublin City as a testing ground for this project. This road network consisted of 30 nodes (road junctions) and 57 edges (road segments). A map of the nodes selected in Dublin city and their labels can be seen in Fig. 3.1.

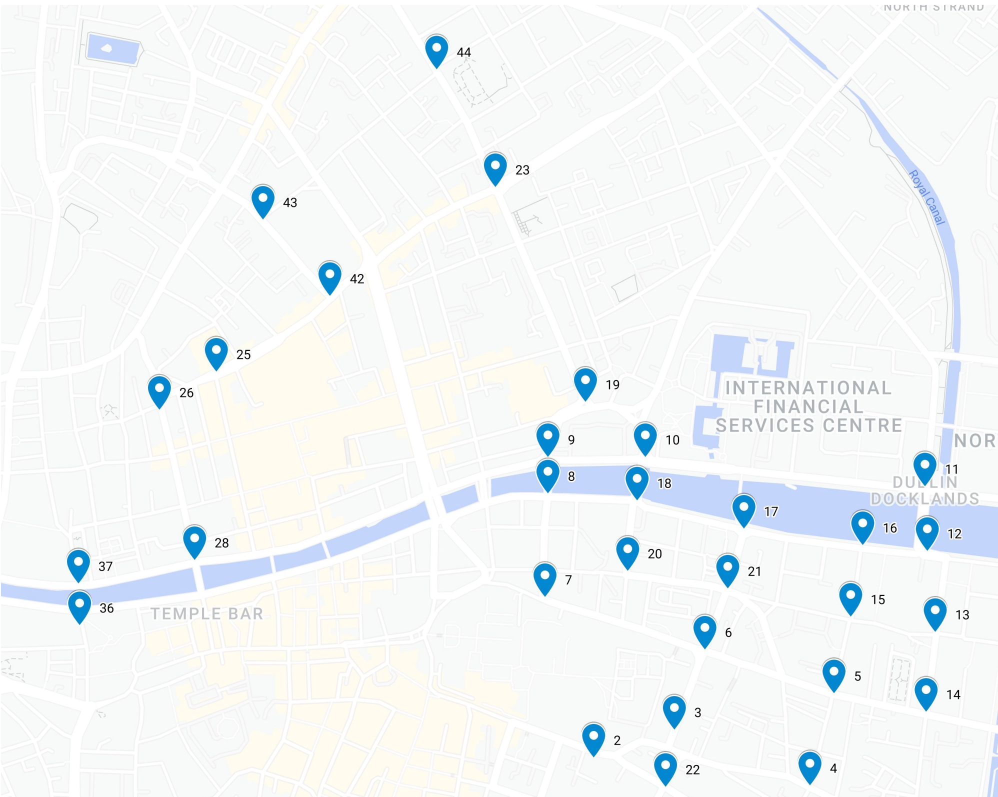


Figure 3.1: Map of nodes and edges used as sample road network

The sample was chosen as it represented a built-up environment and provided strong variation in topography. The road segments along the River Liffey were included to show the impact of less infrastructure. This created a well balanced dataset that included different environments. The size of the road network was chosen so it could be driven in its entirety in a one hour period, for testing purposes, that will be discussed in more detail in Chapter 5.

Each node was given an identification number and each edge was labeled 'node1Tonode2.' For example, the road segment connecting node 8 to node 36 along the River Liffey was labelled '8To36'. For two way road segments an edge was added for each direction.

The latitude and longitude of each node was recorded using google maps and used to calculate the distance between two nodes. This distance calculated between two nodes is an approximation of the length of the road segment. This does not take into account dramatically curved road segments but is a good approximation for the purpose of this project. The formula used to calculate this length is:

$$a = sin^2(\Delta\varphi/2) + (cos\varphi_1 \times cos\varphi_2 \times sin^2(\Delta\lambda/2))$$

$$c = 2 \times atan2(\sqrt{a}, \sqrt{(1-a)})$$

$$d = R \times c$$

where $\varphi$ is latitude, $\lambda$ is longitude, R is earth's radius (mean radius = 6,371km) and angles are in radians. d is defined as the length of a road segment in the road network. Each edge is assigned the value d based on the latitude and longitude of its corresponding nodes.

## 3.2 Shade and time of day calculations

This section outlines the next step in deriving the prediction model. It describes the creation of a solar map with average solar irradiance values for a set of specific time intervals. This process follows a similar approach to Lobaccaro (15) as discussed in Section 2.2.2 but applied to road calculations instead of buildings. This approach is outlined and discussed in this section.

- Step 1: Urban analysis -> Gather digital surface model
- Step 2: Data conversion -> Convert Li-DAR data to raster
- Step 3: Solar mapping -> Create solar maps using ArcGIS tool
- Step 4: Solar radiation analysis -> Average solar radiation values for road segments
- Step 5: Clear sky solar irradiance -> Table of clear sky solar irradiance values

### 3.2.1 Urban analysis

A digital surface model is an elevation model that captures an environment's natural and artificial features. This is required to understand how shade impacts the solar irradiance at any one point.

A Li-DAR point cloud is a collection of 3D points over a space gathered by a laser scan. Each point contains x,y,z coordinates as well as a timestamp and a laser intensity value. This is a commonly used method for creating a digital surface model of an area.

Laefar et al.(36) conducted an aerial laser and photogrammetry survey of a section of Dublin city. This was carried out using a TopEye System across 41 flight paths as displayed in Figure 3.2. The interval between each path flight was 100m so that, with the flights taking place at 300m altitude, each point would be recorded 6 times. This created a set of 1.4 billion laser points. The section highlighted by the red line in Fig. 3.2 represents the area specified in the survey.

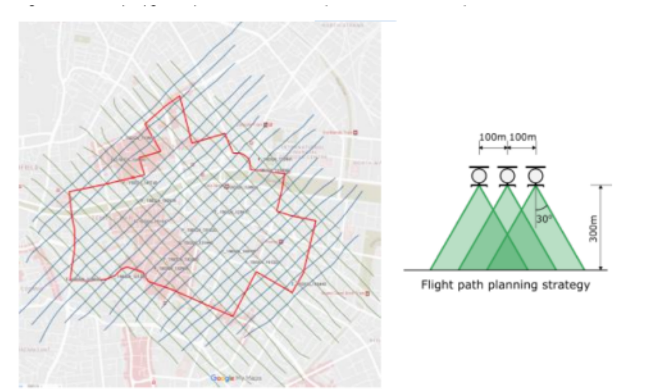


Figure 3.2: Flight paths of aerial laser photogrammetry

The output available from this survey is a set of 78 LAS files each containing the points for a small section of the city. This point cloud was used to create a digital surface map of a section of Dublin city. This aligns with the defined road network to create a local test site for this project.

### 3.2.2 Data conversion

The Li-DAR point cloud data was stored as 78 individual LAS files and were required to be converted into a raster dataset in order to be processed into a solar radiation map. These files were imported into the ArcGIS tool which is also used by Wergertseder (18). The data chosen covers an area approximately from Grand Canal Dock to Smithfield and from Phibsborough to Harcourt Road. This can be seen clearly in Fig 3.3 where the red squares represent the outer limits of the data available in each file.

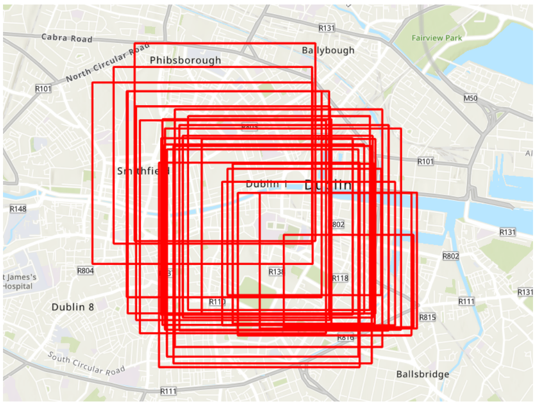


Figure 3.3: LAS files where each square shows the outer bounds of the data for that file

These LAS files were combined by creating an LAS dataset and adding each file. This combines the data into a set that can be visualised as elevation points. This more detailed view can be seen in Fig. 3.4. Each small circle represents an elevation point recorded using Li-DAR.

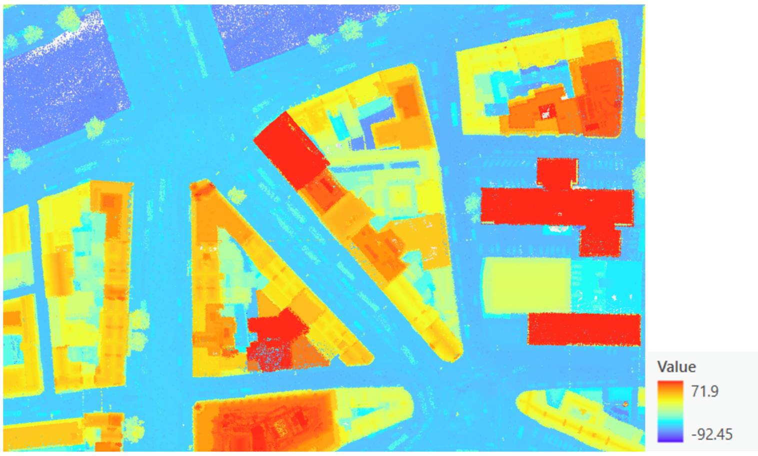


Figure 3.4: Digital surface model at intersection of D'Oiler street and O'Connell Bridge

This LAS dataset could then be converted to a raster data set using the 'LAS Dataset to Raster Conversion' in ArcGIS as discussed in Section 2.1.1. This raster dataset can be seen in Fig. 3.5 The blurred sections around the edges of this raster dataset are due to some outlying data and are considered invalid. The road network is contained to areas that are well defined by the raster dataset.

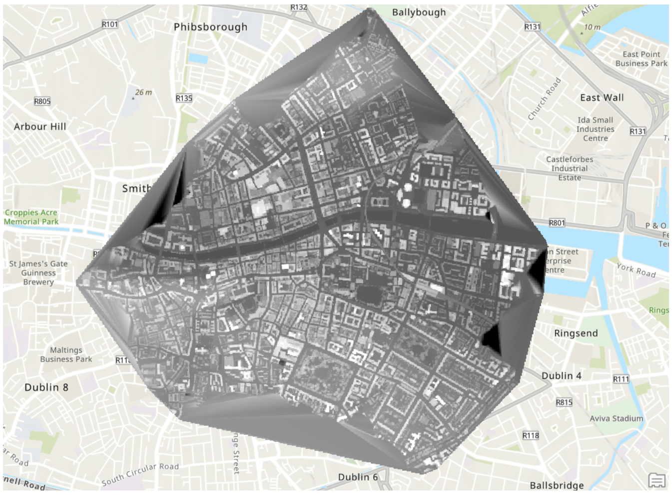


Figure 3.5: Raster dataset of the digital surface model

### 3.2.3 Solar mapping

The ArcGIS software contains the Area solar radiation tool which can calculate the solar irradiance at any point on a map based on atmospheric effects, site latitude and elevation, slope and aspect, daily and seasonal shifts of the sun angle, and effects of shadows cast by surrounding topography as described in Section 2.1.1. The very clear sky solar irradiance was set to have a diffuse proportion of 0.2 and a transmittance of 0.7 as recommended by the documentation (7). Using this tool the raster dataset was converted to a solar radiation map for all required time intervals. An example of this can be seen in Fig. 3.6. Further examples are included in Appendix A1.

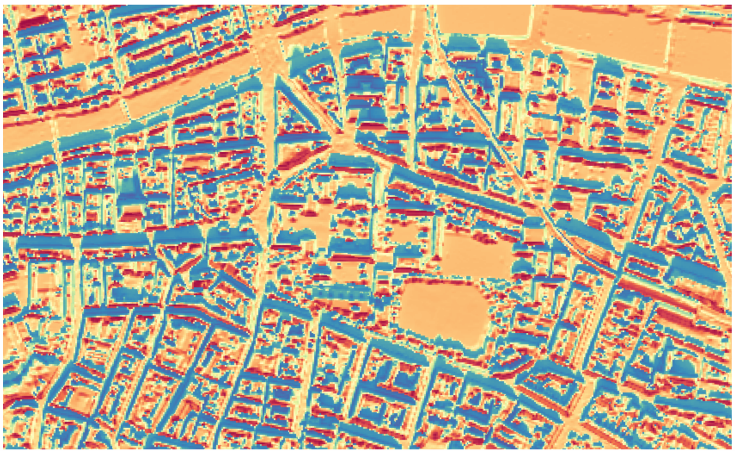

Figure 3.6: Solar map around Trinity College at 11am on March $26^{th}$

### 3.2.4 Solar radiation analysis

Using the Area Solar Radiation tool, maps have been created to show the solar potential across the test area. This solar radiation data needed to be extracted to have average solar irradiance values for each edge in the road network.

ArcGIS allows for the creation of zone data using points, lines or polygons. The roads in the test area were marked using the line tool where each line corresponded to a road edge. The road network represented by zones in the ArcGIS tool can be seen in Fig 3.7.

Figure 3.7: Zonal data recorded over raster dataset

The 'Zonal statistics as Table' tool described in Section 2.1.1 is used to calculate mean solar irradiance values across each edge.

The output table was converted to excel using the 'Table to Excel' tool as described in Section 2.1.1. A sample output table can be seen in Table. 3.1 where the object ID can be matched to an edge in the road network to give the mean solar irradiance along that edge.

| Object ID | Count | Area | Mean |
|---|---|---|---|
| 1 | 60 | 540 | 24.79939006 |
| 2 | 62 | 558 | 21.87171907 |
| 3 | 143 | 1287 | 33.03402524 |
| 4 | 90 | 810 | 23.69199403 |
| 5 | 139 | 1251 | 35.9053963 |
| 6 | 182 | 1638 | 34.06577532 |
| 7 | 77 | 693 | 13.10691821 |
| 8 | 31 | 279 | 26.72527707 |
| 9 | 77 | 693 | 28.35710293 |
| 10 | 92 | 828 | 23.56586856 |

Table 3.1: Sample data for 10 edges produced by the 'Zonal Statistics as Table' tool

### 3.2.5 Clear sky solar irradiance

In order to create a prediction model that can be tested, this process needed to be repeated for multiple time intervals over a variety of days. The model created in the first iteration used time intervals over a one hour period. This seemed feasible and practical to test a large set of nodes within an hour interval.

Further analysis was conducted to understand the change in solar irradiance within the hour to determine if this time interval was sufficient. It was found that the average solar irradiance on a single road could vary by $\pm 60 Wh/m^2$ within the hour. For this reason the prediction interval was changed to be 15 minutes in duration.

The most accurate outcome would be to have an instantaneous prediction model however this is not feasible. Firstly the large amount of data would be too large to store or manage for very little change in accuracy. Secondly, if recording a car's journey, it is not going to be accurate to the minute so a 15 minute interval is feasible for a short journey within Dublin city centre. This 15 minute interval was checked again and it was found that the error was only $\pm 6 Wh/m^2$ from the instantaneous value to the value within the interval.

The overall outcome from this data was a large table that included mean clear sky solar irradiance values for each edge at 52 different 15 minute time intervals. This data is used as the average solar irradiance of an edge at the time requested.

## 3.3 Weather impact

Weather can greatly impact the solar irradiance for solar panels as discussed in previous research highlighted in Section 2.2.3. This is another aspect that is included in the prediction model.

The Open Weather API (37) was chosen to use live and forecast weather data to improve the accuracy of the optimisation algorithm. This was chosen as it is an openly available API that has 90-100% accuracy. The Open weather system uses machine learning algorithms to combine data from 82,000 weather stations globally which include national meteorological agencies, radars and weather satellites. This data is added to the NWP (Numerical Weather Prediction) and combined to produce an API that can provide current and forecast weather data accurate to 500m. Dublin is one of their central cities so this tool fits the needs of this project.

The API can provide weather information for the current time or forecast minutely for 1 hour, hourly for 48 hours or daily for 7 days. It returns a JSON file with variables such as clouds, temperature and humidity. The variable used in this prediction model is cloud cover as studies show this has the greatest impact on solar energy absorption. Temperature, humidity and wind were also considered as potentially influencing factors as discussed by Waterwoth (22) however all of these factors would also be influenced by the motion of the vehicle and heat generated by the engine. For this reason, cloud cover was selected as the only influential weather factor in this project.

The impact of cloud cover on solar irradiance is derived using the formula created by Nevins (20). This formula was chosen due to the large amounts of data recorded over a 3 year period which is discussed in more detail in Section 2.2.3.

$$y = 1 - 0.00243x - (4.24 \times 10^{-5})x^2$$

y represents the fraction of clear sky solar irradiance available and x is the percentage cloud cover. Combining this with the shade and timing data, the current formula for solar irradiance is shown below, where z is the clear sky solar irradiance at the time selected, that was calculated in Section 3.2 and x is the percentage cloud cover.

$$Solar\ irradiance = (1 - 0.00243x - (4.24 \times 10^{-5})x^2) \times (z)$$

## 3.4 Vehicle type

The predictive model so far has focused on the solar irradiance that would be provided to the roof of the vehicle. This section looks at understanding how much energy can be absorbed from this solar irradiance and how much energy is used while travelling a certain distance in a particular vehicle. This section defines a formula to calculate the energy absorbed and the energy consumed by a particular vehicle on a road edge. This section will analyse the features of four types of solar vehicles and how they can be implemented into the prediction model.

### 3.4.1 Lightyear one

Lightyear one is a solar car that is leading the market with its family sized solar vehicle. It is planning to be in production in late 2022 and released in 2023 which confirms the motivation for this project at this time. One of the strong reasons it is leading the market is due to the fact that it only consumes 83 Wh/km (1).

The design mimics that of a modern car with emphasis on expanding the surface area to contribute to the solar absorption. This deisgn can be seen in Fig. 3.8 The solar panels span approximately $5m^2$ and have an efficiency of 20-22% (1).

Lightyear one's chassis is not made up of composites, it is a monocoque. The load bearing structure is made of aluminium skins that are joined using rivets and adhesive bonds (1). This design is crucial to create light structures and prototype rapidly. It is also the main reason the vehicle can run using only 83 Wh/km.

Figure 3.8: Lighyear one solar vehicle

### 3.4.2 Aptera motors

Aptera motors have created a solar vehicle that redesigns current perceptions of a car as seen in Fig. 3.9. Using a three wheel structure and a smooth body the Aptera solar vehicle is 65% more efficient than other vehicles today and dramatically reduces the drag coefficients. The focus is on efficiency in all aspects and Aptera have managed to reduce the energy consumed by the vehicle to 100Wh/mi which is equivalent to 62Wh/km. With this efficiency the Aptera solar vehicle can support 40 miles per day of free driving powered by the sun (2).

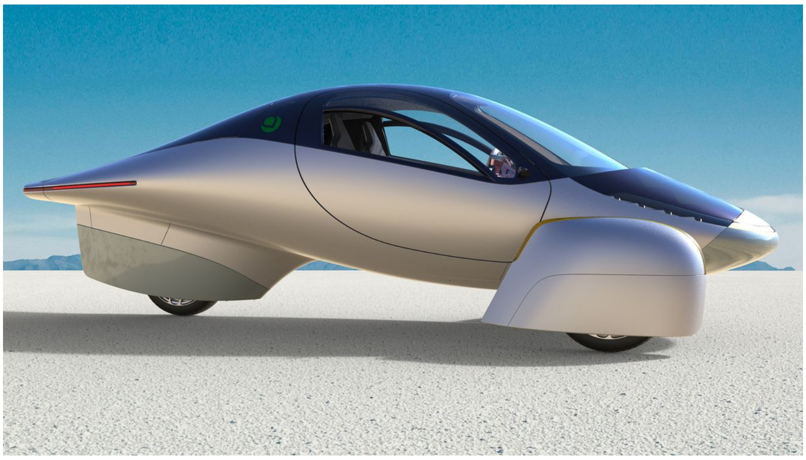

Figure 3.9: Aptera solar vehicle

### 3.4.3 Solar bus

Solar buses have been implemented by Flixbus (38) and Solar Bus Pro (39) by adding solar panels to the roofs of already existing electric buses. This reduces the fuel consumption but is not prioritising relying on 100% solar energy. The efficiency or fuel characteristics of the bus have not been changed and it is still consuming approximately 1kWh/km (4).

Myeongchan Oh proves that this is an inefficient model and it will not be possible to have a solar bus that uses no other form of alternative energy (3). This project will also analyse the feasibility of solar buses. However as seen with Lightyear one and Aptera, a vehicle can be greatly adapted and redesigned to optimise energy usage. With a solar bus, the structure could be adapted to support minimal air resistance, solar panels could be added not only on the roof but on the sides to optimise energy absorption near sunrise or sunset and the weight of the model could be reduced to optimise energy usage. With these adjustments to a solar bus, it may become feasible to operate this vehicle using solar power only.

### 3.4.4 Solar van

Currently solar panels on vans are only used to support the energy needs if a person is living in the van. This adds to the energy generation to power kitchens, lights or other utilities. Currently there is no research that directly discusses the impact of using a self-sustaining solar van. For this study a model of a van will be used based on figures from other solar vehicles and the current energy consumption of an e-van. An e-van typical uses 300Wh/km and has a roof size of approximately $9m^2$ (40). This could support a solar panel area of approximately $8.7m^2$. Similar to the solar bus, this model does not take into account aerodynamic modifications to the vehicle, thus will likely use more energy than it absorbs.

### 3.4.5 Contribution to prediction model

A summary of the values discussed for each vehicle can be seen in Table 3.2.

| Vehicle | PV area ($m^2$) | Peak (Wh) | Efficiency | Energy used (Wh/km) |
|---|---|---|---|---|
| Lightyear one | 5 | 1000 | 20-22% | 83 |
| Aptera | 3.15 | 700 | 20-22% | 62 |
| Solar Bus | 22.62 | 2290 | 20% | 1000 |
| Solar van | 8.7 | 1500 | 20% | 300 |

(40)

Table 3.2: Standard values for solar vehicles

Using these values an approximation of the solar energy absorbed and consumed by the vehicle on a particular edge in the road network can be calculated using the formulas:

$$\textit{Solar energy absorbed} = \textit{solar irradiance} \times \textit{area} \times \textit{time} \times \textit{efficiency}$$

$$\textit{Solar energy consumed} = (\textit{solar irradiance} \times \textit{area} \times \textit{time} \times \textit{efficiency}) - (\textit{energy used} \times d)$$

## 3.5 Summary

The combination of data and formulas discussed in Sections 3.1 to 3.5 make up the predictive model. Firstly, the distance is calculated where $\varphi$ is latitude, $\lambda$ is longitude, R is earth's radius (mean radius = 6,371km) and angles are in radians.

$$a = sin^2(\Delta\varphi/2) + (cos\varphi_1 \times cos\varphi_2 \times sin^2(\Delta\lambda/2))$$

$$c = 2 \times atan2(\sqrt{a}, \sqrt{(1-a)})$$

$$d = R \times c$$

Next the table of clear sky solar irradiance values is used to find the value that corresponds to the specified time of day and road edge. This clear sky solar irradiance value is represented by z in $W/m^2$.

Next the cloud cover (x) at a specific time is extracted from the Open weather API. This is incorporated into the following formula to get the fraction of clear sky solar irradiance (y).

$$y = 1 - 0.00243x - (4.24 \times 10^{-5})x^2$$

The fraction of clear sky solar irradiance (y) is multiplied by the clear sky solar irradiance (z) in $W/m^2$ to get the solar irradiance (i) in $W/m^2$.

$$i = z \times y$$

This value for solar irradiance (i) in $W/m^2$ and the distance (d) in meters are combined with the vehicle information to provide solar energy absorbed and the solar energy consumed. In these equations A is the area of solar panels on the vehicle in $m^2$, e is the efficiency as a percentage and w is the energy used in Wh/km.

$$Solar\ energy\ absorbed(Wh) = i \times A \times t \times e$$

$$Solar\ energy\ consumed(Wh) = (i \times A \times t \times e) - (w \times d)$$

The values calculated using these equations are compared with test data to understand the effectiveness of the predictive model.

# 4 Implementation

The prediction model was implemented into a mobile application so that users can input desired parameters to understand the optimal route to take from point A to point B in their solar vehicle. A data management application was also created for processing and setting up data so that this can be applied to other locations. This chapter will discuss how these applications were implemented by discussing the data, the routing algorithms, the mobile application and the data management application.

## 4.1 Data

Transfer, storage and management of data is a crucial part of any application. The predictive data is in a graph data structure with nodes being road junctions and edges being road segments. It is important to store large amounts of data on the cloud to reduce storage required for the application. It is not scalable to store the data within the application if the intention is for it to grow to many more cities with all times of the year. This section discusses how the data is stored on the cloud for this application.

### 4.1.1 Graph databases

Originally a graph database seemed like the optimal solution for storing the road network. A graph database such as Neo4j is designed to focus on the relationships between nodes and allow for easy traversing from node to node.

Neo4j is a native graph database that manages data in its more naturally connected state, which allows for lightning fast queries and a modifiable data model. For use in the applications it was required to be compatible with Swift, the language used to code the applications. Neo4j is community supported with Swift and unfortunately most of this documentation is out of date and is not well supported. Another consideration was that each road edge will have a wide array of values including solar potential for multiple time intervals, time, direction and distance. With so many attributes there are other more optimal options for storing this data.

### 4.1.2 Document databases

A document database is a data store that uses JSON documents to store data instead of rows and columns. The advantage of a document database is that it is schema less. This schema less structure is an advantage for this road network, because as the application scales, data can be added for direction, lanes and traffic flow which will be different for each edge and therefore require a schema-less structure.

As well as this document databases are easy to maintain and set up. The document database does not deal with foreign keys to display relationships like relational databases. For these reasons, a document style database was chosen for this road network.

### 4.1.3 Firebase

Google Firebase is a well established and well supported document style database. It is designed for the development of mobile and web applications. It includes features such as authentication, google analytics, machine learning and testing that can be implemented into the application as it scales. This was chosen as an optimal database and app support platform for this application.

The Firebase database was set up with two collections; nodes and edges. The node collection kept track of the nodes which are the junctions and stored information such as latitude and longitude as seen in Fig. 4.1. In future this would also store junction traffic configurations.

```
{
  "nodes":{
    "11": {
      "latitude": "53.3428",
      "longitude": "-6.2578"
    }
    "12": {
      ...
    }
  }
}
```

Figure 4.1: Sample data in nodes collection

The edges collection keeps track of the edges, which are the road segments, and stores variables such as distance, predicted energy at specific times or days and average time as seen in Fig. 4.2. In future this would also store lane information and current and future traffic conditions.

```
{
  "edges": {
    "11To12":{
      "From": "11",
      "To": "12",
      "Average_time(s)": 166.16,
      "Distance(km)": 0.689 ,
      "Mar26_7": 29.912,
      "Mar26_7_15": 31.78,
      "Mar26_7_30": 33.456,
      "Mar26_7_45": 33.375,
      "Mar26_11": 69.735
      ...
      "Mar27_7": 26.713,
      ...
    },
    "12To13": {
      ...
    }
  }
}
```

Figure 4.2: Sample data in edges collection

### 4.1.4 Architecture

The architecture for this project is highlighted in Fig. 4.3. This shows how the data management application and the user mobile application interact with the Firebase database. Data is also transferred from the Open Weather API and ArcGIS.

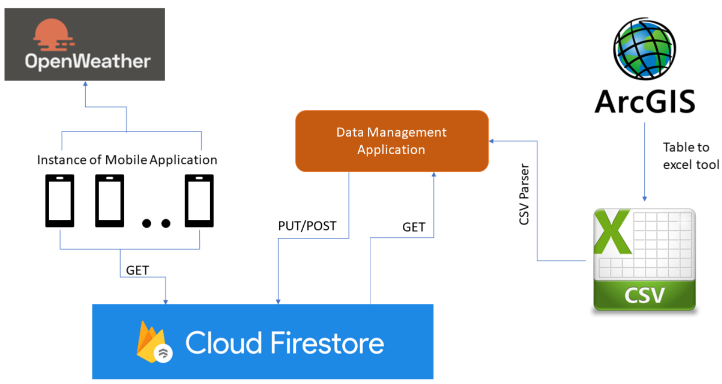


Figure 4.3: Architecture diagram

## 4.2 Implementation algorithms

Once the data had been stored in the database, the next step was to choose a set of algorithms to calculate the most energy efficient route from the database. This section describes how the data graph was designed and what algorithms were used to find the most energy efficient route.

### 4.2.1 Graph design

Each graph edge is calculated using the negative of the formula derived in Chapter 3. The negative is chosen so that the algorithms can be used to minimise the energy consumed instead of maximising the energy absorbed.

$$Edge\ value = (w \times d) - (i \times A \times t \times e)$$

where i is the solar irradiance in $W/m^2$ taking into account weather, time of day, date and shade, d is the length of the edge in Km, A is the area of solar panels on the vehicle, e is the efficiency of the solar panels, t is the time needed to travel the road segment and w is the energy used by the car in Wh/km.

Once each graph edge was calculated, it was evident that there were some negative edge values and thus many shortest route algorithms cannot be used to solve this problem. Sachenbacher highlight a similar problem for electric vehicles (26). The solution to this involved transforming the graph using Johnson's algorithm to convert the weights so that they are all positive values. Once this transformation was complete standard shortest route algorithms such as Dijkstra and A* could be used to solve the problem.

### 4.2.2 Bellman Ford algorithm

The Bellman ford algorithm is used to calculate the shortest path for graphs that include negative weights. This is used within Johnsons algorithm and thus is required for this application. Bellman Ford is outlined in Algorithm 1.

**Algorithm 1** Bellman Ford Algorithm

$\forall v \in V, d[v] \leftarrow \infty$
$\pi(v) \leftarrow nil \forall v$
$d[s] \leftarrow 0$
**for** $i$ *from* $1 \rightarrow n-1$ **do**
  **for** $(u, v) \in E$ **do**
    $d[v] \leftarrow min\{d[v], d[u] + \omega(u, v)\}$
    $\pi(v) \leftarrow u$
  **end for**
**end for**
**for** $(u, v) \in E$ **do**
  **if** $d[v] > d[u] + \omega(u, v)$ **then**
    *return "Negative Cycle"*;
  **end if**
**end for**
*return* $d[v]\ \forall v \in V$

### 4.2.3 Johnsons algorithm

Johnsons algorithm is used to transform the weights of a graph that includes negative values into all positive values as suggested by Sachenbacher (26). This uses the Bellman ford equation to calculate the shortest distance to a new node and then labels each node with this potential. The new weight of edge (u, v) is original weight + potential(u) - potential(v). The algorithm for computing this is outlined in Algorithm 2.

**Algorithm 2** Johnson's Algorithm

*compute* $G'$, *where* $G'.V = G.V \cup \{s\}$, $G'.E = G.E \cup \{(s, \nu) : \nu \in G.V\}$, *and* $\omega(s, \nu) = 0$ *for all* $\nu \in G.V$
**if** $BELLMAN - FORD(G', \omega, s) == FALSE$ **then**
  *print " Input had negative weight cycle"*
**else**
  **for** *each vertex* $\nu \in G'.V$ **do**
    *set* $h(\nu)$ *to the value* $\delta(s, \nu)$ *computed by the* $Bellman - Ford$ *algorithm*
  **end for**
  **for** *each edge* $(u, \nu) \in G'E$ **do**
    $\hat{\omega}(u, \nu) = \omega(u.\nu) + h(u) - h(v)$
  **end for**
  *let* $D = (d_{u,\nu})$ *be a new* $n \times n$ *matrix*
  **for** each vertex u $\in G.V$ **do**
    run DIJKSTRA($G.\hat{\omega}, u$) to compute $\delta(u, \nu)$ for all $\nu \in G.V$
    **for** each vertex $u \in G.V$ **do** $d_{uv} = \delta(u, \nu) + h(v) - h(u)$
    **end for**
  **end for**
  return D

### 4.2.4 Dijkstra algorithm

Dijkstra's algorithm is an uninformed shortest path algorithm that guarantees the optimal solution on a positive directed weighted graph. This was implemented as an initial solution outlined in Algorithm 3. This solution finds the optimal path but requires a large expansion of nodes. For this reason an improvement of A* is suggested.

**Algorithm 3** Dijkstra's Algorithm

$\forall v \in V, d[v] \leftarrow \infty$
$\pi(v) \leftarrow nil \, \forall \, v$
$d[s] \leftarrow 0$
**for** $i$ *from* $1 \rightarrow n-1$ **do**
  **while** $G.V \neq \emptyset$ **do**
    u = EXTRACT-MIN(G.V)
    $S = S \cup \{u\}$
    **for** each vertex $v \in G.Adj[u]$ **do**
      **if** $d[v] > d[u] + \omega(u, v)$ **then**
        $d[v] = d[u] + \omega(u, v)$
        $\pi[v] = u$
      **end if**
    **end for**
  **end while**

### 4.2.5 A* algorithm

A* is an informed optimal shortest route algorithm that guarantees the optimal solution in a positive directed weighted graph. A* functions using the process outlined in Algorithm 4.

**Algorithm 4** A* Algorithm

$\forall v \in V, f[v] \leftarrow \infty$
$\forall v \in V, g[v] \leftarrow \infty$
$\pi(v) \leftarrow nil \, \forall \, v$
$f[s] \leftarrow 0$
$g[s] \leftarrow 0$
**for** $i$ *from* $1 \rightarrow n-1$ **do**
  **while** $G.V \neq \emptyset$ **do**
    u = EXTRACT-MIN-f(G.V)
    $S = S \cup \{u\}$
    **for** each vertex $v \in G.Adj[u]$ **do**
      **if** $f[v] > g[u] + \omega(u, v) + h[v]$ **then**
        $f[v] = g[u] + \omega(u, v) + h[v]$
        $\pi[v] = u$
      **end if**
    **end for**
  **end while**

This differs from Dijkstra's algorithm in the fact that it is informed by a heuristic. A heuristic is designed to be an estimate of the minimum cost from each vertex to the goal.

In this implementation, the heuristic was calculated as the distance in kms from the destination to each node. This is an approximation of which node will have lowest energy usage as those with shorter distances will likely use less energy. The heuristic was calculated using the latitude and longitude of the destination and each edge using the formulas highlighted in Section 3.1.

This algorithm requires additional computation to be done in advance of the search to set up heuristics based on the destination node. Once completed the A* algorithm explores less nodes than Dijkstra's algorithm. This is set as the default solution in the mobile application; 'Drive Solar'.

## 4.3 Drive Solar: User mobile application

The application 'Drive Solar' is an IOS mobile application that aids users in finding the most optimal solar route for their solar vehicle. It takes user inputs of source, destination, date, time, vehicle type and time/energy priority to insert into the prediction model. The app calculates the optimal route and displays the energy consumption for that journey. Other factors such as weather are also displayed to the user to inform them why the values may differ from previous searches. The 'Drive Solar' app takes a simple functionality approach and could be adapted to provide more user friendly features such as map UI, saved routes, default values etc. The current User interface of drive solar can be seen in Fig. 4.4.

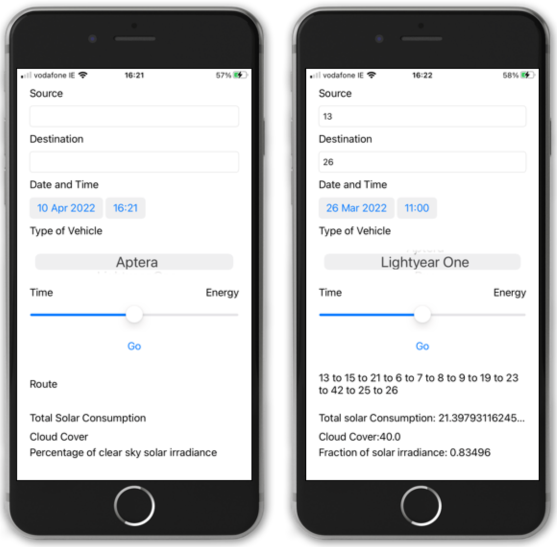


Figure 4.4: User Interface of Drive Solar before and after search

### 4.3.1 Objectives

The app was developed on XCode and can be used on any IOS device that has IOS 14.0 or greater. The objectives of the application are to:

1. Create a user friendly app that allows the user to know the optimal route for their solar vehicle from point A to point B.
2. Incorporate vehicle type, date, time and time vs energy priority as variables that can be adjusted by the user.
3. Display to the user the optimal route to be taken and the total solar consumption that their vehicle is predicted to absorb along that route.
4. Show the impact of weather so the user can understand the benefits of travelling in sunnier conditions.

### 4.3.2 Code structure

The mobile application consists of a main view controller with supporting classes as can be seen in the class diagram in Fig. 4.5

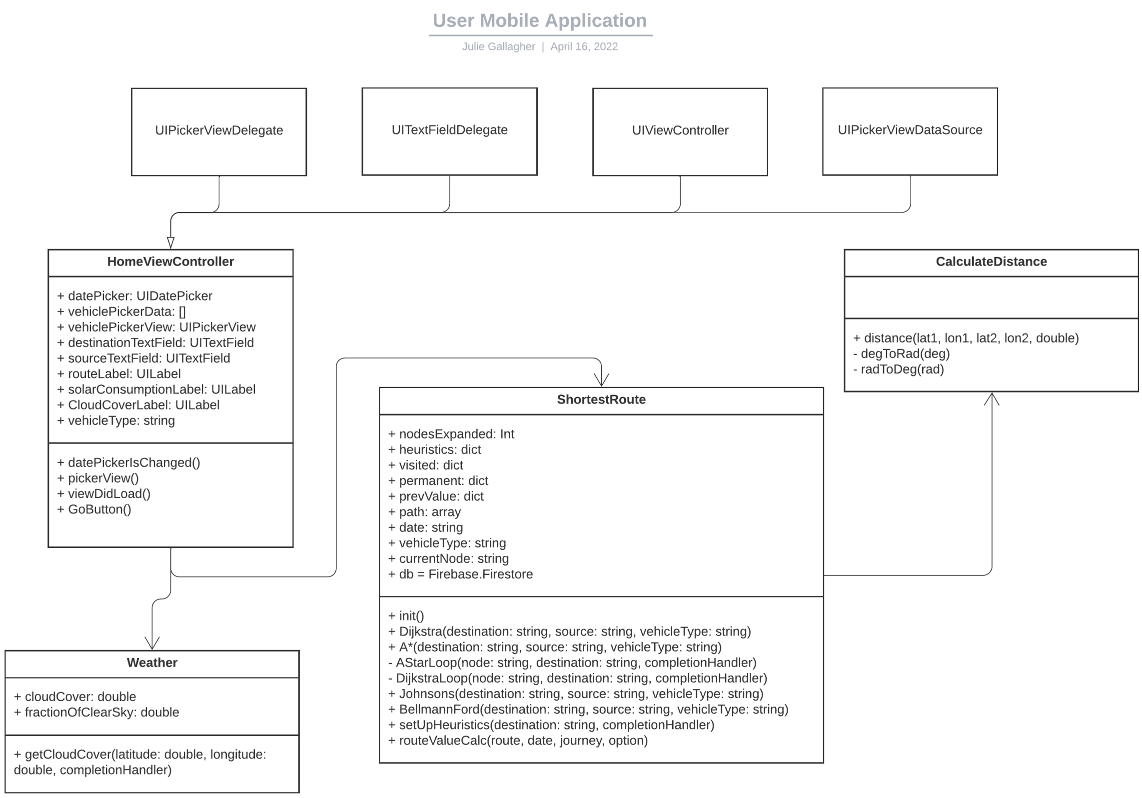


Figure 4.5: User mobile application class diagram

### 4.3.3 Inputs

The inputs entered into the app are determined by the user and provide the elements necessary to calculate the solution from the predictive model.

#### Source and destination

The source and destination can be entered using a text field. Currently, the values inputted are required to be a number corresponding to one of the labeled nodes as seen in Fig. 3.1. If the destination is not reachable using the sampled road network the model will return 'No route'

#### Date and time

The user can select a date and a time using a calendar picker. Currently there is a finite list of dates and times that are available to select. This is due to the fact that a prediction model using the ArcGIS tool requires new maps generated for each time interval. The data available is a sample set for prediction and testing purposes. In future an API would be created to convert a digital surface model with a date and time into the solar potential values for a road network.

#### Vehicle type

A user can select which vehicle they are using with a picker object. The currently available options are Lightyear one, Aptera, Solar Bus or Solar Van. This selection would be expanded to include search functionality for any solar vehicle in the database. The search would return the area, energy used and efficiency values necessary for the prediction model.

#### Priority of time vs energy

The time vs energy priority discussed in Section. 2.2.4 highlights the need to balance the time taken to travel the journey with the energy gained. This is highlighted as a major problem in electric vehicles by Storandt (25), Strehler (24) and De Cauwer (23).

This naturally is included in the prediction model to some extent by including that increased distance, increases the energy used. This has a large influence on the data at the moment due to the current lack of efficiency in solar panels. However, as technology progresses the energy used will have less of an impact and the energy absorbed will have more. For this reason bounded distances would need to be an option for the prediction model.

The user has the option to input their time energy priority preference. With the slider set to energy the algorithm will calculate the most energy efficient route. With the slider set to Time the most distance efficient route is selected. In the centre, the algorithm first calculates the shortest distance route and then bounds it by adding between 0-30% depending on the position of the slider. Then while calculating the most energy efficient route, if the distance is more than the bounded amount then that option is eliminated. This way the most energy efficient route will be selected without increasing the distance by more than a set amount

### 4.3.4 Outputs

The application displays the results of the search to the user with any additional information they may be interested in.

#### Optimal route

The optimal route calculated by the prediction model is displayed. This currently is in the form of a list of nodes that connect the route. This could be improved by providing a map output that displays the route clearly that they can then use to follow driving instructions.

#### Solar energy consumption

The app also outputs the solar energy consumption for that selected optimal route. This output is what is used for testing the accuracy of the prediction model against real-time data.

#### Weather

The weather conditions are also outputted to inform the user of temporary influences over this route calculation. The cloud cover and the fraction of clear sky solar irradiance are displayed. For this reason, a user may chose to travel on another day or at another time if weather conditions improve. This can be tested by inputting future dates and seeing the outcome.

### 4.3.5 Calculation

When the user selects the Go button, the app begins performing the calculation for the optimal route from the selected source to destination under current weather, data and vehicle conditions. It combines the algorithms described in Section. 4.2 to choose the optimal route. This process is demonstrated using a sequence diagram in Fig. 4.6.

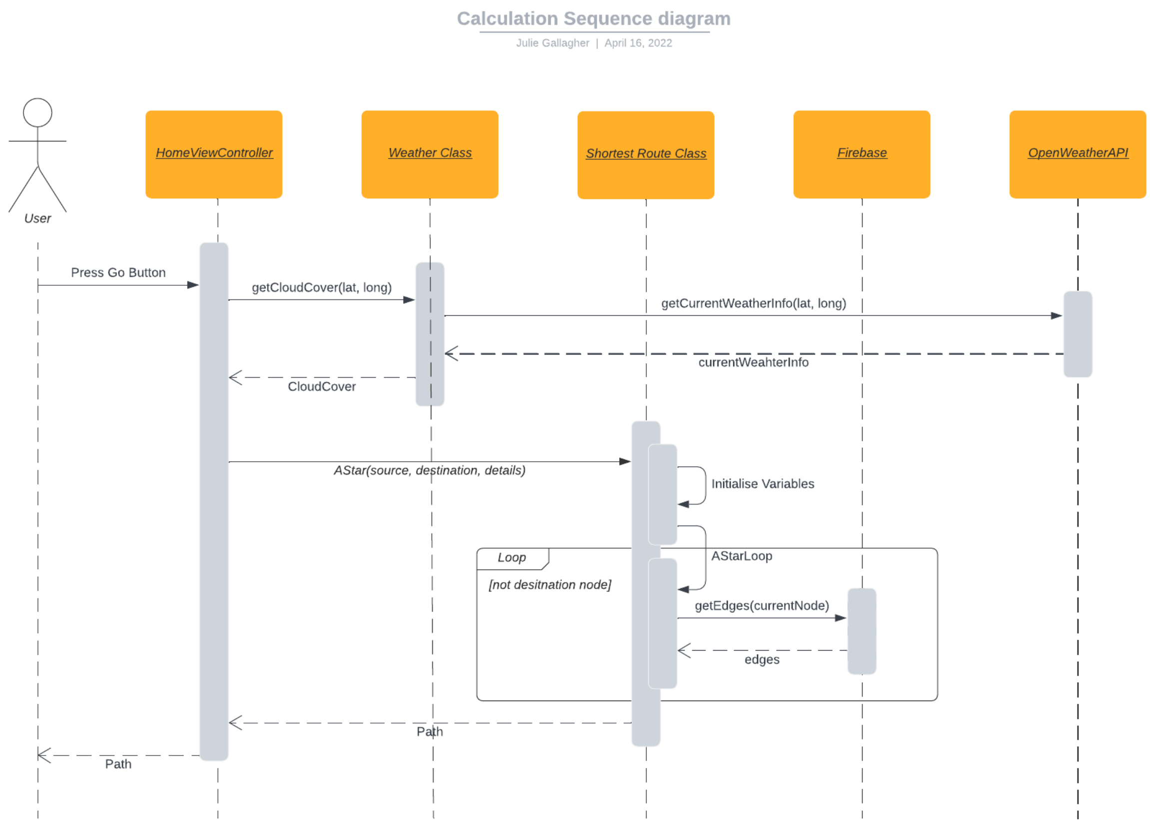


Figure 4.6: Sequence diagram when a user wants to calculate the most energy efficient route

## 4.4 Data Management application

The data management application is designed to control the data processes required for this project. It allows for setting up and reorganising the database. It has functionality for data analysis required for this project.

### 4.4.1 Objectives

This application was also developed in XCode to keep consistent with the user application. It is designed to run on IOS 14.0 or greater. The objectives of this application are to:

1. Set up database by adding nodes and edges in the road network.
2. Import data from CSV files generated by ArcGIS to add predicted solar irradiance values to the database.
3. Perform route calculations to compare solar absorption values with different input parameters.
4. Extract data into CSV files for further analysis.
5. Perform statistical analysis for average dates and upload distance calculations.

### 4.4.2 Code structure

The application centres around a home view controller that has a series of buttons that can be used to initiate any process. This is also supported by additional classes similar to the user mobile application. This structure can be seen in the class diagram in Fig. 4.7.

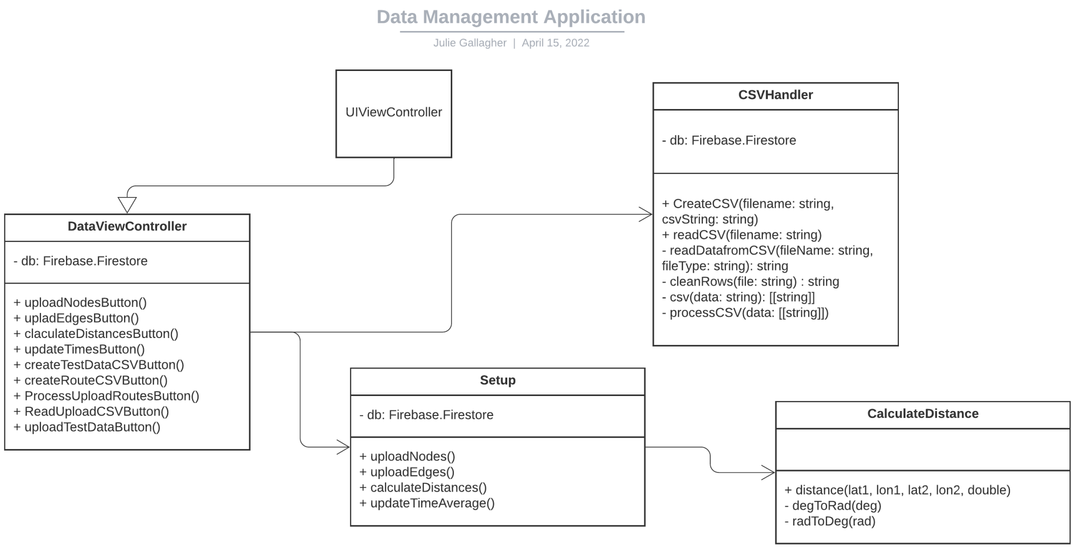


Figure 4.7: Data Management Class Diagram

### 4.4.3 Functions

This section will describe a subset of the functions available in this application. This gives an indication of the kind of calculations it can perform. Other functions not listed here can be seen in the class diagram in Fig. 4.7.

#### Upload nodes and edges

When a new city or location is being added in the road network, the new nodes and edges must be added to the database. This function takes a list of nodes with their longitude and latitude values and a list of edges and uploads them to the database to add new cities to the road network.

#### Read and upload ArcGIS data

This function processes the CSV file containing the predicted clear sky solar irradiance values that is produced by the ArcGIS application. It reads the data in the file and uploads the predicted solar irradiance values for each time interval. This process is represented in a sequence diagram in Fig. 4.8.

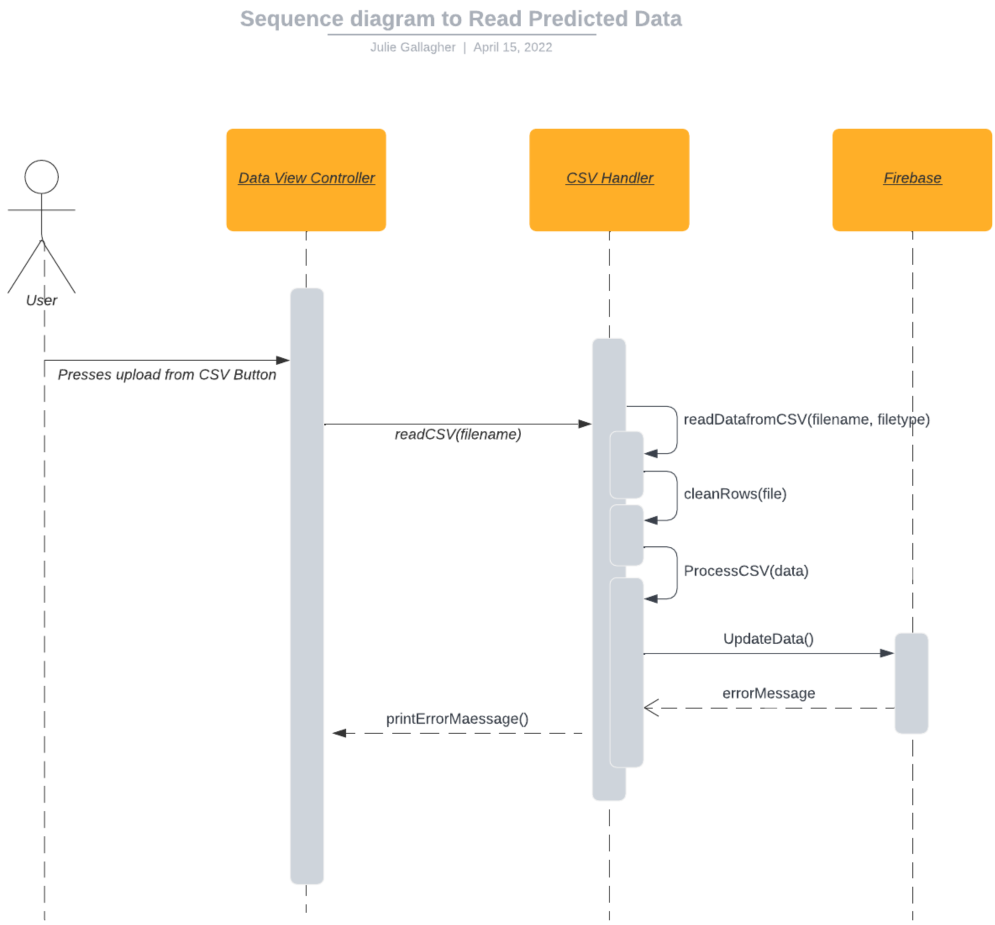


Figure 4.8: Sequence diagram for reading the predicted data from a CSV file

### Create CSV file for route data

When analysing the data, it was necessary to create a CSV file that had tested and predicted values for different routes at different time intervals. This function calculates the solar absorption for a set of routes highlighted in an array. It can be repeated over an array of dates if also required. This is then processed and uploaded into a csv file that can be used for further data analysis.

## 4.5 Summary

The data for this application was stored in a Firebase document database to reduce storage within the application. This data was managed, calculated and controlled by an application that could be used to expand the dataset for different locations or times.

The mobile application 'Drive Solar' has been implemented to provide users with the opportunity to find the optimal route to travel from point A to B in their solar vehicle. This takes user inputs of source, destination, date, time, vehicle type and time vs energy priority.

It outputs the optimal route to travel as well as the amount of solar energy absorbed by the vehicle along that route.

The most energy efficient route algorithms required Johnson's algorithm which includes Bellmann Ford algorithm to transform the graph weights to all positive values. This could then be analysed using Dijkstra and A* to find the most energy efficient route. A* was used as the default in the mobile application to calculate the optimal route while reducing the number of nodes explored.

# 5 Testing methodology

The prediction model and implementation are based on theoretical values. To check that this is an accurate solution testing was conducted to compare the predicted value to the real value. This chapter discusses the testing methodology for multiple iterations to collect the most realistic data to compare against the prediction model. It also discusses how routes were selected to analyse the accuracy of the model in different conditions.

## 5.1 Planning

In advance of recording the final data, it was important to understand the route and timings of the experiment. This ensured that when the data was being recorded no time delays occurred due to routing or other external factors.

### 5.1.1 The Route

The road network being used for this experiment was decided upon in Section 3.1. For each test, the complete set of edges needed to be travelled. Planning this route required considerations for one way streets and one way traffic junctions.

This was planned using a combination of visual configuration and google maps. A route was planned visually to ensure each edge was travelled during the route without excess repetition. Google maps was then used to map edge to edge using Google's 'stops' feature. This ensured that all one way street and traffic configurations were accounted for.

In advance of the first test day, a test route was driven to ensure the route was correct. This test run encountered some road works and areas of excess traffic. The route was adapted again to account for these issues in advance of test day. The route took 55 minutes on this test day which was within the hour as predicted. The final map with all edges that were travelled can be seen in Fig. 5.1.

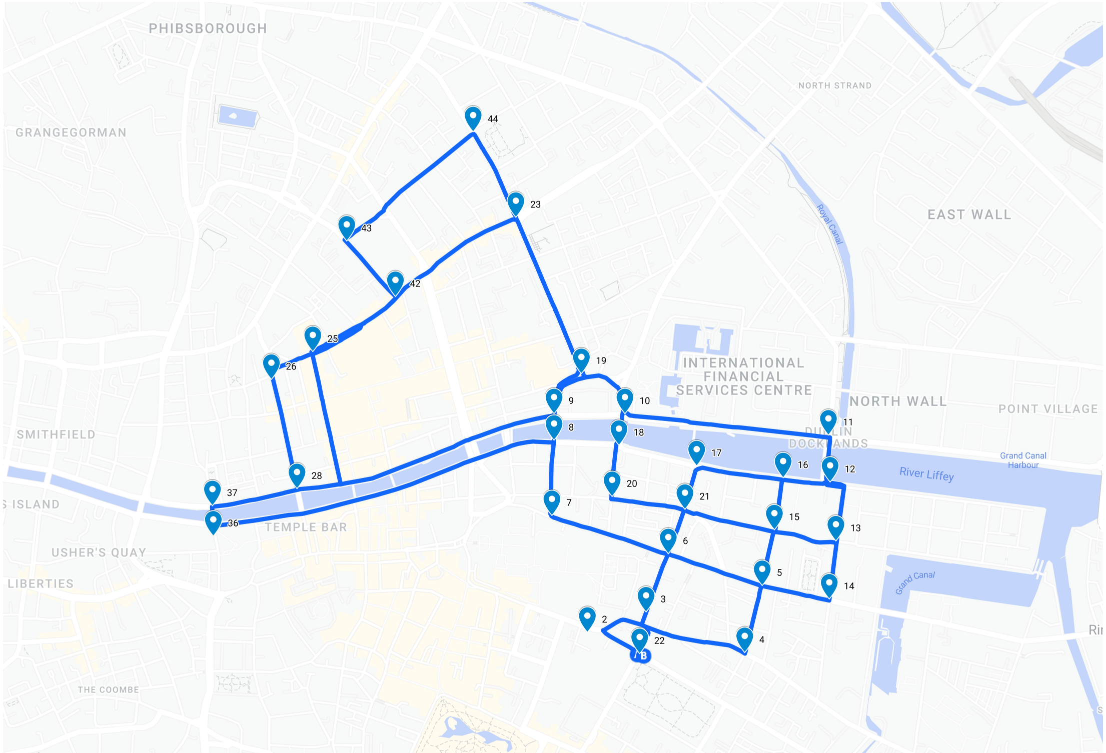


Figure 5.1: Final set of edges

### 5.1.2 Test timing

The test schedule was designed to analyse how effective the prediction model was in a variety of different conditions. The goal was to test two sunny days and two cloudy days. This provides sufficient data in each condition to support conclusions as well as including diverse weather conditions.

For each day of testing, 3 recordings were taken. The recordings began at 07:00 UTC, 11:00 UTC and 15:00 UTC. These time intervals showed variety in the angle of the sun with one set just after sunrise, one set at peak sun and the other a few hours before sunset. Each recording took approximately one hour, but traffic meant that this varied slightly with each recording. By mapping each edge into 15 minute intervals, the delay due to traffic had minimal impact on the results. If the recording ran over an hour, an extra 15 minute interval was added to the prediction set.

The days selected for sunny weather recordings were the $26^{th}$ and $27^{th}$ of March. The days selected for cloudy recordings took place on the $2^{nd}$ and $3^{rd}$ of April. These were recorded at the weekend to try, as much as possible, to eliminate error due to traffic. The times were also selected to avoid rush hour traffic. This kept all recordings between 45 minutes and 1 hour and 15 minutes.

## 5.2 Iterations

The test data was recorded in 2 iterations, as the first iteration had errors that greatly effected the outcome of the data. The methodology was modified for the second iteration to remove these errors.

### 5.2.1 Iteration 1

As there was no access to a solar vehicle, a solar irradiance sensor was used to understand how much solar irradiance the car would receive. The sensor used was the RS PRO Solar Power Meter ISM400. This could be used alongside vehicle type values to estimate the solar absorption and solar consumption of the solar vehicle. These recordings took place on March $18^{th}$, $19^{th}$ and $20^{th}$.

In order to mimic the solar irradiance absorbed by a car the sensor needed to be placed on the outside of the vehicle. The test car being used had no harnessing on the roof so the sensor was placed on the bonnet. The sensor was attached to the windscreen wiper and angled to be perpendicular to the bonnet.

Placing the sensor on the windscreen wiper meant that on occasion when the sun was at a very low angle and coming from behind the car, the solar sensor would be slightly shaded. These points of shade were flagged in the data recording and are marked in the results section. This is in some ways accurate as the solar panels on the bonnet of the car in that case would also be shaded. This method could be improved by creating a rig to attach the solar sensor to the roof.

The difficulty with this recording was, not only was it necessary to know the solar irradiance values and time but it was also necessary to know at what point on the graph the car was at. This could have been done using a solar sensor that included GPS. Unfortunately, the sensor available did not have this and thus a video recording was used. The video could see at every node on the road, the value of the sensor and the time. The video also provides other useful information when it comes to analysing the data. Watching some of the footage could aid in identifying reasons for anomalies and understanding the patterns in the data.

### 5.2.2 Iteration 2

After reviewing the data produced by the first iteration, the data appeared to be more randomised than expected. This was analysed in greater depth for the March $19^{th}$ 7am recording. It was found that the values recorded while facing directly into the sun were much larger than the predicted value and those while driving away from the sun were much less than the predicted value. This suggested that the angle of the sensor on the dashboard greatly contributed to the data.

To test the theory, the solar irradiance sensor was tested outside, tilting the sensor towards and away from the sun, to better understand the influence of angle on the result. This test confirmed that when the solar irradiance sensor was pointed directly at the sun it had a much higher value than when it was pointed away. This was also supported by research conducted by Mamun (41) who's work analyses the effect of the angle of a solar panel on the solar energy absorbed. Based on this information the theory regarding the angle of the sensor was well supported and the testing was run again.

To correct this, the experiment was redesigned to have the sensor parallel to the road as these are the values that are predicted in the model. This also mimics the impact of solar panels that would be placed on the roof of the vehicle.

This discovery shows that angle and positioning of the solar panels would have a great impact on the solar absorption. Vehicles such as Aptera have solar panels at many different angles as they cover the majority of the vehicle. Experiments supported by Mamun (41) could create a more accurate prediction model by including the angles of the solar panels on a vehicle.

## 5.3 Final testing method

After testing and confirming the theory using the second iteration methodology, the testing method was finalised. An image of the test set up can be seen in Fig. 5.2.

Figure 5.2: Test set up for the final methodology

1. Park the test car on a flat road.
2. Place the solar irradiance sensor against the windscreen wiper so the sensing circle is directly parallel to the road.

3. Secure the Solar irradiance to the windscreen wiper in this fixed position.
4. Turn the solar irradiance meter on.
5. Set it to record using integrated solar energy measurement.
6. Set the units to $Wh/m^2$.
7. Again check that the sensor is perfectly level in all directions.
8. Set up a video camera on the dashboard of the car that can record both the value of the sensor and the road ahead.
9. Drive the route outlined in Section 5.1.1.
10. Watch the video and at each node record the current value of the sensor and the time in seconds into a CSV file.
11. The test value for the edge is $\frac{Power_1 - Power_2}{time_1(hr) - time_2(hr)}$.

This produced tables of values that represent the test value at each time interval for each edge. A sample can be seen in Table 5.1. This could then be converted to graphs and processed on an edge by edge and route by route basis.

| **Edge** | **Solar irradiance $2^{nd}$ April at 7am** | **Solar irradiance $2^{nd}$ April at 11am** |
|---|---:|---:|
| 22To2 | 17.382 | 612 |
| 2To3 | 14.4 | 193.778 |
| 3To4 | 17.1 | 476.307 |
| 4To5 | 20.9793 | 339.9069 |
| 5To6 | 21.6 | 119.7 |

Table 5.1: Sample data for 5 test data edges on April 2 at 7 and 11 am

## 5.4 Analysing routes

Once the test data had been gathered it was important to understand how the data changed over different routes on a journey to answer the research question. Four journeys were selected at a range of locations on the road network to test how the prediction model can identify the optimal route. For each journey (source/destination pair) there are multiple route options to take. The journeys and routes compared in this section are highlighted in Table. 5.2.

The Journeys selected in this table were chosen to understand if the prediction model is accurate in a variety of conditions. Journey 1 is the longest route that supports a wide range of conditions. Journey 2 was selected to look at the outcome of a shorter range journey with still a wide variety of options. Journey 3 compares two dramatically different routes to the same destination. Journey 4 sees the impact of very small adjustments in the route.

| Journeys | Route |
|---|---|
| **Journey 1: 13 to 26** | |
| Route 1 | 13 - 14 - 5 - 6 - 7 - 8 - 9 - 19 - 23 - 42 - 25 - 26 |
| Route 2 | 13 - 14 - 5 - 6 - 7 - 8 - 36 - 37 - 28 - 29 - 25 - 26 |
| Route 3 | 13 - 12 - 16 - 17 - 21 - 6 - 7 - 8 - 36 - 37 - 28 - 29 - 25 - 26 |
| Route 4 | 13 - 12 - 16 - 17 - 21 - 6 - 7 - 8 - 9 - 19 - 23 - 42 - 25 - 26 |
| Route 5 | 13 - 12 - 16 - 15 - 5 - 6 - 7 - 8 - 36 - 37 - 28 - 29 - 25 - 26 |
| Route 6 | 13 - 12 - 16 - 15 - 5 - 6 - 7 - 8 - 9 - 19 - 23 - 42 - 25 - 26 |
| **Journey 2: 10 to 4** | |
| Route 1 | 10 - 11 - 12 - 13 - 14 - 5 - 4 |
| Route 2 | 10 - 11 - 12 - 16 - 15 - 5 - 4 |
| Route 3 | 10 - 18 - 20 - 21 - 15 - 5 - 4 |
| Route 4 | 10 - 18 - 20 - 21 - 6 - 3 - 4 |
| **Journey 3: 42 to 19** | |
| Route 1 | 42 - 43 - 44 - 23 - 19 |
| Route 2 | 42 - 25 - 26 - 28 - 29 - 9 - 19 |
| **Journey 4: 22 to 12** | |
| Route 1 | 22 - 2 - 3 - 4 - 5 - 14 - 13 - 12 |
| Route 2 | 22 - 2 - 3 - 4 - 5 - 15 - 13 - 12 |
| Route 3 | 22 - 2 - 3 - 6 - 5 - 14 - 13 - 12 |
| Route 4 | 22 - 2 - 3 - 6 - 5 - 15 - 13 - 12 |

Table 5.2: Journeys and routes selected for analysis

The solar irradiance predicted and tested for each journey could be calculated using the data management application. This produced a CSV with the route values for each date and vehicle type, both energy absorbed and energy consumed. These could then be processed into graphs to visualise the results. These journey graphs are then used to understand the effectiveness of the model to predict the most energy efficient route from point A to point B.

## 5.5 Summary

The testing methodology was designed to focus on obtaining results that could analyse different factors which influence the accuracy of the prediction model. Tests were outlined to understand the effect of time of day, vehicle type, weather conditions and solar power angle. The test route was outlined to contain different environments within Dublin city by including the River Liffey. Multiple iterations were performed to confirm and finalise the testing methodology to be consistent with the prediction model.

Once the test data was obtained a variety of routes for each journey could be analysed using the data management application. This helped answer the research question for routing in clear sky and cloudy conditions.

# 6 Results and Discussion

This chapter outlines sets of results acquired by the project to determine the effectiveness of the prediction model in clear sky and cloudy conditions. It also discusses the impact of choosing different vehicles and how the model prioritises time for a user as well as energy. Each section will discuss the outcome of the experiment and evaluate its relevance to the research questions. Suggestions are made to improve the prediction model in future research and the limitations of this work are discussed.

## 6.1 Road segment analysis in clear sky conditions

This section does preliminary analysis to understand the effectiveness of the model at predicting the solar irradiance of a particular road segment in clear sky conditions. The limitations of this data are discussed in more detail to determine in what way the model could be improved in future work.

### 6.1.1 Road segment analysis at 7:00 UTC

The graphs in Fig. 6.1 compare the predicted and test data from March $26^{th}$ and $27^{th}$ at 7:00 UTC. To test how similar the predicted data was to the test data an error margin of 20% of the mean predicted value was set. If the tested value was within this range then the prediction model was considered accurate for that road segment. From the graphs displayed, the accuracy of the prediction model of a particular road segment in clear sky conditions at 7am is 44%. A similar process was conducted for the recordings tested at 11am and 3pm and the accuracies were 38% and 40% respectively. The results of this analysis can be seen in Appendix A2. This concludes that in clear sky conditions the average solar irradiance of a road segment can be predicted with approximately 40.6% accuracy.

Some of the edges that have a more dramatic discrepancy between the predicted and tested data are highlighted in Table. 6.1. The video footage was analysed to determine the reason for this gap and highlight some limitations with this project. These limitations are analysed in more detail in the following section.

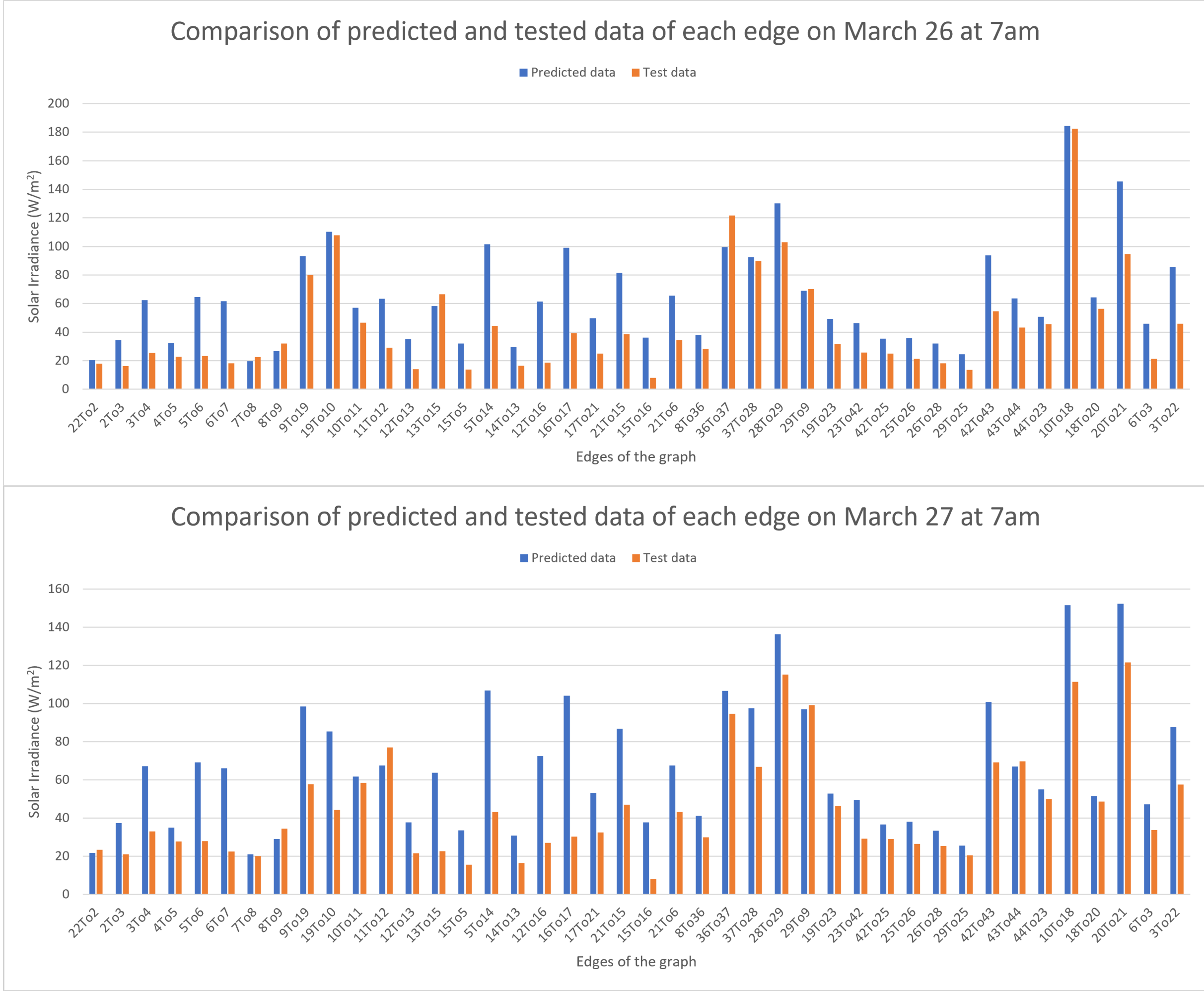


Figure 6.1: Comparison of predicted and tested data on March $26^{th}$ and $27^{th}$ at 7:00 UTC

| Reason | Edges effected |
|---|---|
| Car Shade | 5To6, 6To7, 12To16, 16To17 |
| Traffic | 42-43, 5To14 |
| Construction | 15To16 |
| Lanes | 2To3 |
| Bridge | 9To19 |

Table 6.1: Limitations that caused large discrepancy in data March 26 and 27 at 7 am

## 6.1.2 Discussion of limitations

This section highlights some limitations for this project, identified in the road segment analysis. These limitations have caused some large discrepancy in results as were highlighted in Table. 6.1.

### Car shade

This limitation occurs only on a particular number of edges during a 7am recording. This is due to the positioning of the sensor on the windscreen wiper. With a very low sun angle coming from directly behind the car, the sensor was shaded as can be seen in Fig. 6.2. This is a limitation that makes the test data lower than expected. This does not have any influence on the effectiveness of the prediction model.

Figure 6.2: An image showing how the sensor was shaded by the car

### Traffic

Traffic is the label given to an anomaly that occurs due to longer wait times at different points along a road segment. A road segment can have sections that are partly shaded by buildings and partly exposed to direct sunlight as seen in Fig. 6.3. With traffic or other speed effecting conditions the vehicle can spend more time in one section than another and thus change the solar energy consumed along the road segment. The predictive model estimates the value of the road segment assuming an equal amount of time is spent across the length of the road segment. This causes discrepancy in the results.

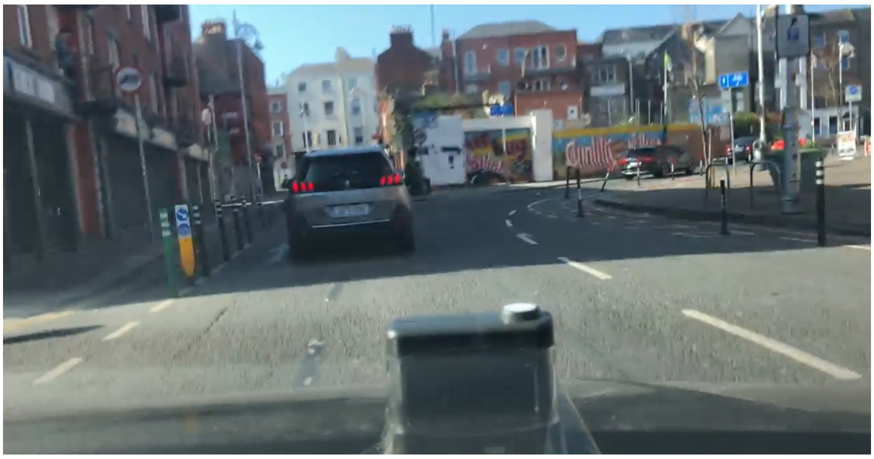

Figure 6.3: A representation of how traffic can impact the prediction model

To improve this, the prediction model could include a traffic prediction or live traffic model. This could weight sections of the road depending on current traffic predictions. Although this would improve the effect of traffic on the model it will not make it 100% accurate, as traffic is an ever-changing factor that cannot be predicted exactly unless in autonomous vehicle environments.

### Lane changing

Another aspect similar to the traffic problem is that a road can contain multiple lanes. Currently the prediction model has one line which represents the route taken down a road which is averaged to find the predicted value. However a wider road can have multiple paths to take down the road in either direction. Similar to the traffic problem, one side of the road can be shaded and one side of the road can be in direct sunlight as seen in Fig. 6.4. This may result in the car experiencing a completely shaded road segment or a road segment in direct sunlight.

Figure 6.4: Road segment from node 5 to 6 at 3pm on April 3rd

To improve this, the prediction model could incorporate different paths to be taken down a road. This can begin by having two different paths for a two way street and then be improved upon by adding multiple lanes depending on the direction intended to drive. This would improve the prediction model to some extent but is not perfectly predictable as it is not possible to predict the exact point at which someone will change lanes.

### Construction

The current digital surface model has slightly changed from what it was in 2015 when the LiDAR dataset was recorded. This can be seen when comparing the solar irradiance on the map against what is visible from the video recording. The map may appear that the street is in direct sunlight and the video may show that the road is completely shaded. This can be seen in Fig. 6.5 where the blue line in the map shows the road segment which appears to be in direct sunlight. In reality the road is completely shaded due to construction on the right hand side. This could be improved by using a more up to date digital surface model of Dublin.

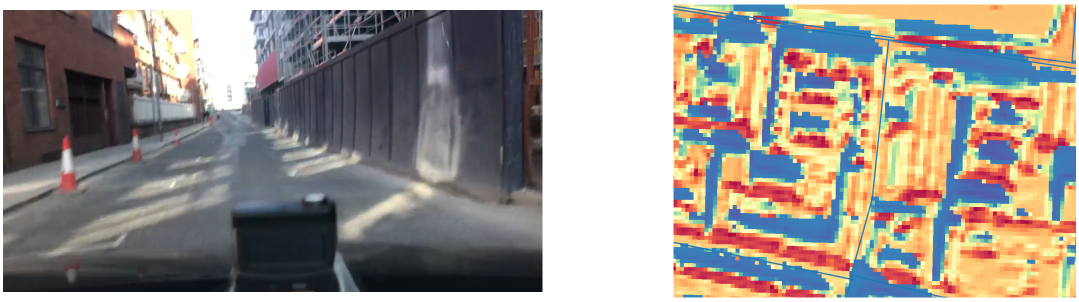

Figure 6.5: Representation of changes in solar irradiance due to construction

### Bridge

This is an unusual limitation but occurs on two of the edges in the road network. This occurs when there is an overhead bridge on a road. The prediction model shows there to be an area of direct sunlight whereas the car is driving underneath the bride and thus becomes shaded. The effect of this can be seen in Fig. 6.6. This could be improved upon by having more qualitative information on the digital surface model. If it was understood that a bridge was at a certain location then this could be given an approximated value representing shaded conditions.

Figure 6.6: A representation of how an overhead bridge can impact the prediction model

### Shade from other vehicles

While driving, particularly in a lower sun angle environment, it is possible to be shaded from other vehicles such as buses or trucks. An example of this occurring can be seen in Fig. 6.7. Unfortunately this aspect is unpredictable and it is unlikely that a solution to this could be included in the prediction model.


Figure 6.7: An image of the test car being shaded by another vehicle.

#### Summary

Various limitations to this project are evident on individual road segments that cause discrepancies larger than 20% of the mean predicted value. This greatly impacts the accuracy of the prediction model on an individual road segment. These limitations could be improved upon in future works to increase the accuracy of the prediction model.

## 6.2 Route analysis in clear sky conditions

The small details along a road segment dramatically impacted the overall accuracy of the prediction model. This section will analyse the accuracy of the model when viewed over a journey and its multiple route options. The analysis of each route was simulated using the Lightyear One vehicle and was recorded on a range of dates at a range of times using the Journeys defined in Section 5.4.

The graph in Fig. 6.8 shows a comparison of the energy absorbed as tested and as predicted by the model in clear sky conditions on March $27^{th}$. The absorption value is used here to determine if the prediction model can predict the amount of energy absorbed along a route. As the amount of energy used is the same for both test and predicted data it is less of an indication of the accuracy of the experiment. A similar analysis was conducted on March $26^{th}$ and the graphs for this can be seen in Appendix A3.

When combining March $26^{th}$ and March $27^{th}$ data, it is found that 58% of the time the route suggested by the predicted model that absorbs the most energy from the solar panels is the route with the highest absorption in practice also. This measurement of accuracy does not compare the difference in solar irradiance values but only if the route predicted is the optimal route.

The graphs show that even when the optimal route is not selected by the prediction model it is often the second best route in practice. The solar absorption values predicted are very similar to those in test.


Figure 6.8: Comparison of predicted and tested data for solar absorption along a Journey

From the different route analysis, it can be concluded that the prediction model is less accurate at predicting the optimal route when only small differences are made as seen in Journey 4 with only a 33% chance of selecting the optimal route. On the other hand Journey 3 had a 100% success rate as the routes were dramatically different. Journey 1 and 2 had similar success with 50% of the time the predicted route being selected. This shows that change in length of the Journey does not effect the accuracy of the prediction model.

The prediction model can accurately predict large differences between two routes but struggles to differentiate two very similar routes.

Next the energy absorbed was combined with approximate energy used by the vehicle while travelling journey 1. The results of this are displayed in Fig. 6.9. This was also conducted for all other routes at every time frame which can be seen in Appendix A3.

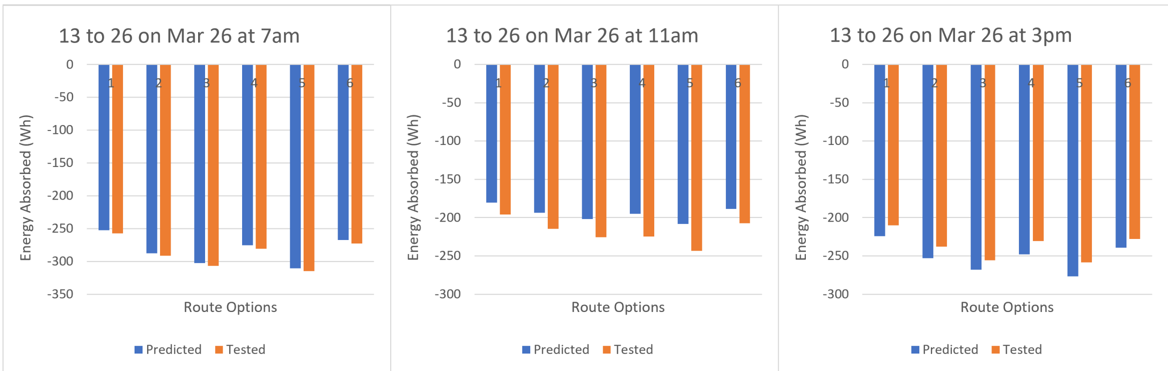


Figure 6.9: Comparison of predicted and tested data for solar energy consumed along Journey 1

83% of the time the optimal energy efficient predicted route was the optimal energy efficient route to take according to the test data. This is higher than the accuracy of the absorption calculation as the energy used is calculated as the same for both the test and prediction model as there was no access to a solar vehicle while conducting this project. For this reason, the impact of the absorption has a smaller effect than the energy used and the accuracy appears higher.

It is also observed that all of the energy consumed values are negative. This confirms that with the current technology, using a solar vehicle in Dublin does not seem feasible to self-sustain while driving. Even at peak solar times the vehicle is loosing 200Wh of energy on an approximately 5 minute journey which can increase to 300Wh in off peak solar conditions. With improvement in solar panel efficiency and solar vehicle technologies this may change and the prediction model is still effective by simply changing the vehicle parameters.

In clear sky conditions the predictive model choose the route with the most energy absorbed in 58% of cases. This increases to 83% for energy consumption. This is concluded using data across a variety of routes in 3 time intervals over two days.

## 6.3 Analysis in cloudy weather conditions

This section will look at a similar set of data as discussed in the previous sections but with more diverse weather conditions. This section will analyse the effect of weather on the solar irradiance and how weather influences the effectiveness of the prediction model.

### 6.3.1 Predicting and classifying weather

The weather forecast is very difficult to predict particularly for within a 15 minute interval and at a specific location. When tested a day in advance the weather forecast often predicted very different conditions to what was present on the day. The effect of this meant that the predicted data and tested data could be drastically different.

Current weather data from sources such as Open weather API are also not particularly accurate and thus can cause great differences between predicted and tested data. The optimal way to determine the cloud cover at the time would be either to have image processing for satellite images or to have sensors around the city to approximate the current cloud cover.

The cloud cover was measured at the time of recording using grid analysis of a photograph, due to the dramatic inaccuracy of other platforms. This value was used to create the prediction model to determine if it was still possible to predict the solar irradiance on each road segment if the weather was recorded live. In order to automate this in a city environment, laser cloud base recorders would need to be in operation in the city.

This cloud cover value was classified for the purpose of analysis to relate data sets with similar weather conditions. The classifications are listed in Table 6.2.

| Weather Classification | Cloud cover |
|---|---|
| Heavy Cloud | 80-100% |
| Medium Cloud | 50-80% |
| Light Cloud | 5-50% |
| Clear sky | 0-10% |

Table 6.2: Cloud classifications

This section will compare a sample of results in heavy and light cloud conditions similar to the way it was conducted for clear sky data. More results in different conditions can be found in Appendix A4.

### 6.3.2 Analysis of individual road segments under heavy and light cloud

The graphs in Fig. 6.10 show the impact cloud can have on the solar irradiance. The heavy cloud conditions see a dramatic decrease in solar irradiance whereas light cloud conditions see a very similar irradiance to that of a clear sky. More results for individual route analysis in different cloudy conditions can be seen in Appendix A4.

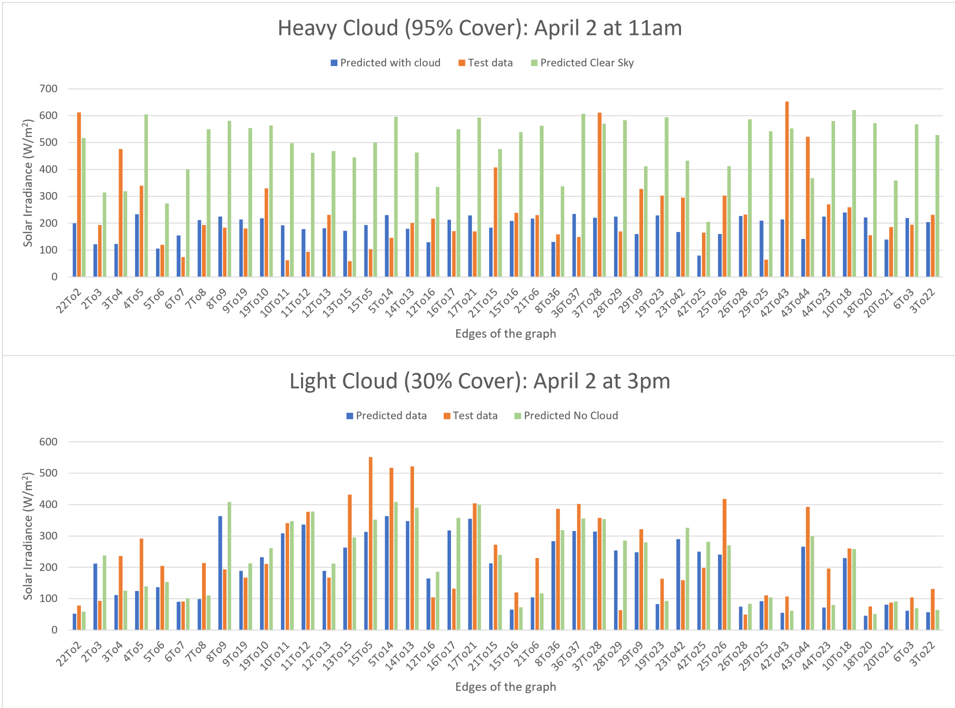


Figure 6.10: Comparison of predicted and tested data at each edge under heavy and light cloud conditions

In both conditions it is clear to see that some edges were more impacted by cloud than others. In the heavy cloud graph the majority of the edges are comparable to the predicted with cloud data. In some cases, edges such as 37To28 are more similar to clear sky conditions. This demonstrates a small break in the clouds which is difficult to include in the prediction model. In light cloud conditions the majority of edges are similar to the clear sky recording and the predictions with light cloud. However in some case such as edge 28To29 there was a cloud overhead and thus there was a dramatic decrease in solar irradiance.

Scattered cloud is very difficult to predict on an individual road segment as it is almost impossible to know at exactly what point a vehicle will be shaded by cloud and when it will be in direct sunlight. Uniform cloud is easier to predict as it is more of a constant shade across the duration of the journey.

Similar to the analysis for sunny data, the accuracies were calculated based on how many edges were within 20% of the mean predicted value. The accuracies were 46%, 26% and

27% for light, medium and heavy cloud respectively. This totals to an accuracy of 35% when predicting the solar irradiance of an individual road segment in cloudy conditions. It appears to be more feasible to predict the solar irradiance in light cloud conditions on individual road segments. These accuracy values are still much lower than was recorded for clear sky conditions.

The prediction model is not very effective at predicting the solar irradiance along a road segment in cloudy conditions. Clouds are ever-changing and can dramatically increase or decrease the solar irradiance in any location at a particular point in time. This may be more predictable as an average over longer durations but is not very effective when analysing individual road segments.

### 6.3.3 Route analysis in cloudy conditions

The graphs in Fig. 6.11 show the energy absorbed and energy consumed along Journey 1 in light and heavy cloud conditions. Similar graphs in a variety of cloud conditions can be seen in Appendix A5 for all Journeys.

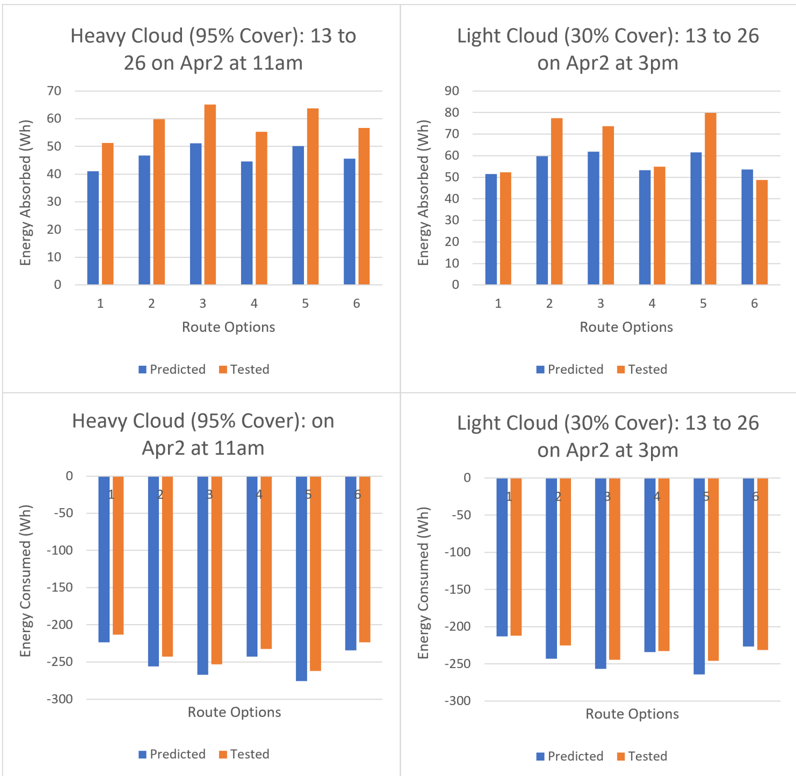


Figure 6.11: Comparison of predicted and tested data for Journey 1 under heavy and light cloud conditions

In total it was found that 45% of the time the route predicted to absorb the most solar energy, in reality absorbed the most energy also. This is slightly lower than for sunny conditions which is expected. In cloudy conditions, the error margin increases due to changes in the cloud structure as discussed in the previous section and thus the prediction model is less accurate.

Under light cloud conditions the accuracy was 63%. Under medium cloud conditions the accuracy was 25% and under heavy cloud conditions the accuracy was 38%. This shows that the accuracy is lowest for medium cloud cover. This is due to the fact that with medium cloud cover there is more of an even distribution of areas with cloud and areas with direct sunlight. This causes approximately half of the predicted values to be to high and half of them to be too low. This can be seen in Appendix A4. With light and heavy cloud conditions there is only a small number of edges where the error gap occurs. In light cloud the gap occurs when there is a cloud overhead and in heavy cloud conditions the gap occurs when there is a break in the clouds.

When analysing the energy consumed the accuracies are 88%, 75% and 100% for light, medium and heavy cloud conditions. This again shows that the medium cloud is most difficult to predict. These values conclude a total accuracy in cloudy conditions of 90%. This is higher than for sunny conditions even though it has just been shown that the model is less accurate in cloudy conditions. The reason for this is that the energy used by the vehicle is the same for predicted and test data, as there was no access to a solar vehicle. Therefore the energy used in the equation is considered 100% accurate. In cloudy conditions the energy absorbed is lower and thus contributes less to the overall accuracy of the consumption model. For this reason the accuracy appears higher. Energy consumption in this model is not the best way to measure accuracy as the energy used is consistent for test and predicted data.

Under cloudy conditions the solar irradiance is much lower and thus the total energy consumed is even lower than that under sunny conditions. The same route at 11am produced values as low as -270Wh in cloudy conditions in comparison to -240Wh in sunny conditions. This shows that under cloudy weather conditions using a solar vehicle is even less feasible.

It is also important to note that the conclusions drawn for cloudy conditions are based off a smaller dataset. The entire data collected for cloudy conditions was over a two day period so each cloud category has approximately two test runs to work off. Therefore more datasets could be gathered to further confirm the accuracy values suggested here.

Under cloudy conditions it is more difficult to predict how much energy is absorbed by the solar vehicle. This is the most difficult under medium cloud conditions. Although the accuracy for energy consumed is technically higher this is influenced by the fact that energy used is a constant in the prediction and test data. Thus the energy absorbed is a better measure and has an accuracy of 45%.

## 6.4 Comparison of vehicles

The graphs in Fig. 6.12 show a comparison of different vehicles on Journeys at 11am on March 26th. The maximum energy route was selected for each journey to compare optimal performance of the vehicles.

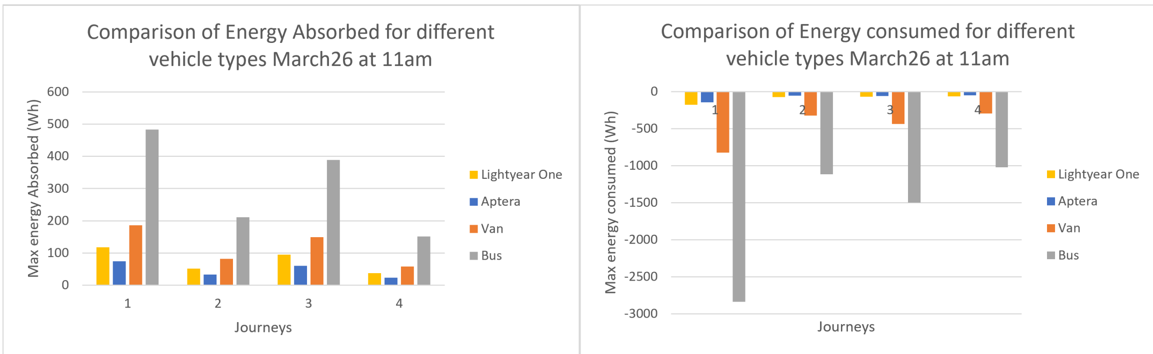


Figure 6.12: Comparison of Vehicle type across journeys on March 26 at 11am

From the graph it is clear that currently the van and bus are least energy efficient as the energy that they use does not balance out with the energy absorbed. This is due to the design of the vehicles that have not been modified for aerodynamic efficiency. These sample solar bus and van are based on traditional bus and van structures with solar panels attached to the roof. This structure could be adapted so that the vehicle consumes less energy per km similar to adaptations made to Lightyear One and Aptera.

The energy absorbed by the vehicle increases with the area of the solar panels. If modifying the vehicle structure is not possible, the energy used can still be supported by solar energy in a hybrid vehicle. For buses this can save up to 500Wh for an approximately 5 minute journey. The emphasis should still be to add solar panels to the roof where possible to reduce energy required from fossil fuels even if the vehicle is not self-sustaining.

Lightyear One and Aptera are similar in that they are designed for efficiency and it is evident that the energy consumed is much higher than that for a bus or a van. Lightyear One absorbs a larger amount of energy than Aptera due to its larger surface area of solar panels. Aptera however has a higher energy consumed which further emphasises the importance of designing for efficiency in solar vehicles. Although Aptera absorbs less energy, it also uses less which results in a higher energy consumed than Lightyear One.

All vehicles produced negative energy consumed values while driving at 11am in March at peak solar conditions. This shows that with current technologies in Ireland, the solar vehicle is not a feasible solution if only used while driving. This energy balance however could be supported by also parking the vehicle in direct sunlight and then optimising the energy while driving using the Drive Solar application.

## 6.5 Comparison of time vs energy

This section is going to analyse in more detail the effect of Drive Solar when looking at a particular journey. It determines which routes are time and energy optimal and which route would be selected by Drive Solar based on the users preferences.

Journey 3 from 42 to 19 can be taken using two routes which can be seen in Fig. 6.13.


Figure 6.13: 2 routes highlighted for Journey 3

Using a google maps approach the green line 'Route 1' is the most efficient route according to time constraints. When examining the energy constraints this varies.

At 7am in sunny conditions the most energy efficient route is the green line 'Route 1.' This route is most time/distance efficient and thus the vehicle will use less energy while travelling this route. At 7am there is not enough solar irradiance to balance out the energy used by the vehicle over a distance.

At 11am in sunny conditions however the orange route 'Route 2' is selected as the most energy efficient route. Although this route is slightly longer the energy absorbed by the vehicle at this time is much greater and can counter balance energy used. This again is affected by weather conditions, so in heavy cloud at 11am the green line 'Route 1' is selected as the optimal route again.

The algorithm for calculating energy consumed includes the energy absorbed and the energy used by the vehicle along a route. This algorithm naturally takes into consideration the time/distance required to travel the route. With very long distances the energy used will be too great to counteract and is unlikely to be selected as the optimal route. The time vs energy priority addition to the app further emphasises this by not selecting routes outside a certain distance extra to travel.

The distance along 'Route 1' is 1.67km and the distance along 'Route 2' is 1.97km. Therefore if the user sets their time energy priority at time or within 18% of the shortest distance than the app will return 'Route 1'. This is the optimal route for that person even when it is not the most energy efficient as the user has emphasised their need for a faster route at this time.

The most energy efficient route is not always the most time efficient route but is likely to be impacted by time due to the energy used by the vehicle. Similar results for the other Journeys can be seen in Table. 6.3.

| **Journey** | **Best Time Route** | **Best Energy Route at 7am** | **Best Energy Route at 11am** | **Best Energy at Route 7am with Cloud** |
|---|---|---|---|---|
| 1 | 1 | 1 | 1 | 1 |
| 2 | 1 | 3 | 3 | 3 |
| 3 | 1 | 1 | 2 | 1 |
| 4 | 1 | 4 | 4 | 4 |

Table 6.3: Sample of how different variables effect what route is selected by Drive Solar

Other Journeys such as 4 and 2 select a different route to the time efficient route in all conditions listed here. This is due to a much larger difference between the energy consumed on each route.

## 6.6 Summary

The accuracy of the prediction model under all conditions are summarised in Table. 6.4.

| **Cloud cover** | **Individual Road segment accuracy** | **Energy absorbed accuracy** | **Energy consumed accuracy** |
|---|---|---|---|
| Clear sky | 40.6% | 58.3% | 83.3% |
| General Cloud | 35% | 45% | 90% |
| Light Cloud | 46% | 62.5% | 87.5% |
| Medium cloud | 26% | 25% | 75% |
| Heavy cloud | 27% | 37.5% | 100% |

Table 6.4: Accuracy Table

This table summarises some of the statistics presented in the results section. It focuses on the accuracy of the prediction model under different conditions. This in combination with other key findings will be concluded and related to the research questions in the following section.

# 7 Conclusion

This section highlights the key findings of this project and the conclusions that can be drawn from the research. It also conducts a project analysis to understand the strengths and limitations within the project as well as what challenges were faced. Finally this section will discuss future work that can be done to improve upon the project presented in this dissertation.

## 7.1 Result Conclusions

The results presented in this paper successfully answer the stated research question and sub questions. This section provides answers to each research sub question and analyses the overall response to the research question as a whole. It will also discuss other key findings that were discovered throughout this project.

**To what extent can a model predict the average solar irradiance of a road segment at a defined time on a clear day or in cloudy weather conditions?**

The results show that a model can predict the average solar irradiance of a road segment to a 40.6% accuracy in clear sky conditions and to a 35% accuracy in cloudy conditions. This low accuracy on an individual road segment is due to some limitations within this project such as traffic, vehicle shade and construction as discussed in Section 6.1.2. With improvements to these limitations in future work the accuracy of this model could be greatly increased. Using the current method, the model is not effective at predicting the solar irradiance on individual road segments.

**To what extent can a model predict the optimal solar energy efficient route for a solar vehicle on a clear day or in cloudy weather conditions?**

The results show that the model can predict the optimal absorption route with 58.3% and 45% and the optimal consumed route at 83% and 90% accuracy for clear sky and cloudy conditions respectively. This result is a great improvement from individual edge analysis.

With averages over a route the errors due to individual road segments have a smaller impact.

The route analysis also showed that the length of the route does not effect the accuracy of the prediction model. It was found that the prediction model is more effective at predicting solar irradiance for 2 very different routes than for minor changes in the route. With Drive solar being more effective for larger differences in the route, users can make the right decisions when it is truly necessary.

This shows the potential impact that the Drive Solar application could have on the population. By successfully choosing the most energy efficient route while driving the users are saving energy and contributing towards a greener energy future.

### How does the solar vehicle selected determine the feasibility of a self sustaining solar powered vehicle?

The solar vehicle selected can have a dramatic impact on the feasibility of self sustaining solar powered vehicles. Through analysis Aptera was found to be the most feasible solar vehicle. This was still producing negative values for energy consumed along a journey however with some support from energy generated from parking, this is a feasible solution. Lightyear one is slightly less efficient but functions similar to Aptera. On the other hand the solar bus is not feasible using current bus designs. The energy absorbed by the solar panels is not enough to outweigh the energy consumed. The solar panels can simply support the energy consumed in a hybrid vehicle. This also applies to analysis for hybrid solar vans. Drive Solar is still an applicable application to improve solar consumption while driving in hybrid solar vehicles.

### How can the model include a users desire for the most time efficient as well as the most energy efficient route?

The most time efficient route is naturally included in the energy calculation as the more time spent driving, the more energy is used. This is further emphasised using bounded distances in the Drive Solar application to limit the excess distance travelled by the user to achieve higher solar energy.

In current conditions it is found that often the most energy efficient route is the most time efficient route due to more energy being lost than gained from the solar panels. With increasing technological development in the field, this bounded distances aspect of the application will have a bigger impact.

### 7.1.1 Other key findings

While analysing the effectiveness of the prediction model through this project some other key findings were discovered that could benefit and support future work.

The weather analysis in cloudy conditions produced some conclusions. Firstly, the current weather model using Open Weather API does not produce accurate enough results to use in the prediction model. Live cloud cover measurements are required to keep the prediction model accurate. As well as this it was found that medium cloud conditions had the lowest accuracy in the prediction model due to a more even distribution of cloud and direct sunlight. Finally, it was concluded that scattered cloud was more difficult to predict and caused more errors in the prediction model.

Time of day greatly influences the amount of energy consumed by a solar vehicle. Peak solar hours can multiply the solar energy absorbed along a route. Additions to the application could include choosing the optimal time to travel a defined route.

Finally, it was discovered how much of an impact the angle of a solar panel can have on the energy consumed. Including the angles of the panels could be a great improvement to the prediction model if there was an ability to test the results on a solar vehicle.

### 7.1.2 To what extent can a model predict the optimal solar energy efficient route for a solar vehicle?

The model designed in this experiment predicts the route with the most energy absorbed with a 51.65% accuracy and chooses the route with the most energy consumed with a 86.65% accuracy. This concludes that the model can effectively predict the optimal energy efficient route for a solar vehicle. This model varies in accuracy depending on weather conditions with the most accuracy in clear sky conditions and the least accuracy in medium cloud conditions. Some limitations are highlighted that prevent this model from being more accurate. This could become a more accurate model by improving some of these limitations.

The Drive Solar application effectively implements this model into a user friendly application so that choosing the optimal route for a solar vehicle becomes a widespread practice as solar vehicles are released.

## 7.2 Project analysis

### 7.2.1 Challenges

This section will describe the main challenges and what actions were taken to overcome them.

The first challenge was encountered when looking for digital surface model data. Attempts were made to transform the digital twin of the docklands, contact Dublin City Council, contact Ordinance survey Ireland but all were unsuccessful. The LiDAR data used for this project was found eventually by contacting Dr. John Connolly in the geography department who provided resources linked to the LiDAR dataset used.

There was difficulty encountered when trying to convert the solar prediction map to a graph style dataset that could be used for the application. Image processing and combining the solar map with Open Street Map data was all considered. This was solved using the Zonal statistics as table tool to convert the zone lines into a table including the data. This could then be exported to excel and parsed through the mobile application into the Firebase dataset.

The asynchronicity of the firebase database calls caused a number of challenges when trying to implement various functions for the mobile application. For example the get edges function needed for Dijkstra's algorithm was now asynchronous. This was solved by converting the algorithms into recursive implementations. Other functions were altered to use completion handlers or dispatch queues to solve the asynchronicity problems.

The lack of GPS in the solar irradiance sensors provided challenges when trying to match the solar irradiance values to specific nodes on the node map. This was solved using video footage which needed to be analysed for each occurrence. This limited the number of tests that could be run due to the time required to process the data. This could be improved in future work by including a GPS in the test sensor.

Challenges encountered delayed the progress of the project at different points but were all solved to some extent so that the project could continue. In some cases this required slightly limiting the scope to account for changes in design.

### 7.2.2 Strengths and Limitations

This project provided a comprehensive solution to develop a prediction model to optimise the routes of solar powered vehicles and test the accuracy of this model. The model was successful and produced an accuracy of 83% under clear sky conditions. The project successfully addresses the research question and sub questions as outlined in Section. 1.4

with conclusive results supported by tested data.

Due to some assumptions made and limited scope of the project, the model had some limitations and the project did not have the capacity to investigate these further. Firstly the errors discussed in Section. 6.1.2 were addressed as limitations that caused anomalies in the datasets. As well as this the limitation due to uniform and scattered cloud was also discussed in Section 6.3.2.

The formula designed for calculating energy used also was considered a limitation. This used a simple distance times energy used per distance equation. This does not take into account repeated stop start in traffic conditions as discussed by Liu (27) or the elevation gain as discussed by Storandt (25). This energy used equation was also assumed for the tested data and was not tested itself. This was the main cause of the increase in accuracy for cloudy weather conditions.

After developing the application to work with Open weather API, it was found that the current weather data provided by this platform had a very low accuracy. To replace this the cloud cover was calculated using a grid calculation of a photograph. This solution could not be adapted for use in the Drive solar application without the use of laser based cloud recorders. This limited the accuracy of the model in the application in comparison to the data analysed.

The lack of access to a solar vehicle was also a limitation for this project. The absorption, efficiency and energy used was taken as constant values. In reality this would greatly differ depending on the angle of the solar panels as discussed in Section. 5.2.2 as well as the current state of charge of the vehicle. With access to a solar vehicle the predicted data could have been compared against more realistic outcomes and other factors such as angle of solar panels and state of charge would have also been analysed.

## 7.3 Future work

This project provides a large scope for future development in the field. Some aspects of this project can be investigated further to improve the accuracy of the results by mainly addressing the limitations as discussed in Section. 7.2.2.

The prediction model could be improved by adding live traffic information and lane configurations. This would allow sections of the road to be weighted differently depending on where the vehicle is more likely to be due to traffic or lane configurations. The effectiveness of such model could be analysed to determine to what extent it would benefit the prediction model with the cost of more data processing and storage.

The weather model was moderately successful at predicting the solar irradiance based on current observed cloud conditions. It was found that the forecasting model was ineffective and thus this could be further investigated to find a more accurate forecasting model. This could be done by adding laser based cloud recorders around a city to track current cloud cover. The forecast model could also be improved by considering the impact of scattered clouds and creating a system to detect when anomalies in the cloud might occur. A solution could be implemented similar to google maps where the energy absorbed by each user using the app is tracked and thus a better indication of cloud cover can be measured from the energy absorbed by all users at any point in time.

Investigation could also be completed into the effectiveness of using AI algorithms in lieu of the shortest route algorithms. Algorithms such as Deep Q learning and SARSA could be used to explore the environment based on sets of test data and determine best policies for navigating the route. This would dramatically reduce computation but with the risk of not finding the optimal route in all cases.

The algorithm to calculate energy used could also be updated. This could be based off approximate time duration to travel a route but may also take into account traffic conditions to account for repeated stop start effect. This could be tested by monitoring the energy used by a solar vehicle while driving the test route.

The process for generating the maps and transferring them to Firebase through the data management application takes significant calculation and time. To improve this an API could be created to input a digital surface model and output the solar irradiance on all the roads at a specified time. An API such as this would make this project more scalable and significantly reduce repetitive calculation.

Finally, the testing was done assuming that solar irradiance values translate into constants for an actual solar vehicle. There was no consideration for the angle of the solar panels, or other factors that may influence absorption. Future work can be conducted to test the accuracy of this using a solar vehicle. These models may be developed to consider angle of solar panels and state of charge as other factors that will effect the model.

Due to this being a new field, the research to date is very limited. This project acts as an introduction to the potential effect of work in the area. The future work outlined in this section will expand this project to become a more accurate application.

## 7.4 Summary

The research outlined in this paper successfully answers the research question defined for this project. It shows that the predictive model effectively predicts the most energy efficient route for a solar vehicle. This project encounters some significant limitations such as traffic, energy used calculations and the lack of access to a solar vehicle. Many of the limitations reduce the accuracy of the prediction model or have caused some contributing factors to be omitted. With future developments in the area this prediction model can become a more accurate solution.

By increasing the energy absorbed by a solar vehicle, Drive Solar can aid in the transition to the widespread use of self-sustaining solar vehicles.

# Bibliography


[1] Django Mathijsen. The role of composites in getting the solar car to our driveways: Lightyear one. *Reinforced Plastics*, 65(4):178–187, 2021.

[2] Aptera motors, Dec 2021. URL `https://aptera.us/`.

[3] Myeongchan Oh, Sung-Min Kim, and Hyeong-Dong Park. Estimation of photovoltaic potential of solar bus in an urban area: Case study in gwanak, seoul, korea. *Renewable Energy*, 160:1335–1348, 2020.

[4] Naveed ur Rehman, Mohamad Hijazi, and Muhammad Uzair. Solar potential assessment of public bus routes for solar buses. *Renewable Energy*, 156:193–200, 2020.

[5] Hannah E Daly and Brian P Ó Gallachóir. Future energy and emissions policy scenarios in ireland for private car transport. *Energy Policy*, 51:172–183, 2012.

[6] las dataset to raster (conversion)—arcgis pro | documentation 2022, 2022. URL `https://pro.arcgis.com/en/pro-app/2.8/tool-reference/conversion/las-dataset-to-raster.htm`.

[7] an overview of the solar radiation toolset—arcgis pro | documentation 2022, 2022. URL `https://pro.arcgis.com/en/pro-app/2.8/tool-reference/spatial-analyst/an-overview-of-the-solar-radiation-tools.htm#:~:text=The%20Area%20Solar%20Radiation%20tool,for%20an%20entire%20geographic%20area`.

[8] zonal statistics as table (spatial analyst)—arcgis pro | documentation 2022, 2022. URL `https://pro.arcgis.com/en/pro-app/2.8/tool-reference/spatial-analyst/zonal-statistics-as-table.htm`.

[9] table to excel (conversion)—arcgis pro | documentation 2022, 2022. URL `https://pro.arcgis.com/en/pro-app/latest/tool-reference/conversion/table-to-excel.htm`.

[10] Rendy Adhi Rachmanto, I Nyoman Sutantra, Bambang Sudarmanta, and Unggul Wasiwitono. Energy management system in series-parallel hybrid solar vehicle. *Journal of Advanced Research in Fluid Mechanics and Thermal Sciences*, 72(2):158–169, 2020.

[11] Dunbar P Birnie III. Analysis of energy capture by vehicle solar roofs in conjunction with workplace plug-in charging. *Solar Energy*, 125:219–226, 2016.

[12] Luchang Bai, Youtong Zhang, Hongqian Wei, Junbo Dong, and Wei Tian. Digital twin modeling of a solar car based on the hybrid model method with data-driven and mechanistic. *Applied Sciences*, 11(14):6399, 2021.

[13] Christiaan Oosthuizen, Barend Van Wyk, Yskandar Hamam, Dawood Desai, and Yasser Alayli. The use of gridded model output statistics (gmos) in energy forecasting of a solar car. *Energies*, 13(8):1984, 2020.

[14] Lalith Pankaj Raj Nadimuthu and Kirubakaran Victor. Performance analysis and optimization of solar-powered e-rickshaw for environmental sustainability in rural transportation. *Environmental Science and Pollution Research*, pages 1–12, 2021.

[15] Gabriele Lobaccaro, Malgorzata Maria Lisowska, Erika Saretta, Pierluigi Bonomo, and Francesco Frontini. A methodological analysis approach to assess solar energy potential at the neighborhood scale. *Energies*, 12(18):3554, 2019.

[16] Deepak Kumar. Mapping solar energy potential of southern india through geospatial technology. *Geocarto International*, 34(13):1477–1495, 2019.

[17] Tao Hai, Ahmad Sharafati, Achite Mohammed, Sinan Q Salih, Ravinesh C Deo, Nadhir Al-Ansari, and Zaher Mundher Yaseen. Global solar radiation estimation and climatic variability analysis using extreme learning machine based predictive model. *IEEE Access*, 8:12026–12042, 2020.

[18] Paulina Wegertseder, Peter Lund, Jani Mikkola, and Rodrigo García Alvarado. Combining solar resource mapping and energy system integration methods for realistic valuation of urban solar energy potential. *Solar Energy*, 135:325–336, 2016.

[19] Seongha Park, Yongho Kim, Nicola J Ferrier, Scott M Collis, Rajesh Sankaran, and Pete H Beckman. Prediction of solar irradiance and photovoltaic solar energy product based on cloud coverage estimation using machine learning methods. *Atmosphere*, 12 (3):395, 2021.

[20] Michelle G Nevins and Jennifer N Apell. Emerging investigator series: quantifying the impact of cloud cover on solar irradiance and environmental photodegradation. *Environmental Science: Processes & Impacts*, 23(12):1884–1892, 2021.

[21] Abdoulatif Bonkaney, Saïdou Madougou, and Rabani Adamou. Impacts of cloud cover and dust on the performance of photovoltaic module in niamey. *Journal of Renewable Energy*, 2017, 2017.

[22] Damon Waterworth and Alona Armstrong. Southerly winds increase the electricity generated by solar photovoltaic systems. *Solar Energy*, 202:123–135, 2020.

[23] Cedric De Cauwer, Wouter Verbeke, Joeri Van Mierlo, and Thierry Coosemans. A model for range estimation and energy-efficient routing of electric vehicles in real-world conditions. *IEEE Transactions on Intelligent Transportation Systems*, 21(7):2787–2800, 2019.

[24] Martin Strehler, Sören Merting, and Christian Schwan. Energy-efficient shortest routes for electric and hybrid vehicles. *Transportation Research Part B: Methodological*, 103: 111–135, 2017.

[25] Sabine Storandt. Quick and energy-efficient routes: computing constrained shortest paths for electric vehicles. In *Proceedings of the 5th ACM SIGSPATIAL international workshop on computational transportation science*, pages 20–25, 2012.

[26] Martin Sachenbacher, Martin Leucker, Andreas Artmeier, and Julian Haselmayr. Efficient energy-optimal routing for electric vehicles. In *Twenty-fifth AAAI conference on artificial intelligence*, 2011.

[27] Chenglin Liu, Jianqiang Wang, Wenjuan Cai, and Yuzhao Zhang. An energy-efficient dynamic route optimization algorithm for connected and automated vehicles using velocity-space-time networks. *IEEE access*, 7:108866–108877, 2019.

[28] Mahnoosh Alizadeh, Hoi-To Wai, Anna Scaglione, Andrea Goldsmith, Yue Yue Fan, and Tara Javidi. Optimized path planning for electric vehicle routing and charging. In *2014 52nd Annual Allerton Conference on Communication, Control, and Computing (Allerton)*, pages 25–32. IEEE, 2014.

[29] Okan Arslan, Barış Yıldız, and Oya Ekin Karaşan. Minimum cost path problem for plug-in hybrid electric vehicles. *Transportation Research Part E: Logistics and Transportation Review*, 80:123–141, 2015.

[30] Sören Merting, Christian Schwan, and Martin Strehler. Routing of electric vehicles: Constrained shortest path problems with resource recovering nodes. In *15th Workshop on Algorithmic Approaches for Transportation Modelling, Optimization, and Systems (ATMOS 2015)*. Schloss Dagstuhl-Leibniz-Zentrum fuer Informatik, 2015.

[31] Ki-Beom Lee, Mohamed A Ahmed, Dong-Ki Kang, and Young-Chon Kim. Deep reinforcement learning based optimal route and charging station selection. *Energies*, 13 (23):6255, 2020.

[32] Mehrija Hasičić, Damir Bilić, and Harun Šiljak. Sensor fusion for solar car route optimization. In *2016 5th Mediterranean Conference on Embedded Computing (MECO)*, pages 456–459. IEEE, 2016.

[33] Damir Bilić, Mehrija Hasičić, and Harun Šiljak. Practical implementation of solar car optimized route estimation. In *2016 XI International Symposium on Telecommunications (BIHTEL)*, pages 1–5. IEEE, 2016.

[34] Mehrija Hasicic, Damir Bilic, and Harun Siljak. Criteria for solar car optimized route estimation. *Microprocessors and Microsystems*, 51:289–296, 2017.

[35] Mehrija Hasicic and Harun Siljak. Putting the sc in score: Solar car optimized route estimation and smart cities. In *Modeling and Optimization in Green Logistics*, pages 75–86. Springer, 2020.

[36] Debra F Laefer, AVV Saleh Abuwarda, L Truong-Hong, and H Gharibi. Aerial laser and photogrammetry survey of dublin city collection record. 2015. *URL https://geo. nyu. edu/catalog/nyu_2451_38684*, 2015.

[37] OpenWeatherMap.org. One call api: Weather data for any geographical coordinate. URL https://openweathermap.org/api/one-call-api.

[38] Flixbus places solar panels on buses 2022, 2022. URL https://www.sustainable-bus.com/alternative-drive-coach/flixbus-places-solar-panels-on-buses-on-board-equipments-are-green-powered/.

[39] Solar panels for the bus industry - less co2 & less fuel 2022, 2022. URL https://solarbus.pro/.

[40] Martin Weiss, Kira Christina Cloos, and Eckard Helmers. Energy efficiency trade-offs in small to large electric vehicles. *Environmental Sciences Europe*, 32(1):1–17, 2020.

[41] M.A.A. Mamun, M.M. Islam, M. Hasanuzzaman, and Jeyraj Selvaraj. Effect of tilt angle on the performance and electrical parameters of a pv module: Comparative indoor and outdoor experimental investigation. *Energy and Built Environment*, 3(3):278–290, 2022. ISSN 2666-1233. doi: https://doi.org/10.1016/j.enbenv.2021.02.001. URL https://www.sciencedirect.com/science/article/pii/S2666123321000179.

# A1 Solar Maps


Figure A1.1: Sample of a generated solar map on April 3 at 7am

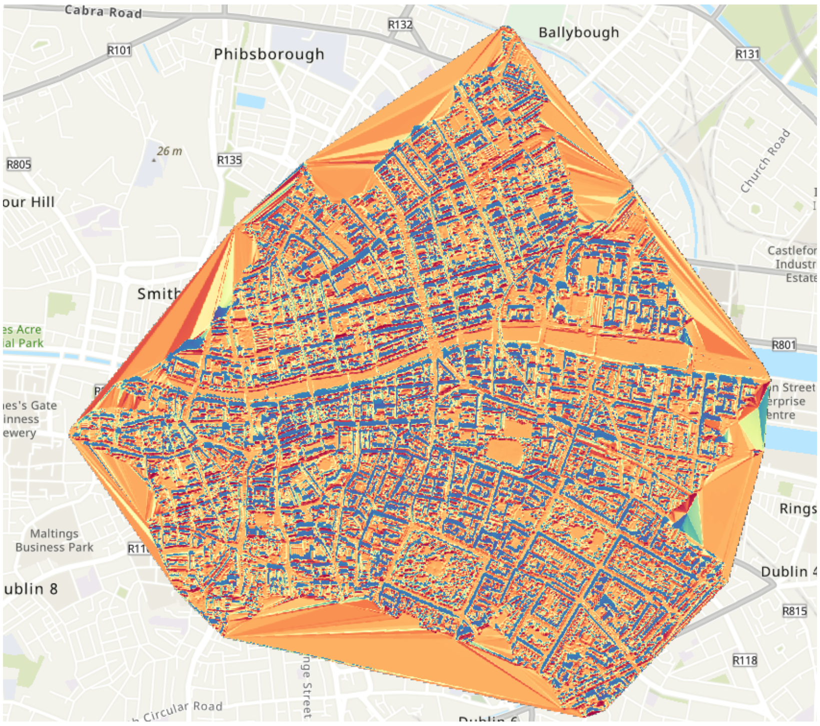


Figure A1.2: Sample of a generated solar map on April 3 at 11am

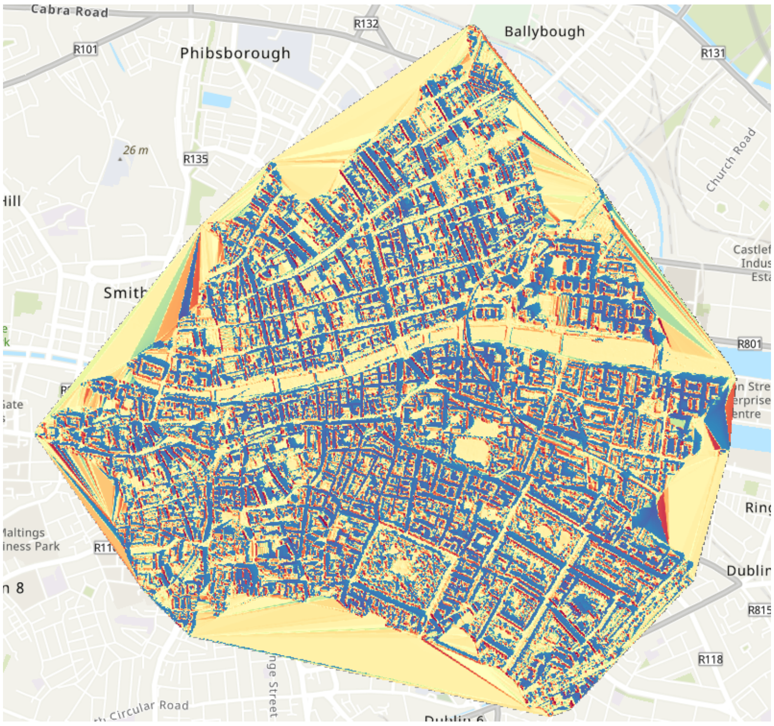


Figure A1.3: Sample of a generated solar map on April 3 at 3pm

# A2 Individual road segment analysis at 11am and 3pm

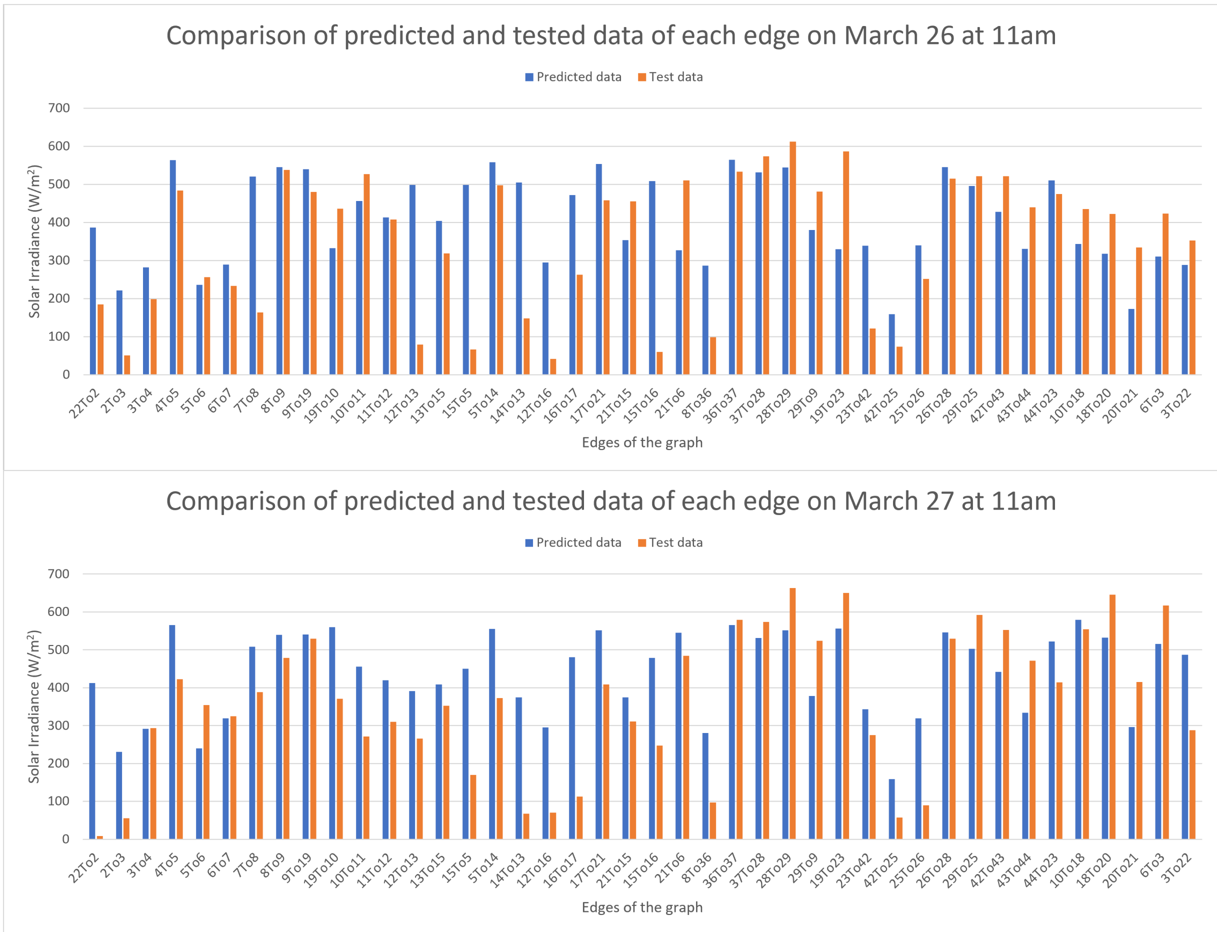


Figure A2.1: Comparison of predicted and tested data on March 26 and 27 at 11:00 UTC

| Reason | Edges effected |
|---|---|
| Traffic | 25To26, 8To36, 7To8, 12To13, 14To13 |
| Construction | 16To17, 15To5 |
| Lanes | 2To3, 12To16 |
| Bridge | 4To5 |

Table A2.1: Reasons for large discrepancy in data March 26 and 27 at 11 am

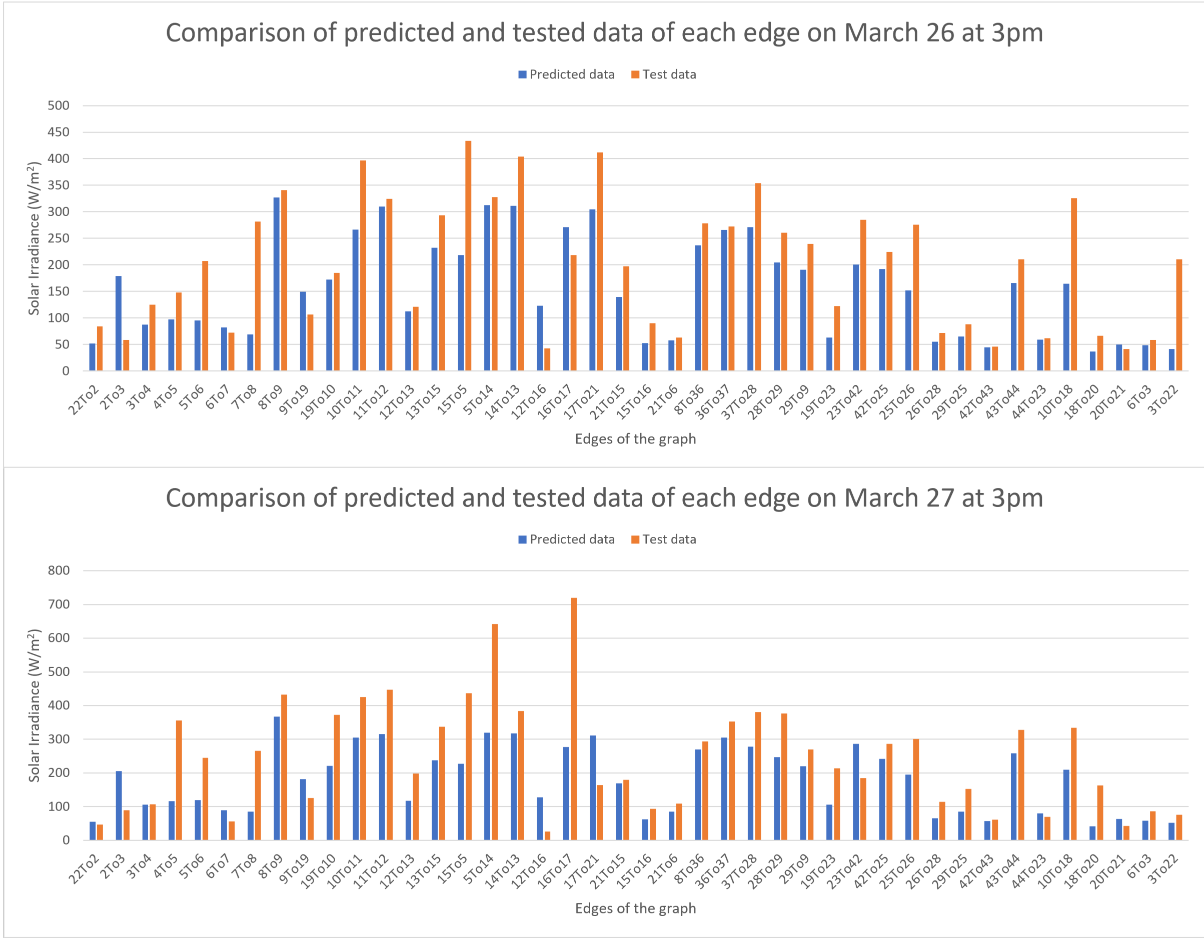


Figure A2.2: Comparison of predicted and tested data on March 26 and 27 at 15:00 UTC

| Reason | Edges effected |
|---|---|
| Traffic | 4To5, 7To8, 5To14, 16To17, 10To18, 18To20, 3To22 |
| Lanes | 2To3 |

Table A2.2: Reasons for large discrepancy in data March 26 and 27 at 3 pm

# A3 Route analysis in clear sky conditions


Figure A3.1: Route analysis conducted on March 26th for the energy absorbed by a solar vehicle

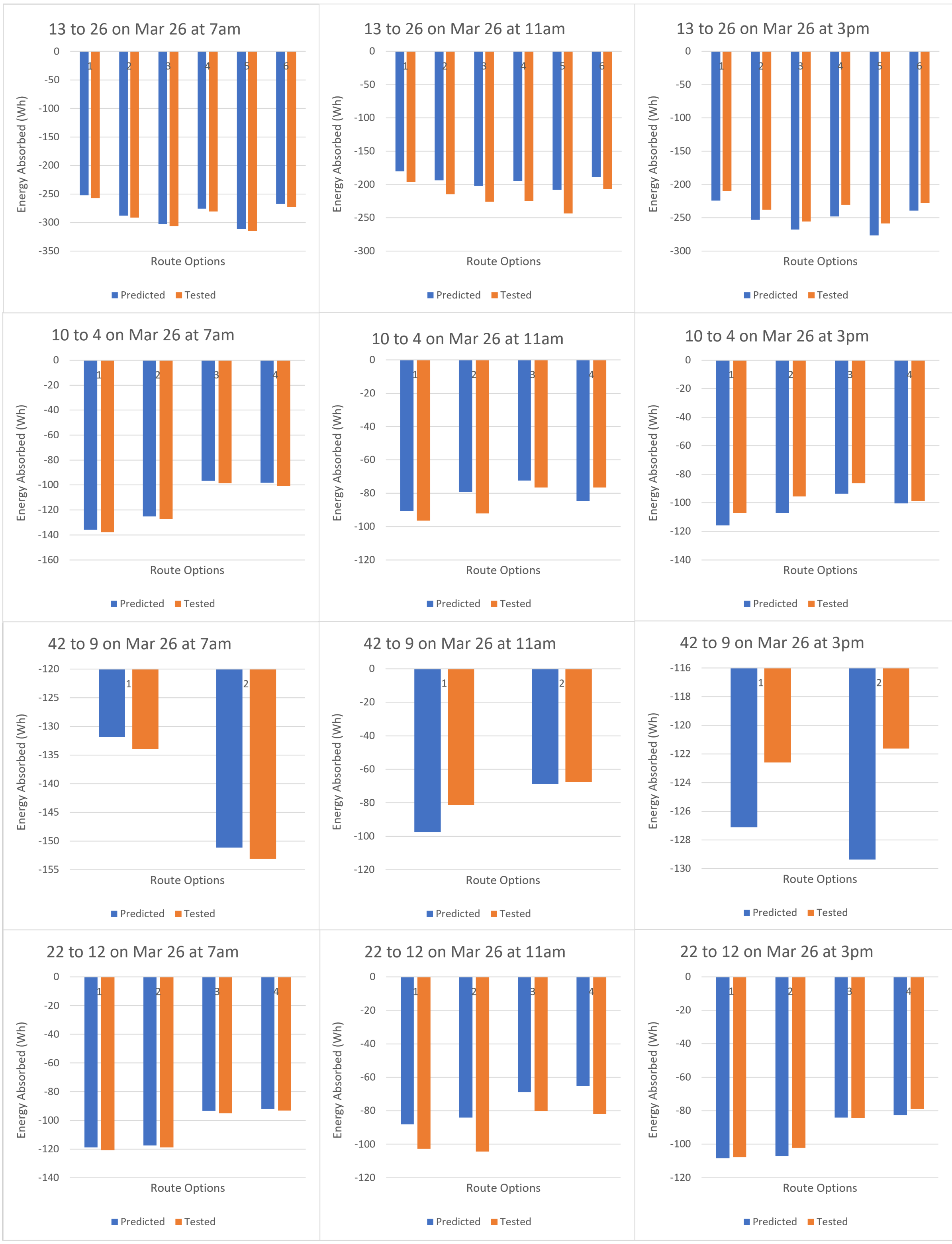


Figure A3.2: Route analysis conducted on March 26th for energy consumed by a solar vehicle

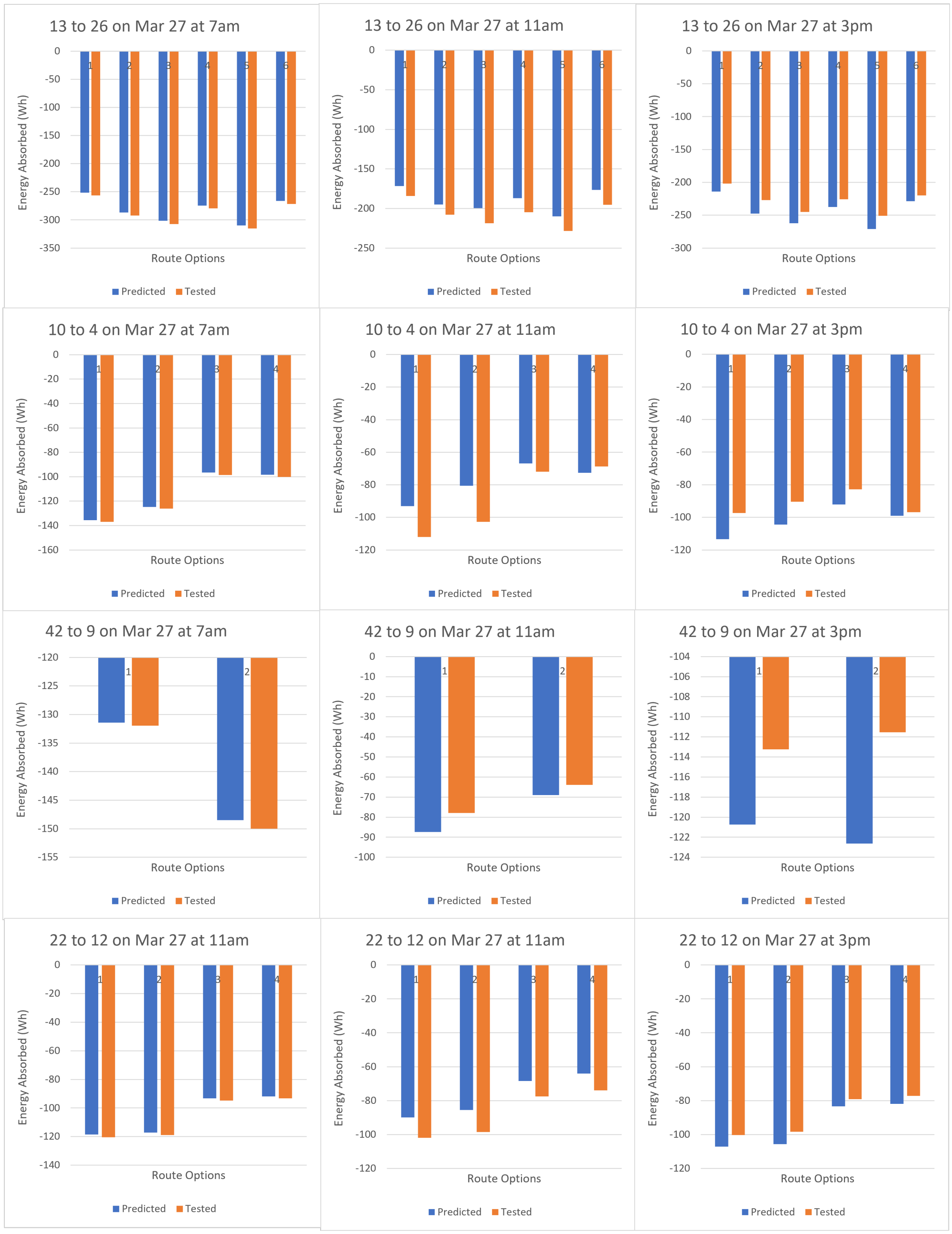


Figure A3.3: Route analysis conducted on March 27th for energy consumed by a solar vehicle

# A4 Individual road segment analysis in cloudy conditions

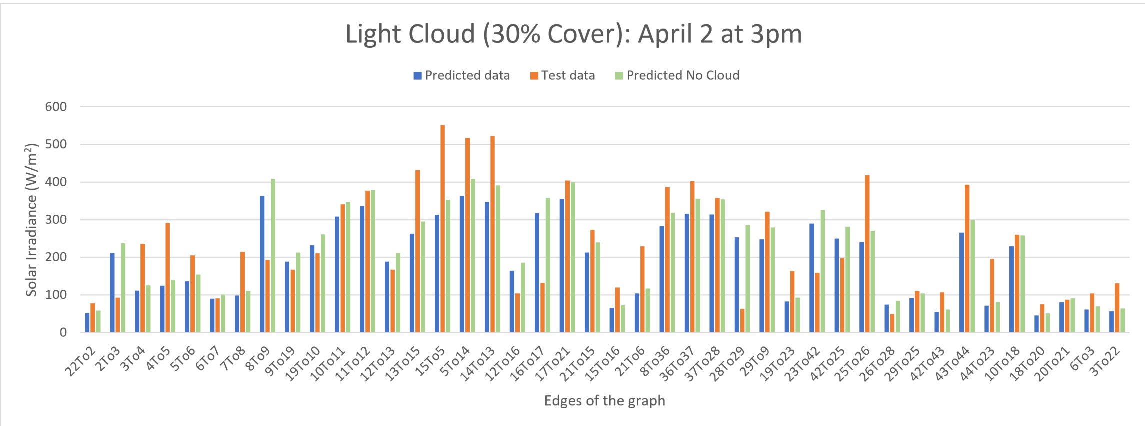


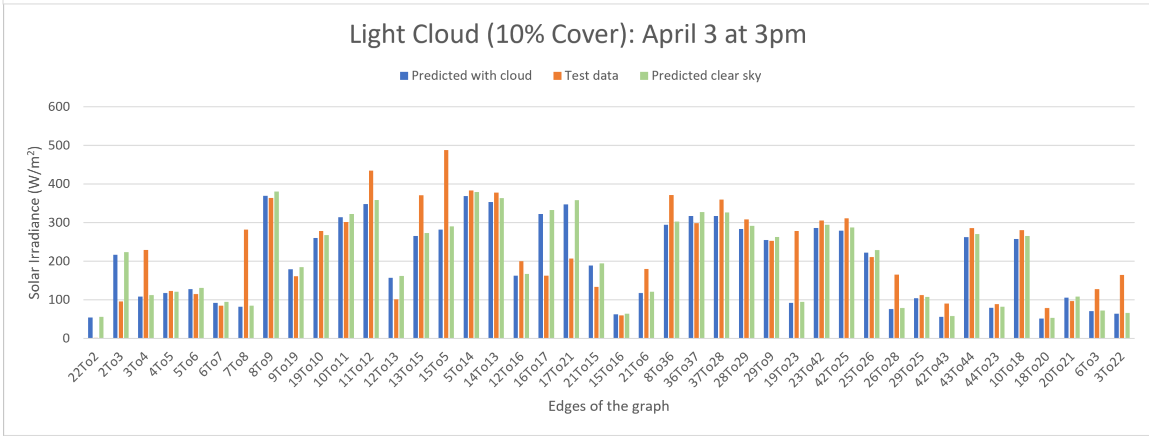


Figure A4.1: Individual road segment analysis for light cloud

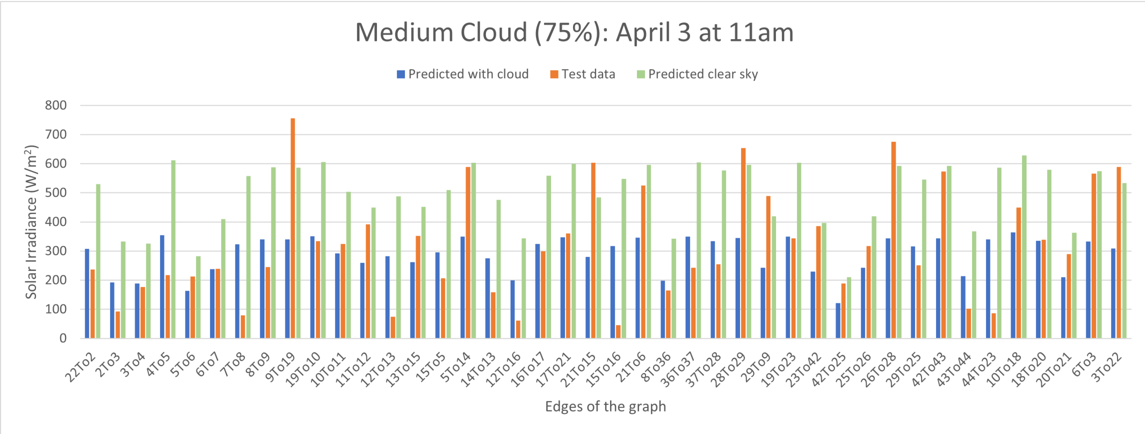


Figure A4.2: Individual road segment analysis for medium cloud

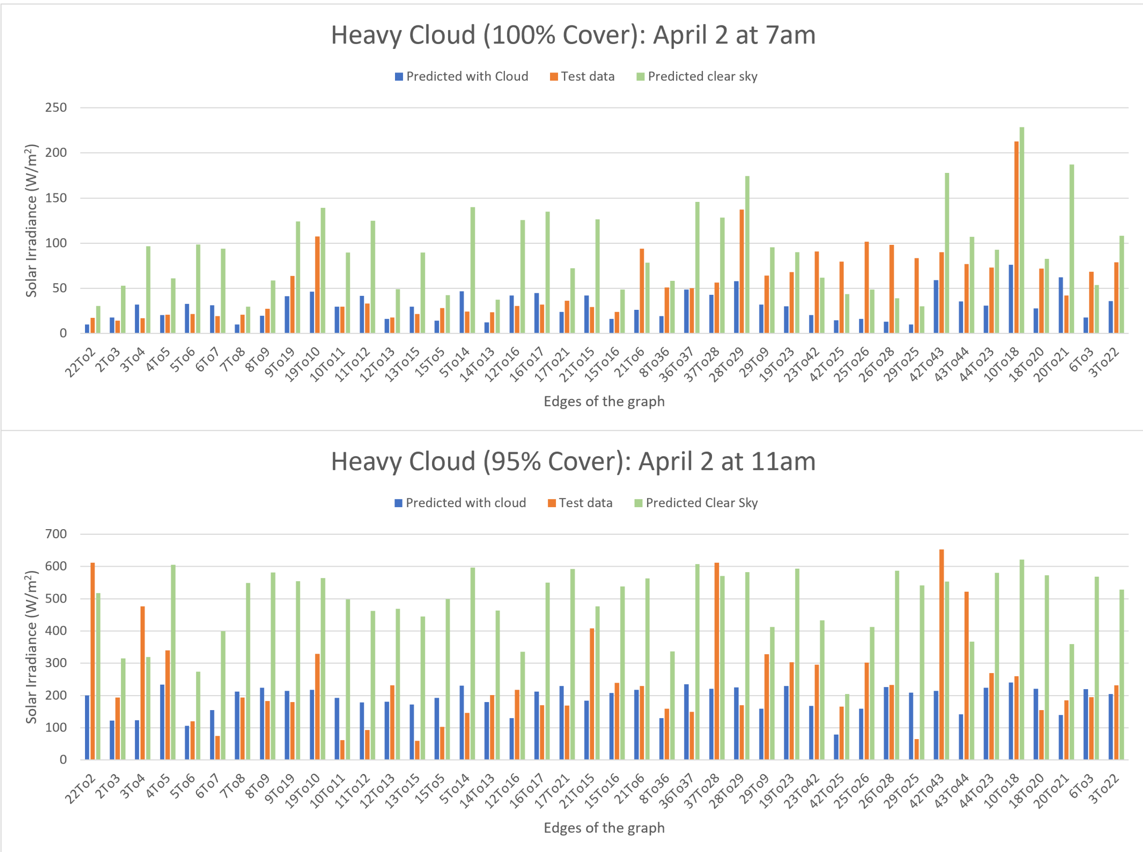


Figure A4.3: Individual road segment analysis for heavy cloud

# A5 Route analysis in cloudy conditions


Figure A5.1: Route analysis conducted in light cloud conditions for the energy absorbed by a solar vehicle

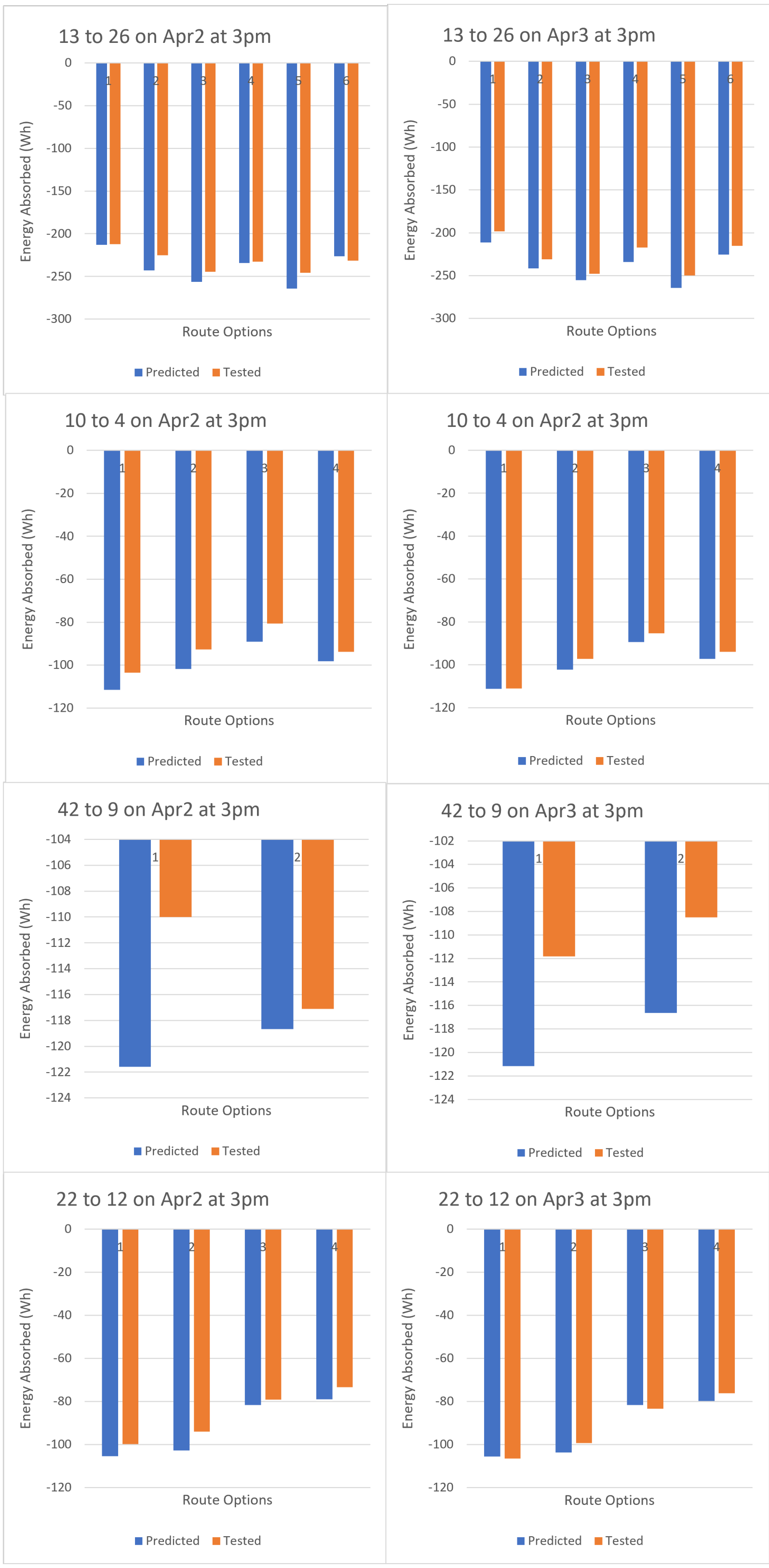


Figure A5.2: Route analysis conducted in light cloud conditions for the energy consumed by a solar vehicle

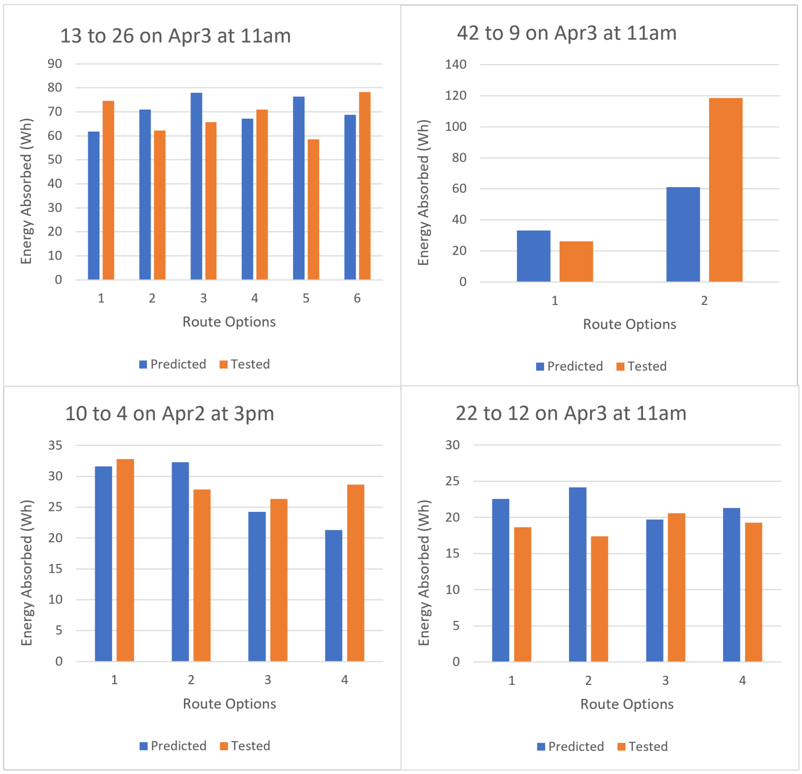


Figure A5.3: Route analysis conducted in medium cloud conditions for the energy absorbed by a solar vehicle

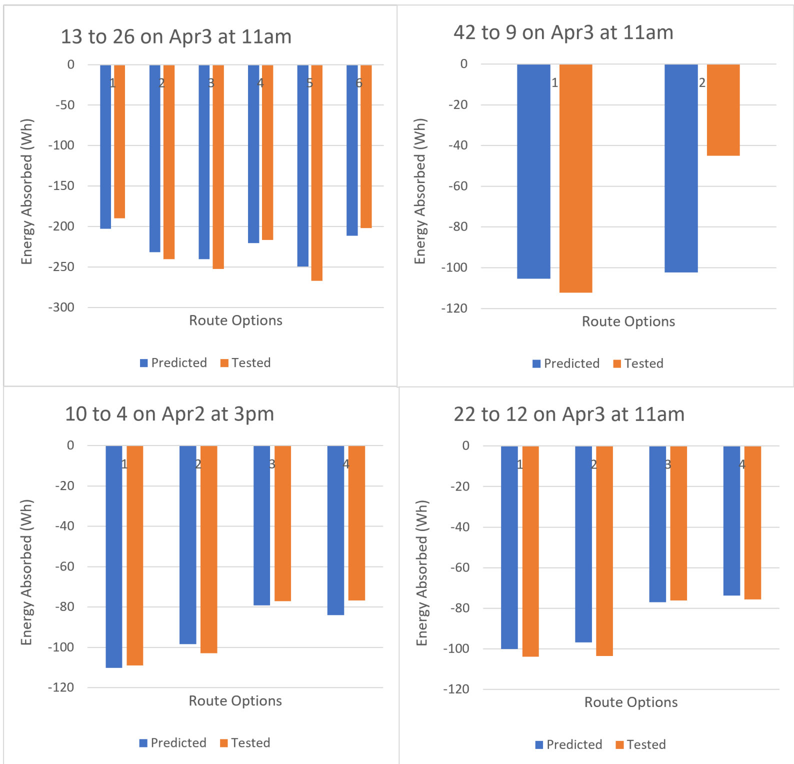


Figure A5.4: Route analysis conducted in medium cloud conditions for the energy consumed by a solar vehicle

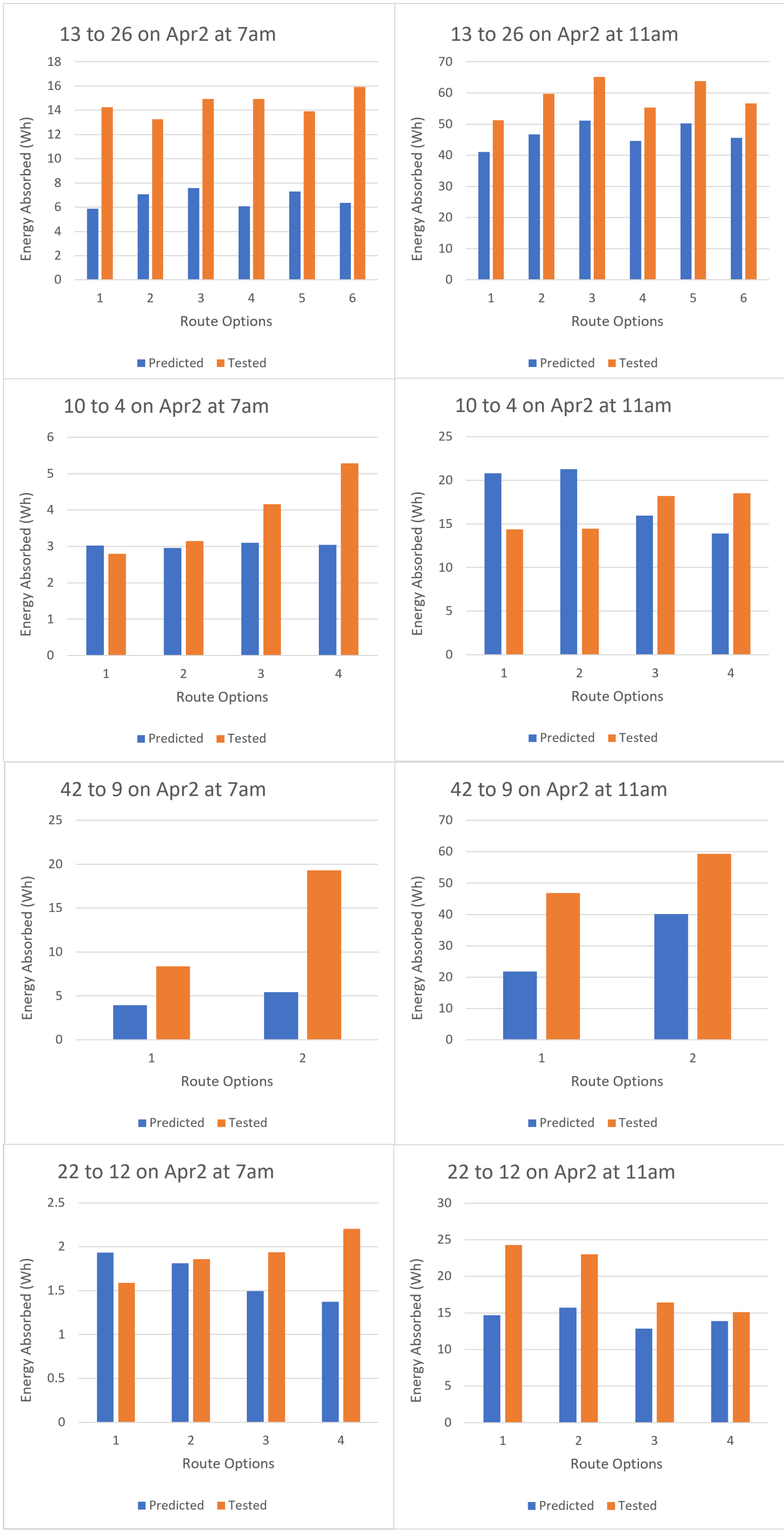


Figure A5.5: Route analysis conducted in heavy cloud conditions for the energy absorbed by a solar vehicle

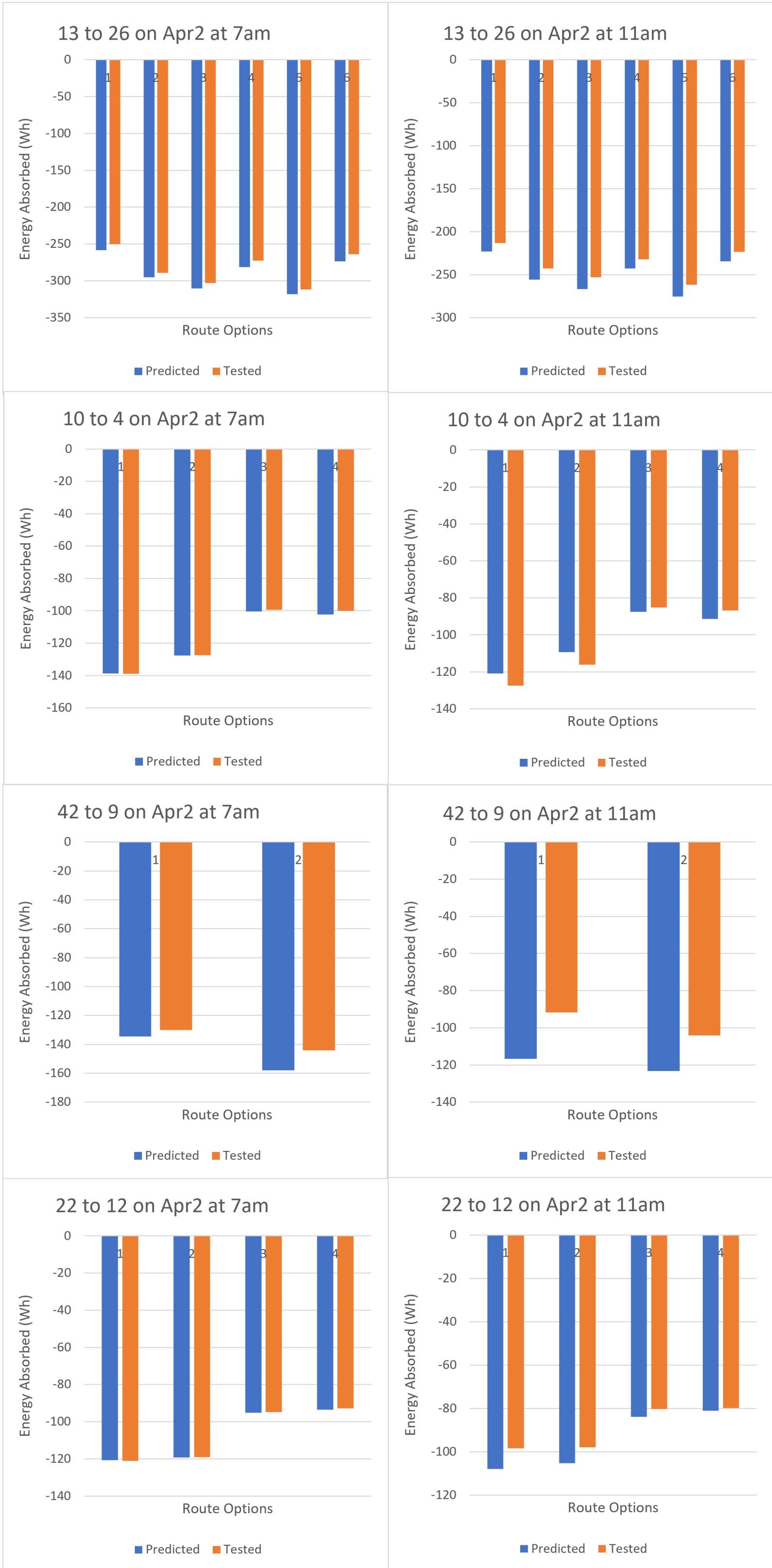


Figure A5.6: Route analysis conducted in heavy cloud conditions for the energy consumed by a solar vehicle

# A6 Vehicle Analysis


Figure A6.1: Comparison of vehicles travelling optimal route for each journey March 26